SANDIA REPORT

SAND201X-XXXX
Unlimited Release
Printed October 2017

Modular Accident Analysis Program (MAAP) – MELCOR Crosswalk: Phase II, Analyzing a Partially Recovered Accident Scenario

Nathan Andrews, Troy Haskin and Chris Faucett
Sandia National Laboratories

Prepared by
Sandia National Laboratories
Albuquerque, New Mexico 87185 and Livermore, California 94550

Sandia National Laboratories is a multimission laboratory managed and operated by National Technology and Engineering Solutions of Sandia, LLC, a wholly owned subsidiary of Honeywell International, Inc., for the U.S. Department of Energy's National Nuclear Security Administration under contract DE-NA0003525.

Issued by Sandia National Laboratories, operated for the United States Department of Energy by National Technology and Engineering Solutions of Sandia, LLC.

Available to DOE and DOE contractors from
U.S. Department of Energy
Office of Scientific and Technical Information
P.O. Box 62
Oak Ridge, TN 37831

Telephone: (865) 576-8401
Facsimile: (865) 576-5728
E-Mail: reports@osti.gov
Online ordering: http://www.osti.gov/scitech

Available to the public from
U.S. Department of Commerce
National Technical Information Service
5301 Shawnee Rd
Alexandria, VA 22312

Telephone: (800) 553-6847
Facsimile: (703) 605-6900
E-Mail: orders@ntis.gov
Online order: https://classic.ntis.gov/help/order-methods/

SAND201X-XXXX
Printed October 2017
Unlimited Release

Modular Accident Analysis Program (MAAP) – MELCOR Crosswalk: Phase II, Analyzing a Partially Recovered Accident Scenario

Nathan Andrews, Troy Haskin and Chris Faucett
Severe Accident Analysis Department
Sandia National Laboratories
P. O. Box 5800
Albuquerque, New Mexico 87185-MS0748

Abstract

Following the conclusion of the first phase of the crosswalk analysis, one of the key unanswered questions was whether or not the deviations found would persist during a partially recovered accident scenario, similar to the one that occurred in TMI-2. In particular this analysis aims to compare the impact of core degradation morphology on quenching models inherent within the two codes and the coolability of debris during partially recovered accidents. A primary motivation for this study is the development of insights into how uncertainties in core damage progression models impact the ability to assess the potential for recovery of a degraded core.

These quench and core recovery models are of the most interest when there is a significant amount of core damage, but intact and degraded fuel still remain in the core region or the lower plenum. Accordingly this analysis presents a spectrum of partially recovered accident scenarios by varying both water injection timing and rate to highlight the impact of core degradation phenomena on recovered accident scenarios.

This analysis uses the newly released MELCOR 2.2 rev. 9665 and MAAP5, Version 5.04. These code versions, which incorporate a significant number of modifications that have been driven by analyses and forensic evidence obtained from the Fukushima-Daiichi reactor site.

ACKNOWLEDGMENTS

This work was prepared by Sandia National Laboratories for the United States Department of Energy and the United States Nuclear Regulatory Commission.

MAAP analyses in this report were contributed by the Electric Power Research Institute (EPRI).

Sandia National Laboratories is a multimission laboratory managed and operated by National Technology and Engineering Solutions of Sandia LLC, a wholly owned subsidiary of Honeywell International Inc. for the U.S. Department of Energy's National Nuclear Security Administration under contract DE-NA0003525.

TABLE OF CONTENTS

FIGURES

TABLES

NOMENCLATURE

1F1	Fukushima-Daiichi Unit 1
BAF	bottom of active fuel
BSAF	Benchmark Study of the Accident at the Fukushima Daiichi Nuclear Power Station
BWR	boiling water reactor
CRD	control rod drive
CV	control volume
DOE	Department of Energy
EPRI	Electric Power Research Institute
FP	fission product
hr	hour
IC	isolation condenser
J	joule
K	Kelvin
kg	kilogram
LP	lower plenum
m	meter
MAAP	Modular Accident Analysis Program
MCAP	MELCOR Cooperative Assessment Program
MCCI	molten core concrete interactions
MPa	Megapascal
MSIV	main steam isolation valve
MSL	main steam line
MW	megawatt
NEA	Nuclear Energy Agency
NCG	non-condensable gas
OECD	Organization for Economic Cooperation and Development
PCV	primary containment valve
PWR	pressurized water reactor
RPV	reactor pressure vessel
s	second
SNL	Sandia National Laboratories
SOARCA	State-of-the-Art Reactor Consequence Analyses
SRV	safety relief valve
TAF	top of active fuel
TEPCO	Tokyo Electric Power Company
TMI	Three Mile Island
µm	micron
USNRC	United States Nuclear Regulatory Commission

1. INTRODUCTION AND DISCUSSION

1.1. Review of Phase I Results

The Modular Accident Analysis Program (MAAP)-MELCOR Crosswalk Phase 1 Study was completed in November 2014, documenting differing behavior of the MAAP5 and MELCOR severe accident analysis codes during a stylized Fukushima Daiichi Unit 1 (1F1) event scenario. [1]

The diverging behavior of the MAAP5 and MELCOR codes was brought to light by a DOE sponsored analysis of 1F1. This unit, based on international expert consensus, experienced significant core damage and saw core relocation ex-vessel due to a lack of water injection. The original DOE study applied the MELTSPREAD and CORQUENCH codes to identify a range of plausible ex-vessel conditions given ex-vessel core debris relocation transients established by MAAP5 and MELCOR. Of particular concern to these analyses were the reactor pressure vessel (RPV) pressure at time of lower head breach, the fraction and temperature of molten core debris relocation into containment and the rate of core debris relocation into containment. The Crosswalk sought to find the origin of these key divergences as well as any others that occurred during the in-vessel phase of a severe accident. [1]

Accordingly, in the MAAP-MELCOR Crosswalk, relevant code deviations that could lead to a significant difference in system behavior were identified and attributed to the relevant models within the two codes. Deviations are described in more detail in the Modular Accident Analysis Program (MAAP)-MELCOR Crosswalk Phase 1 Study. These deviations included: [1]

- Core energy balance
- RPV response
- Containment response
- Fuel assembly collapse
- Fuel canister failure
- Extent of downward relocation of particulate debris
- Flow and heat transfer area in the degraded core
- Fraction of core forming solid or molten debris
- Core region failure mechanism
- Rate of core debris slumping
- Molten fraction of debris slumping to lower plenum
- Molten fraction of debris in the lower plenum
- In-vessel hydrogen generation

At a high level, the MAAP5 program predicted core relocation behavior similar to that which occurred at Three Mile Island Unit 2 (TMI-2) in which a crucible was formed in-core. The outer crust of this crucible insulated a significant amount of molten mass. On the other hand, the

MELCOR program predicted a significantly higher amount of particulate debris within the core region. The increased porosity of the MELCOR debris leads to a higher steam and gas flow rate through the core. Subsequently, there is more convective heat removal and more in-vessel hydrogen generation. [1]

1.2. Study Purpose and Objective

Following the conclusion of the first phase of the crosswalk analysis, one of the key unanswered questions was whether or not the deviations found would persist during a partially recovered accident scenario, similar to the one that occurred in TMI-2. In particular phase two aims to compare the impact of core degradation morphology on quenching models inherent within the two codes and the coolability of debris during partially recovered accidents. [1]

These quench and core recovery models are of the most interest when there is a significant amount of core damage, but intact and degraded fuel still remain in the core region or the lower plenum. Accordingly this analysis presents a spectrum of partially recovered accident scenarios by varying both water injection timing and injection rate to highlight the impact of core degradation phenomena on recovered accident scenarios.

This analysis uses the newly released MELCOR 2.2 rev. 9665 and MAAP 5, Version 5.04, which incorporate a significant number of modifications that have been driven by analyses and forensic evidence obtained from the Fukushima-Daiichi reactor site. [2] [3] In particular, the analyses performed and insights gained from participating in the OECD/NEA BSAF Phase I Project highlighted several key areas where MELCOR 2.1 could be enhanced by improving model robustness and implementing new dedicated models to better capture phenomenological behavior and key boundary conditions that strongly affect the source term. [4]

1.3. Relevant Code Modifications from MELCOR 2.1 to MELCOR 2.2

MELCOR 2.2 is a significant official release of the MELCOR code with many new models and improvements. This section provides a quick review and characterization of new models added, significant code changes and their impact on analyzing the Fukushima-Daiichi accidents. More detailed information is found in “Quicklook Overview of Model Changes in MELCOR 2.2: Rev 6342 to Rev 9496” as well as the User Guide and Reference Manuals. These changes have made it possible for 500-hour long source term calculations of Fukushima-Daiichi Power Station to be performed in under 50 hours of computational time. [5]

Code improvements have been directed in the following areas to better simulate the Fukushima-Daiichi Power Station response: detailed safety system modeling, ex-vessel behavior and code performance during core reflood. These improvements to MELCOR 2.1 mark a significant advancement to the MELCOR code resulting in the recent increment in the version number to 2.2. [5]

The accident progressions in both 1F2 and 1F3, where alternative water injection was introduced across various core degradation states, required improving code robustness and performance during reflood. One key set of changes temporally relaxes the rate-of-change of the quench velocity and causes the quench velocity to be smoothly driven to zero within a small distance of the pool level. Several model corrections and numerical improvements to the MELCOR quench

model were developed and implemented and have significantly improved the robustness of the code for reflood conditions. [5]

Akin to this, a temporal relaxation model was introduced within the code. Many physical processes in MELCOR are modeled by correlation based relationships developed from steady-state experiments. These models do not represent the time it takes for these processes to respond as conditions change. As a result, temporal "rate-of-change" aspects of MELCOR simulations are not expected to be highly accurate and numerical instabilities can be magnified when sudden changes occur. Temporal relaxation is a simple way to introduce a user-imposed time-scale based model that limits how quickly processes being modeled can change in time. This has made it significantly easier to perform forensic analysis of core oxidation and relocation behavior for this analysis and improved code robustness. [5]

In the case of core degradation, SNL and the USNRC decided to take a prudent "wait-and-see" approach to changing the phenomenology of core degradation within MELCOR. Future changes to this portion of the code will be highly informed by entry into the reactor pressure vessel and/or the primary containments of each Fukushima-Daiichi unit. That said, assessment is currently underway of MELCOR crust formation and molten pool/crust formation modeling with a focus on steam permeability to severely damaged core regions and its effects on hydrogen generation, sensible heat gain and convective heat loss from such degraded regions. This is partly motivated by recent MELCOR/MAAP crosswalk studies comparing the two code modeling paradigms and also from deep analysis of the Fukushima Daiichi Unit "three peaks" time period where we believe there is evidence of core degradation processes affecting hydrogen generation and PCV pressurization. This investigation could result in further refinement of MELCOR core degradation modeling. [5]

This crosswalk analysis, utilizes several of the key modifications to the MELCOR software made within version 2.2. In particular, this analysis makes use of the quench and temporal relaxation models implemented since the original crosswalk analysis. Additionally, insights gained from the core degradation analysis contained within this report will be used to modify and update the MELCOR COR package, which houses core degradation modeling, as necessary.

1.4. Plant Models and Phenomenological Representations

The plant models and parameters are described in-depth in the Phase I analysis and thus not presented here. How the two codes represent the physical phenomena of core degradation, system behavior, lower plenum behavior and hydrogen generation is also not addressed. Similar to the plant models, this phenomenological information is contained in-depth within the original crosswalk analysis. [1]

1.5. Accident Scenario

The accident scenario developed by EPRI and SNL for this analysis is stylized after the accident progression of Fukushima Daiichi Unit 1. However, this accident scenario is for the purpose of code comparison and not for Fukushima Daiichi forensic efforts. The behavior of key systems in the plant can be seen in Table 1-1. This accident scenario is identical to the first phase scenario with two key exceptions: SRV seizure is assumed to occur at 3.0 hours instead of 7.0 hours and water injection enters via the downcomer at a specified time. [1]

Table 1-1. Behavior of key systems in simulated Fukushima accident scenario

System	Behavior
Main Steam Line Isolation Valve (MSIV)	MSIV closure signal at 52.5 s after SCRAM.
	MSIV open area reducing from fully open to fully closed over a 3 s interval from the time of the closure signal.
Control Rod Drive (CRD)	At reactor scram it is assumed that the CRD injection flow ceases.
Feedwater System	The feedwater system is assumed to inject for the first 60 s following the initiating event.
	The feedwater injection transient is an imposed boundary condition; the detailed injection transient can be seen in Figure 1-1.
	The specific enthalpy of feedwater is assumed to be 792 kJ/kg.
Safety Relief Valve (SRV)	SRV seizure is assumed to occur at 3 hours after SCRAM.
	All discharge through the seized SRV is assumed to go into the suppression pool.
Isolation Condenser (IC)	IC heat removal is assumed to be constant with pressure at 42.4 MW per train.
	The periods of IC operation are shown in Table 1-2.
Water Injection into Downcomer	Varying timing and amounts. Please see Table # for a full listing of cases.

The cumulative feedwater flow into the RPV can be found in Figure 1-1. This value was held constant between the two codes. Both MELCOR and MAAP also used the same isolation condenser operation periods, which are shown in Table 1-2.

The decay heat for this analysis was generated using ORIGEN. Methods and results are summarized in Cardoni, 2014. [6]

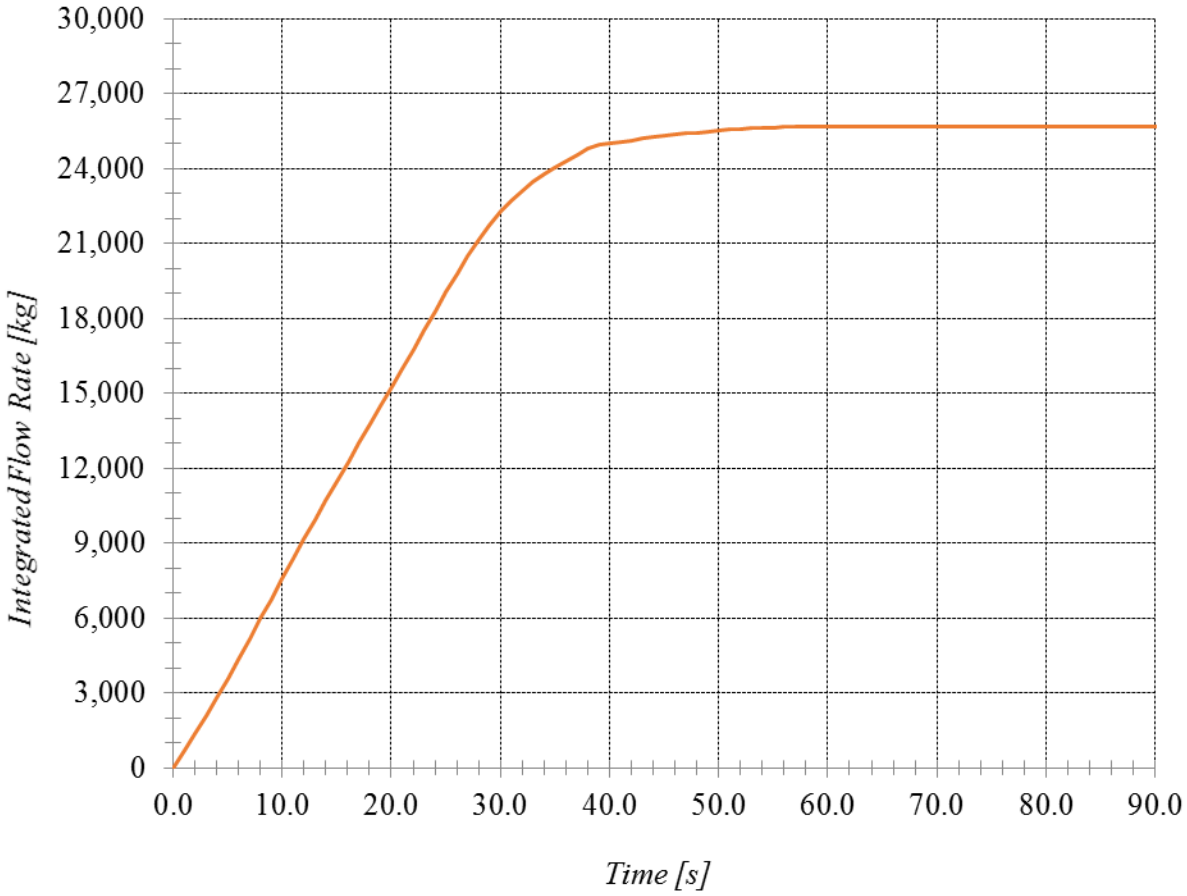

Figure 1-1. Cumulative feedwater flow into the RPV

Table 1-2. Isolation condenser operation parameters

Time Isolation Condenser Operation Starts (s)	Time Isolation Condenser Operation Ceases (s)	Number of IC Trains Operating (#)
360	400	2
1,860	1,980	1
2,280	2,400	1
2,760	2,880	1

The behavior of the main steam line isolation valve, control rod drive mechanism, feedwater system, safety relief valve and the isolation condenser behavior were made constants between the two codes. This ensures that the differences in system behavior during the accident sequence originate from the differing in-core phenomenological treatment of the two codes.

Unlike Phase I of the crosswalk analysis, a spectrum of cases was run, instead of a single realization. The goal of this analysis is to highlight the difference between the two codes found during a partially recovered accident. To fully capture the divergent behavior, different timings

and rates of water injection into the downcomer were simulated. The full case matrix can be seen in Table 1-3. The injection delay refers to the amount of time after 5.0 kg of in-vessel H_2 is generated, which is used as surrogate for the onset of core damage. This timing was different for MAAP and MELCOR. These two parametric studies allow the comparison of how both injection rate and injection timing affect overall core damage progression. A singe representative case was chosen for a more in-depth comparison between the two programs; this was "Case 4" with an injection rate of 5.0 kg/s and a delay of 1.0 hour. (Case 4 and Case 9 are the same, but the cases are presented sequentially for easier comparison.) The timing of the onset of core damage for both programs was 3.6 hours; the point at which 5.0 kg of H_2 was generated.

Table 1-3. Case matrix for the MELCOR-MAAP Crosswalk, Phase II

Case	Injection Rate (kg/s)	Injection Delay (hours)
1	0.0	1.0
2	1.0	1.0
3	2.5	1.0
4	5.0	1.0
5	15.0	1.0
6	20.0	1.0
7	5.0	0.00
8	5.0	0.25
9	5.0	1.0
10	5.0	2.0
11	5.0	3.0
12	5.0	5.0

This reference case was chosen because the injection rate is representative of the amount of injection needed to make up for loss of water coverage from steam generation in the early stages of the accident scenario. Additionally, starting injection one hour after the onset of core damage allows this analysis to better examine the effect of core degradation models on a partially recovered accident, similar to TMI-2. Such an accident necessarily needs to have both a sufficiently damaged core and a portion of intact fuel remaining in the active core region when injection begins. The reference case meets both of these criteria.

1.6. Comparison Methodology

The behavior of the codes as they progress through the prescribed accident sequences will be evaluated according to event timings and simulated behavior. Key areas addressed are the system response behavior, core degradation, hydrogen generation and quenching behavior.

The full list of relevant parameters compared is shown below and grouped by the four key areas of interest. It is believed that this list covers relevant behavior for this accident scenario that can be compared between MELCOR and MAAP. These four areas of interest are compared for the two parametric studies performed on injection rate and injection timing. They are also compared for the single representative reference case of 5.0 kg/s water injection at a delay of 1.0 hour from the onset of core damage.

Since the Phase I crosswalk analysis, insights from the State-of-the-Art Reactor Consequence Analysis (SOARCA) Peach Bottom Uncertainty Analysis have led SNL researchers to change the estimation of the ZrO_2-UO_2 melt interaction temperature from 2800 K in the Crosswalk Phase I analysis to 2500 K in the SOARCA analysis. In order to capture the effect of this change, a single realization was run with the reference case and the SOARCA best estimate value of this melting temperature. This analysis is presented in its own stand-alone chapter. For all other analyses in this report, the Crosswalk Phase I melting point of 2800 K was used to obtain MELCOR results. [6]

- System response behavior
    - RPV water level
    - Primary system pressure
    - Steam dome temperature
    - Drywell Pressure
    - Wetwell Pressure
    - Wetwell Temperature
- Core degradation
    - Fuel temperature
    - Debris location
    - Core support plate and shroud failure
- Quenching behavior
    - Debris coolability
    - Effectiveness of water cooling
- Hydrogen generation
    - Total mass generation
    - Generation rate and timings

1.7. Report Scope

This report compares the results from the second phase of the MAAP-MELCOR Crosswalk. It is a joint effort of the USNRC, SNL and EPRI and covers the conclusions from ongoing discussions of these three organizations. Preliminary results of this analysis were presented at the 2017 Annual Cooperative Severe Accident Research Program (CSARP) and MELCOR Cooperative Assessment Program (MCAP) in order to gain the insight of other international partners and severe accident modeling experts.

This report maintains a similar structure to the original crosswalk report; however, instead of presenting plots in the appendices section, they are included in the body of the report to support the conclusions drawn.

Separate chapters of this report cover:

- Executive summary discussing major conclusions from the report
- Introduction to the problem and codes
- Scenario description, plant models and analysis methodology
- Representative reference case comparison
- Constant injection delay cases analysis
- Constant injection rate cases analysis
- Comparison of reference case's MELCOR analysis to State-of-the-Art Reactor Consequence Analysis fuel melting temperature assumptions
- Conclusions and planned future work

2. REPRESENTATIVE REFERENCE CASE

This chapter discusses in-depth a single representative realization that captures the impact of both core degradation modeling representation and debris coolability on the progression of a partially recovered severe accident similar to what occurred at TMI-2. This representative case has an injection rate of 5.0 kg/s (79 gpm), which corresponds to the necessary amount of injection to makeup boil-off when the primary system depressurizes. With this injection rate, reflooding does not occur immediately and software programs are exercised against a problem with a significant amount of core damage. Injection into the downcomer began 1.0 hours after the onset of core damage, which was taken to be the time when 5.0 kg of hydrogen was generated. This number was identical between the two codes and is a simple, objective way to compare the beginning of gap-release during a severe accident.

2.1. Core Degradation Characterization

This section provides an analysis of the core degradation progression of the representative case. Included is a discussion of the fuel temperature and a characterization of fuel in the lower plenum. Core degradation serves as the primary driver in this scenario for primary system response, containment response and long-term coolability.

2.1.1. Nodalized Core Temperature

The progression of the core region temperature for the MAAP simulation is presented in Figure 2-1; the MELCOR results are presented in Figure 2-2. In the MAAP simulation, the heat-up of the core begins at 3.75 hours in the upper half of the fuel in the central region. From here it spreads both axially and radially. By 4.25 hours, fuel assemblies in the upper third of the core have already begun to fail. This fuel relocates downwards and contributes to the heatup of the lower two thirds of the core. Simultaneously, core degradation expands outwards, blocking flow to upper regions of the core and leading to even more fuel failures. Radial expansion can particularly be seen in the lower third of the core from 5.0 to 6.0 hours.

The agglomerated fuel mass, sitting in the lower half of the core, eventually forms a molten pool as it is no longer coolable. This molten pool gradually grows and forms a hemispherical shape, which is flat on the top.

As water refloods the core, it does not have a significant impact on the overall temperature profile of the degraded fuel. However, this water does cool the peripheral regions of the molten pool, forming a crust with poor heat transfer qualities. This exterior crust inhibits heat transfer out of the central molten region to the exterior. Intact fuel elements in the core are fully quenched by the reflood when they remain in rod geometry. Progressive quenching of exterior fuel elements can be seen from 8.0 to 10 hours at the core mid-level. This molten pool remains beyond the 15 hours shown in Figure 2-1 to the end of the 24 hour simulation.

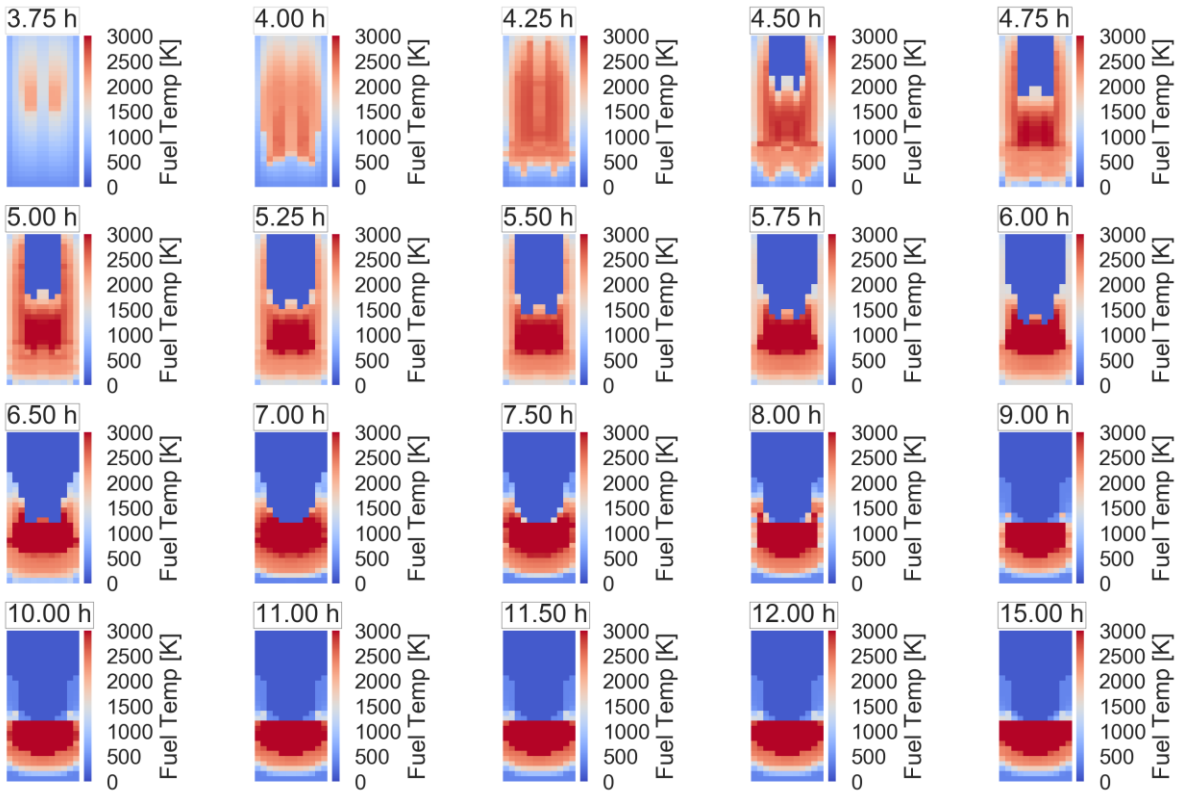

Figure 2-1. Nodalized core temperature for MAAP simulation of the reference case, injection rate of 5.0 kg/s and 1.0 hour delay

In the MELCOR simulation, a significantly different core damage progression is predicted. Instead of a large molten pool that gradually progresses downwards through the core, the MELCOR simulation predicts the formation of particulate debris that relocates to the lower plenum after failing the core plate. The failure of core plate structures in MELOR occurs rapidly after debris builds up on them. This debris is then quenched in the lower plenum and provides a flow of steam to the core. This steam fuels oxidation but also removes a portion of heat from the core region.

In the MELCOR simulation, the first fuel assembly failures occur just before 4.25 hours into the simulation. This initial failure occurs in the top third of the core in the central ring. From here the hot temperatures in this region expand both downwards and radially. Eventually the entirety of both the first and second ring of the core relocate to the lower plenum. The third ring is also failed at the core midpoint.

During the accident scenario, the fuel in the MELCOR simulation experiences damage and candling. However, it retains a relatively intact cylindrical geometry. This means that when injection begins and the core is eventually reflooded, the fuel remaining in the core region is rapidly quenched relative to MAAP. It can be seen that the core is fully cooled by 15.0 hours into the simulation.

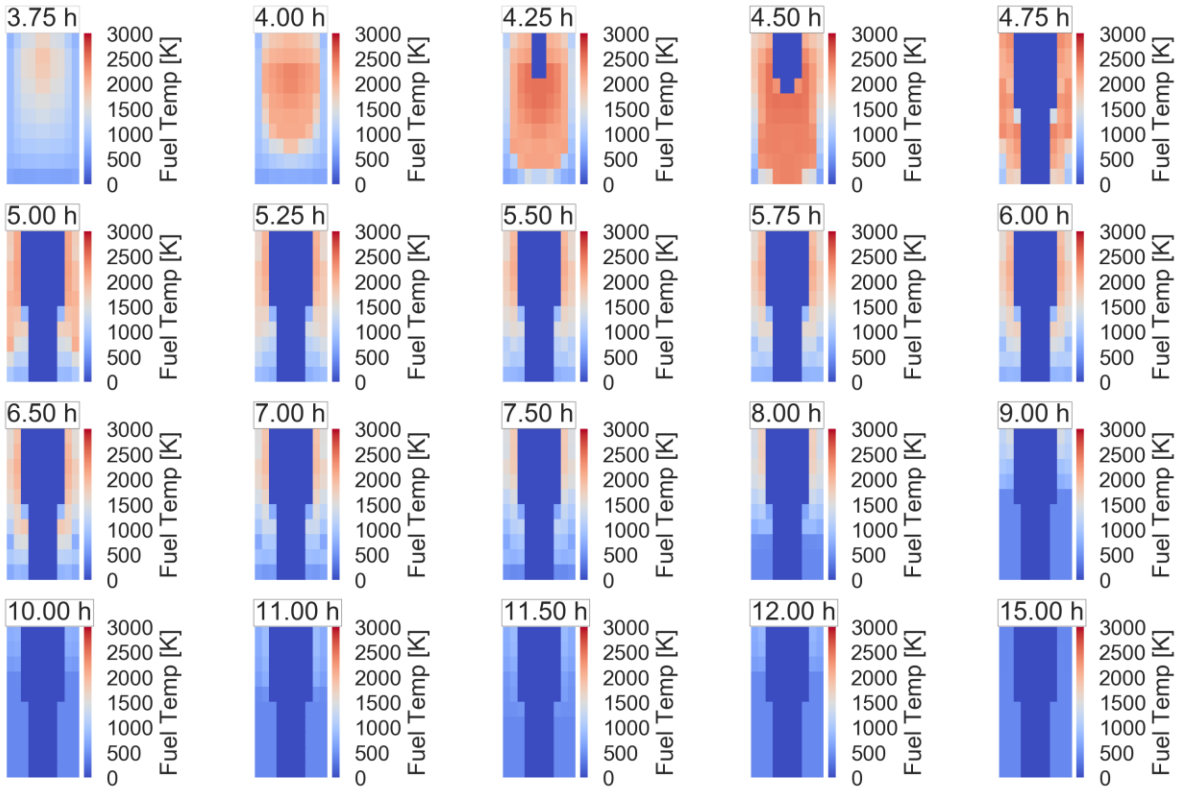

Figure 2-2. Nodalized core temperature for MELCOR simulation of the reference case, injection rate of 5.0 kg/s and 1.0 hour delay

2.1.2. Progression to Core Recovery

In order to highlight the large variation in the quenching behavior of the two codes, enlarged snapshots of the fuel temperature before and after quenching are presented here. In Figure 2-3, fuel temperature for both MAAP and MELCOR are presented immediately before water injection into the downcomer begins. At this point a large portion of the core has relocated to the lower plenum in the MELCOR simulation. In both simulations, there is a significant amount of damage in the upper third of the core. Additionally, the temperatures predicted by both codes in the lower two thirds of the core is rising. Also at this point, the nascent formation of the molten pool in the core of the MAAP simulation is evident while in MELCOR the fuel temperatures are not hot enough for this to occur.

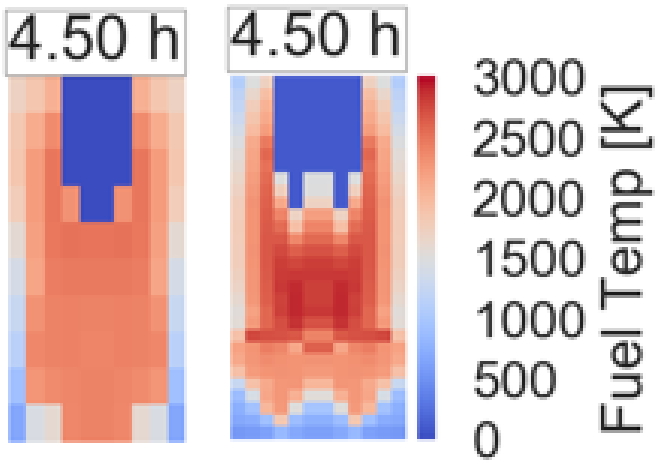

Figure 2-3. Fuel Temperature for reference case with injection delay of 1.0 hour and injection rate of 5.0 kg/s, prior to water injection at 4.5 hours for MELCOR (left) and MAAP (right)

The fuel temperatures for both MAAP and MELCOR 5.4 hours after the start of injection can be seen in Figure 2-4. At this point the remaining fuel in the active core region has been fully quenched in the MELCOR simulation. In the MAAP simulation, there is a large molten pool that has formed in the lower third of the core. This molten pool is not fully quenched at this point. In fact an insulating oxide crust has formed on the bottom surface of the pool. The gradual decrease in temperature from the center of the crucible, which is near 3000 K to the bottom exterior of the crucible, which is near the coolant temperature, can be seen.

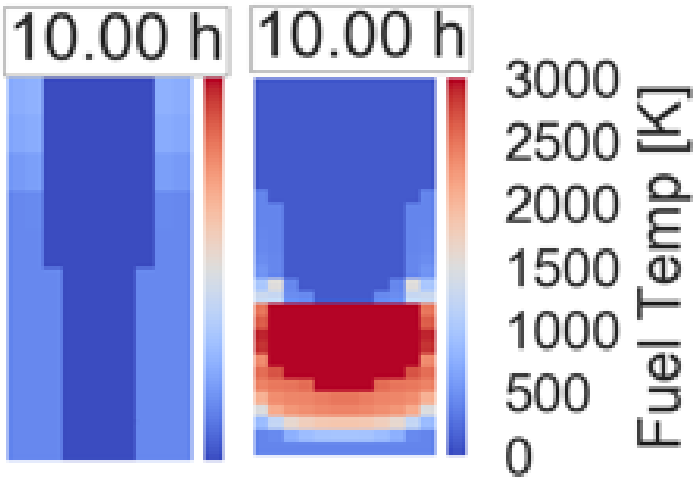

Figure 2-4. Fuel Temperature for reference case with injection delay of 1.0 hour and injection rate of 5.0 kg/s, following water injection at 10.0 hours

2.1.3. Fuel Temperatures

As implied by the nodalized diagrams of the core degradation progression there is a large divergence in the fuel temperature plots of the reference scenario. Fuel temperatures for both MAAP and MELCOR are presented in Figure 2-5.

In MELCOR, fuel nodes can be easily classified into two different groups. The first group increases in temperature drastically to near the time-at-temperature failure criteria. When it reaches the threshold it immediately fails and relocates. In the reference case, all of these fuel failures and relocations occur before 5.0 hours into the simulation. These are seen dropping to 0 K, which simply represents failure. The second group of fuel nodes in the MELCOR simulation also rises in temperature quickly following boil-off of water in the core. However, the fuel failure threshold is not reached for these nodes, and they are gradually quenched. Full quenching occurs just before 15 hours into the simulation.

MAAP fuel nodes in the simulation can be grouped into three separate groups, all immediately spike following loss of cooling. The first group fails and relocated between 4 hours and 8 hours into the simulation. The second group undergoes quenching and returns to a temperature near the coolant. The third, which is part of the crucible that is formed remains relatively constant in temperature from 5 hours to the end of the simulation. This is attributed to the insulating nature of outer crucible layers.

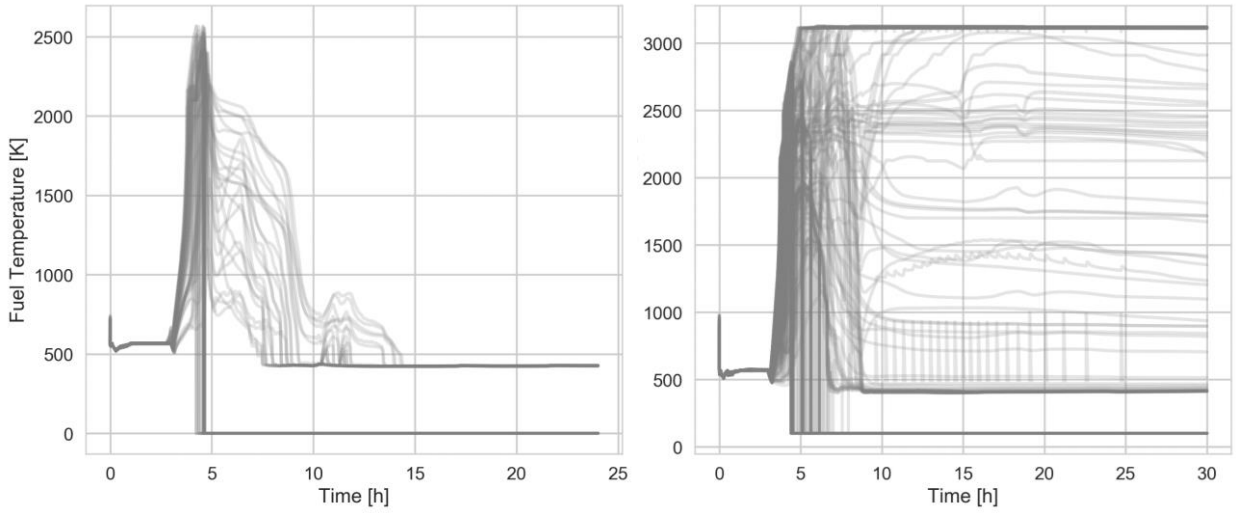

Figure 2-5. Fuel temperature for reference case with injection delay of 1.0 hour and injection rate of 5.0 kg/s, showing MELCOR (left) and MAAP (right)

2.1.4. Lower plenum Characterization

During the simulation, MELCOR relocates a significant amount of fuel debris to the lower plenum, whereas fuel debris in MAAP remains in the core region. This difference is illustrated in **Error! Reference source not found.** which shows the mass of molten material in the lower plenum for both the MAAP and MELCOR simulation. In the MELCOR simulation, this molten material is eventually fully quenched, which leads to increased steam cooling, relative to MAAP, in the core region. The quenching of this molten material also leads to a spike in the steam dome

temperature, which is shown in Figure 2-9. When this molten material is quenched it becomes a fully cooled form of particulate debris in the lower plenum region.

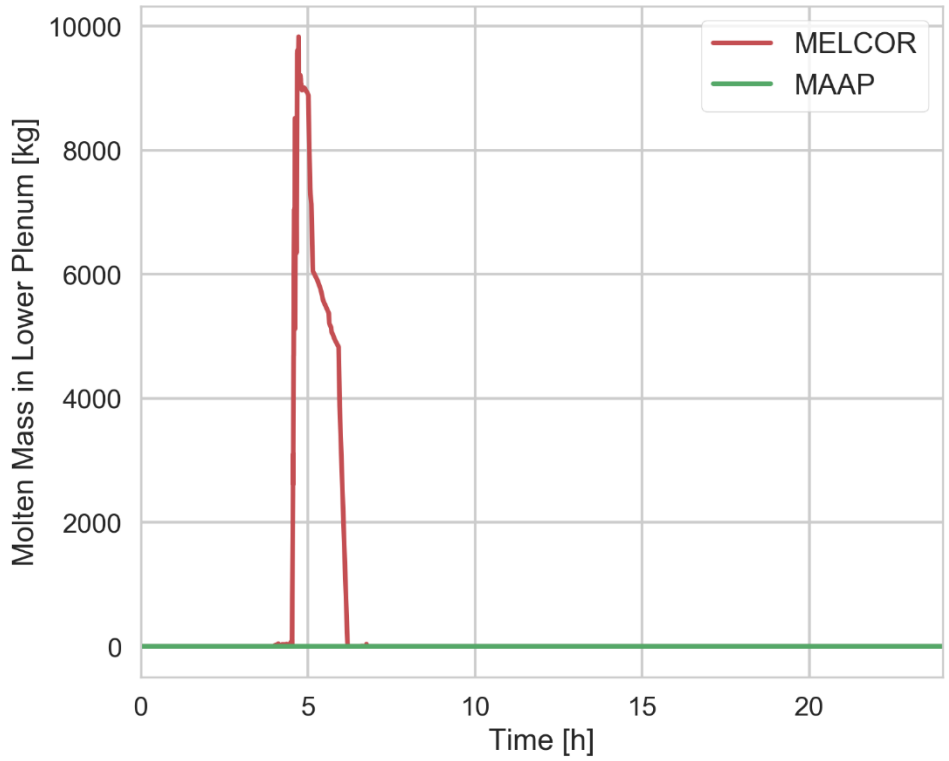

Figure 2-6. Molten mass in the lower plenum for reference case with injection delay of 1.0 hour and injection rate of 5.0 kg/s

2.2. Primary System Behavior

In this section the primary system behavior of MAAP and MELCOR is compared for the reference case. Included are analyses of RPV water levels, RPV pressure, steam dome temperature and in-vessel hydrogen generation. In this section it is demonstrated that the differences in core degradation representation and phenomenological assumptions drive the key differences seen in the behavior of the primary system.

2.2.1. Reactor Pressure Vessel Water Level

Until the onset of core damage at 3.6 hours in the accident, both MELCOR and MAAP show very similar water levels in the RPV. After this point, the water level in MELCOR compared to MAAP is lower. This is due to the fact that the core plate in the MELCOR case fails whereas in MAAP it does not. This allows damaged fuel material to relocate to the lower plenum. In the lower plenum, this fuel debris is quenched. As time progresses the decay heat of this debris in the lower plenum continues to be cooled through the boiling of water in the lower plenum. Water level is plotted in Figure 2-7.

As the reflooding progresses and reaches the core region, both MAAP and MELCOR simulations show a leveling off when the water level is near 1.0 m below TAF. At this time, a

portion of the core is filled with steam generated by the quenching of hot fuel debris. After the debris is able to be fully cooled by liquid water, the water level increases to above TAF.

Another factor contributing to the more rapid reflood in the MAAP simulation is the less effective heat transfer out of the molten crucible that is formed. The crust of the crucible is composed of oxides, and there is subsequently less conductive heat transfer to the outer surface, compared to both the particulate debris and nominally intact geometry (candling has still occurred) found in the MELCOR simulations.

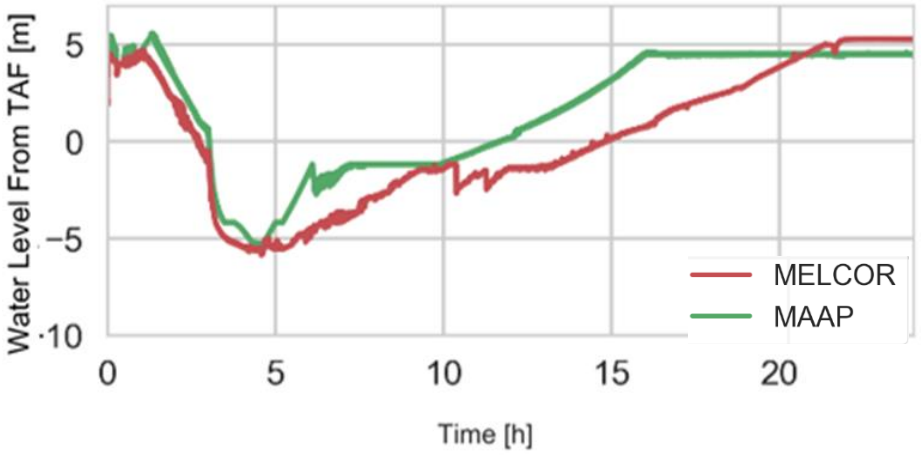

Figure 2-7. Water level for reference case with injection delay of 1.0 hour and injection rate of 5.0 kg/s

2.2.2. Primary System Pressure

The primary system pressure is shown in shown in Figure 2-8. A fundamentally identical response is seen in both the MAAP and MELCOR simulations until the point of depressurization. Here the MELCOR simulation experiences a slightly slower depressurization relative to MAAP. This difference in depressurization is likely attributable to three factors: 1) slightly different modeling of the primary system and SRVs, 2) increased steam generation in the MELCOR lower plenum, and 3) increased H_2 generation in MELCOR. The last two of these would lead to a higher pressure in the containment and thus a lower depressurization rate.

A large spike in the primary system pressure of the MELCOR simulation can be seen centered around 4.9 hours. This spike is due to the relocation to the lower plenum and subsequent quenching of the two innermost rings.

Following this spike, both the MELCOR and the MAAP analysis demonstrate pressure oscillations when the water level increases to BAF. When it reaches BAF, it begins to boil until all heat can be removed without boiling.

The long-term pressure of the MELCOR simulations are higher than that of MAAP due to the increased pressure in the MELCOR containment. This increase in pressure is resultant from the fact that MELCOR generates more H_2 relative to MAAP, which is a function of the differing core degradations.

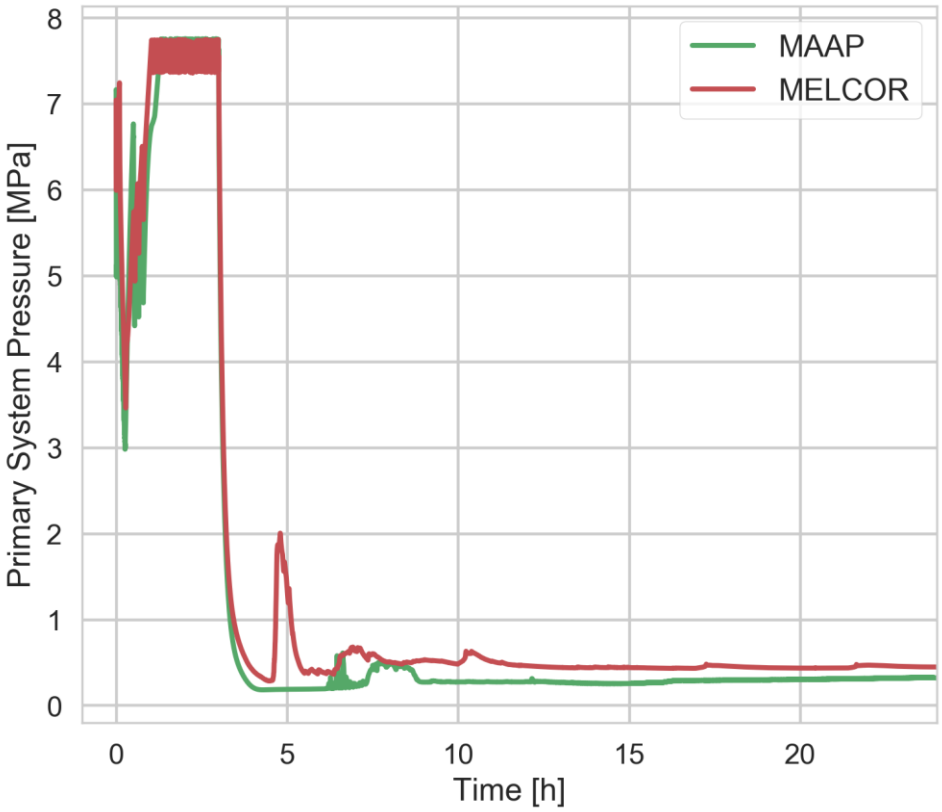

Figure 2-8. Primary system pressure for reference case with injection delay of 1.0 hour and injection rate of 5.0 kg/s

2.2.3. Steam Dome Temperature

The increased steam dome temperature in MELCOR, relative to MAAP, is a direct result of the relocation of fuel to the lower plenum in the MELCOR simulation. When the fuel relocates to the lower plenum, it is quenched, generating steam. This steam provides cooling to the core and also feeds zirconium oxidation reactions. This results in a significantly higher temperature by the time steam reaches the steam dome from the lower plenum. This is indicated by the coincident spikes in both the steam dome temperature and the amount of unquenched molten mass in the lower plenum at 4.9 hours. After this mass is fully quenched, the steam dome temperature decreases.

A second increase is seen in both the MAAP and MELCOR simulations as the quench front reaches the bottom of the active core region, near 6.5 hours. When there an increased amount of water is boiled and the top of the core is cooled by this steam. This leads to the observed increase in steam dome temperature.

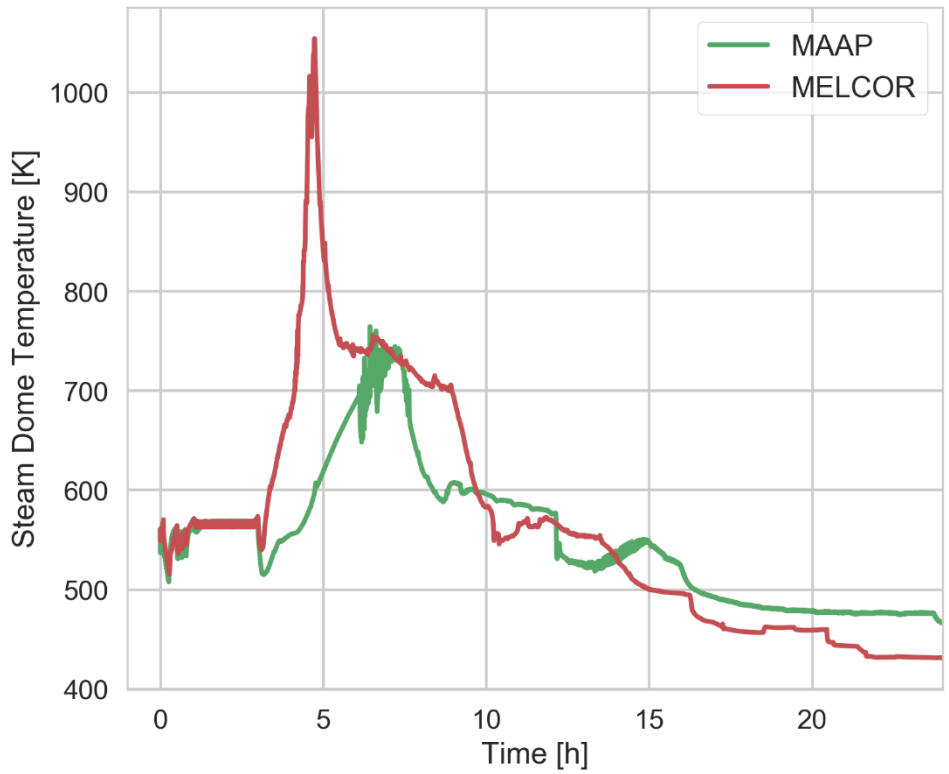

Figure 2-9. Steam dome temperature for reference case with injection delay of 1.0 hour and injection rate of 5.0 kg/s

2.2.4. In-vessel Hydrogen Generation

In the first phase of the MAAP-MELCOR Crosswalk analysis, one of the key takeaways is that the mass of in-vessel hydrogen generation in MAAP simulations is often half that of the same MELCOR simulation. This difference is due to differing representations of core degradation. The molten pool and related channel blockage that are formed in MAAP simulations inhibit the oxidation of zirconium while increased steam generation in the MELCOR lower plenum bolsters the oxidation of intact fuel materials. [1]

The same differences between MAAP and MELCOR in-vessel hydrogen generation were found in this analysis. These differences are plotted in Figure 2-10. The total mass of H_2 generated in MELCOR is over twice that of MAAP at the end of the five hour long phase of initial core damage. This difference persists until the end of the simulation. A small increase in the total amount generated in the MAAP analysis occurs when the quench front reaches the bottom of the core and additional steam is generated. This steam leads to additional oxidation of the remaining available zirconium.

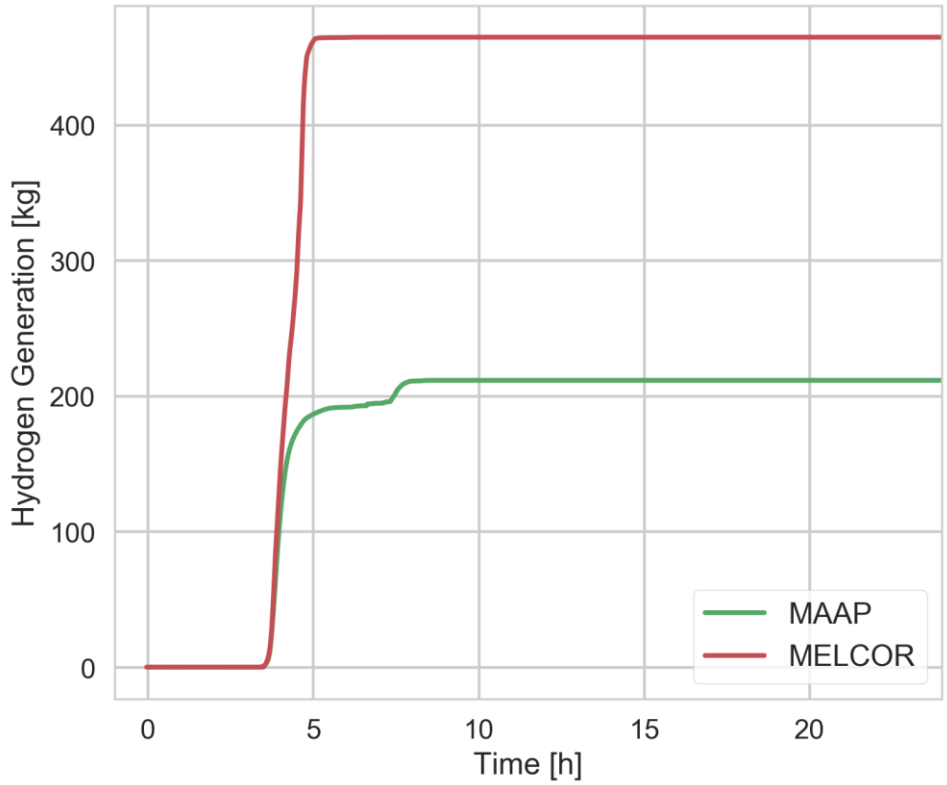

Figure 2-10. Hydrogen generation for reference case with injection delay of 1.0 hour and injection rate of 5.0 kg/s

2.3. Drywell and Wetwell Behavior

Drywell and wetwell behavior are presented in this section. Key divergences in late-time behavior are fully attributable to differences that occur during the early stages of the core damage progression.

2.3.1. Containment Pressure

The drywell and wetwell behavior for both codes track one another with near identical agreement. During the initial phase of core degradation, which starts at 3.6 hours into the simulation, a difference in pressure is established between the MELCOR and MAAP simulations. This difference can be attributed to the nearly 250 kg of additional hydrogen generated in the MELCOR simulations. This additional hydrogen generation leads to a pressure difference in the MELCOR drywell that is 75 kPa higher than the MAAP simulation. After this pressure differential is established by 5.0 hours into the simulation, it persists until the end of the simulation at 24 hours. Drywell pressure for both MAAP and MELCOR are shown in Figure 2-11; similarly wetwell pressures are shown in Figure 2-12.

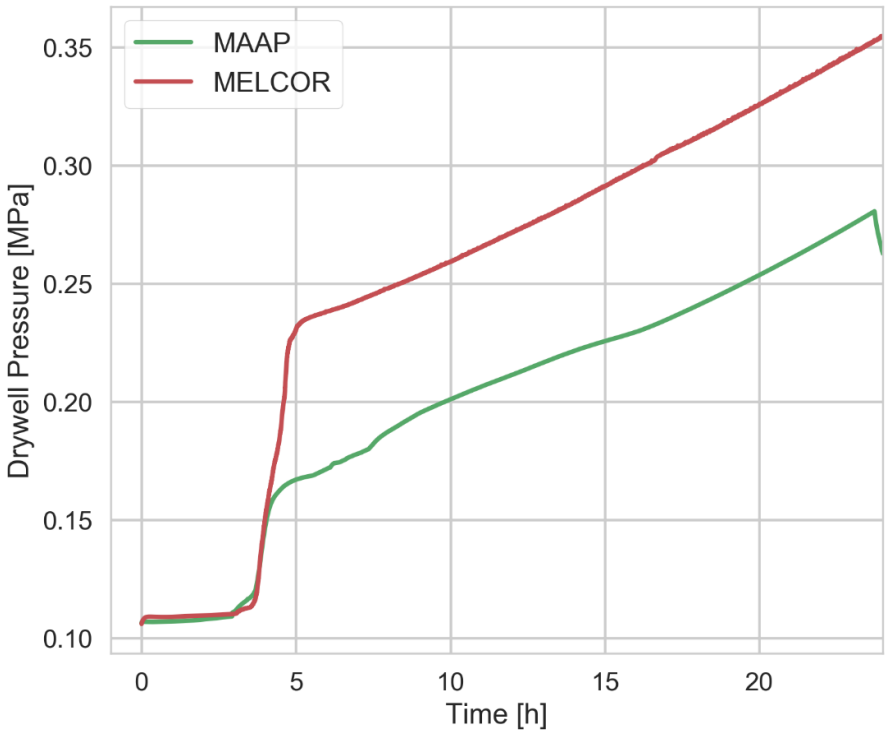

Figure 2-11. Drywell pressure for reference case with injection delay of 1.0 hour and injection rate of 5.0 kg/s

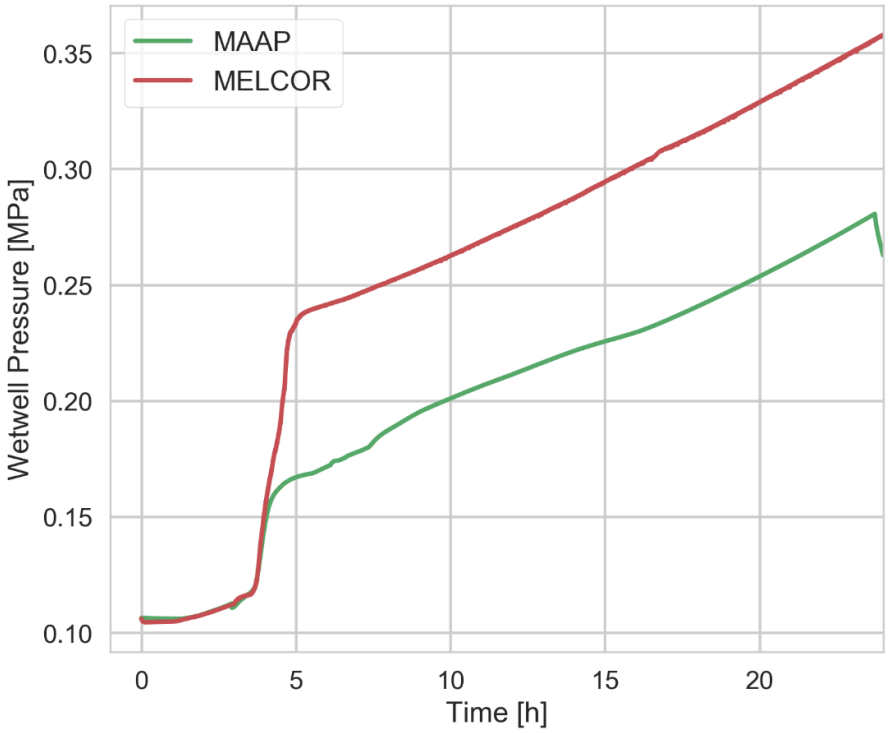

Figure 2-12. Wetwell pressure for reference case with injection delay of 1.0 hour and injection rate of 5.0 kg/s

2.3.2. Wetwell Temperature

Until the relocation of fuel into the lower plenum, which occurs between 4.0 and 5.0 hours, in the MELCOR simulation, bulk wetwell temperatures in MAAP and MELCOR are within a few degrees difference of each other. After fuel relocates to the lower plenum, additional steam is generated. This steam increases in temperature as is moves through the core and is eventually condensed in the wetwell.

A difference in temperature of near 10 K is established by seven hours into the transient. This difference in temperature remains until the end of the simulation at 24 hours. A short plateau in the MAAP simulation occurs after the initial phase of core damage. Then, when the water level in the MAAP simulation reaches BAF during reflood, a second increase in the wetwell temperature occurs, due to boiling (quenching) in the lower region of the core.

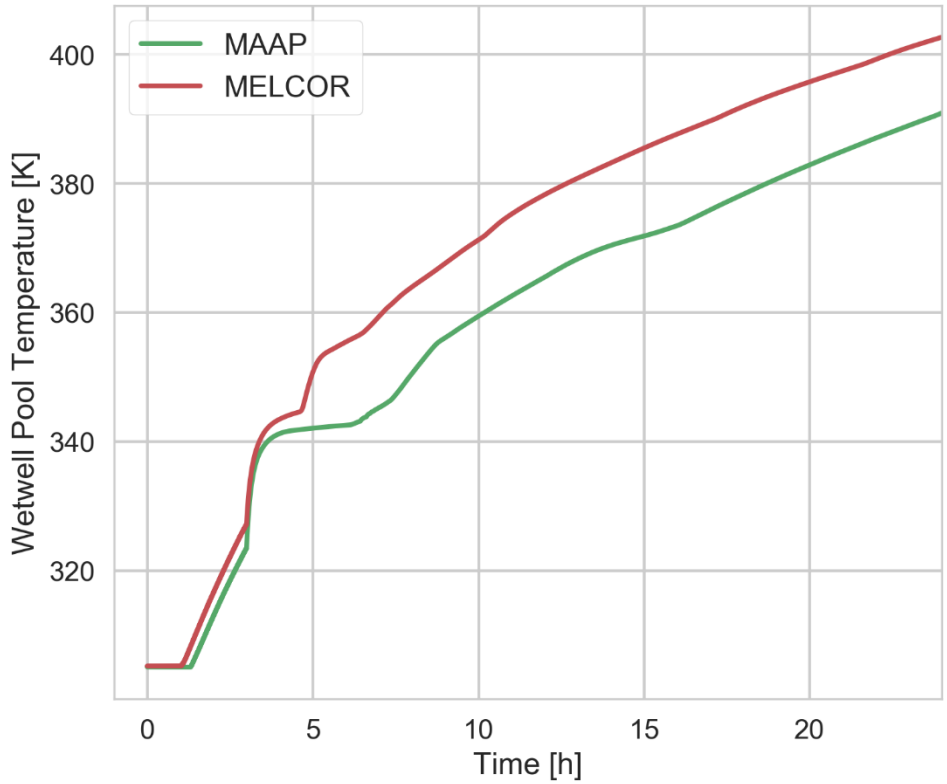

Figure 2-13. Wetwell temperature for reference case with injection delay of 1.0 hour and injection rate of 5.0 kg/s

2.4. Effectiveness of Water Injection

During a partially mitigated severe accident, one of the key metrics of interest is how effective water cooling and injection is at removing decay heat at various stages of the severe accident. In order to evaluate this several analyses were performed:

- The total amount of convective heat transfer from both steam and water cooling for the entire 24 hours of the simulation
- Core blockage fraction in the core region predicted by both software codes from 3.75 hours to 15 hours

2.4.1. Convective Heat Losses

The large differences in the convective heat transfer to coolant are further demonstrated by Figure 2-14. From the figure, the total amount of heat transfer via convective cooling in MELCOR is higher during the entire course of the severe accident simulation. This difference is particularly noticeable in the late stages of the simulation, where MELCOR removes over ten times as much energy through convection.

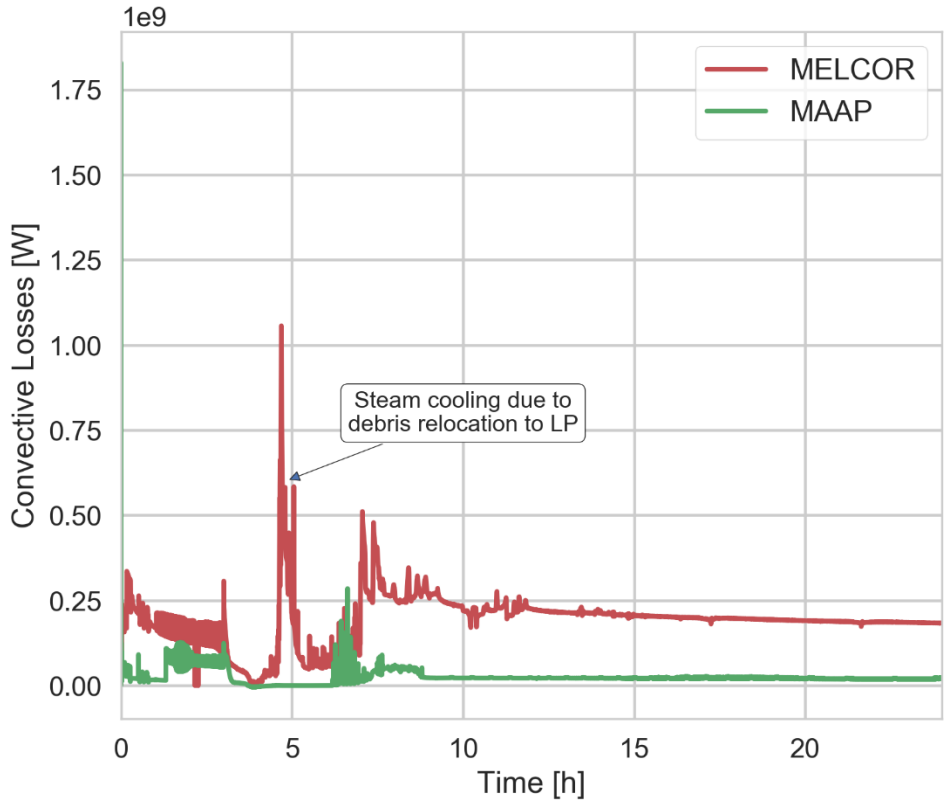

Figure 2-14. Convective heat transfer of reference case with injection delay of 1.0 hour and injection rate of 5.0 kg/s

A spike in convective heat transfer can be seen in the MELCOR simulation at the time of fuel relocation to the lower plenum. This fuel is quenched in the lower plenum and generates steam

which cools the core region. Both contribute to the increase in convective heat transfer. In both the MELCOR and MAAP simulations, heat removal through convection oscillates when core boiling occurs. This can be seen both during boil-off and reflooding.

2.4.2. Core Blockage Fraction

The core blockage fraction for both MAAP and MELCOR are presented in Figure 2-15 and Figure 2-16 respectively. Core blockage fraction is represented here as the fraction of total core volume that is solid in any given core node. It should be noted that a volume fraction of 0, indicates that no fuel exists in a region and that intact fuel has a non-zero fuel solid fraction.

It can be seen that MAAP predicts the formation of blockage that first extends radially in the bottom third of the core. As the molten pool then extends axially, it further blocks the core region, limiting the ability of steam and water to reach hot core materials. This crucible has a core blockage fraction at or near 1.0.

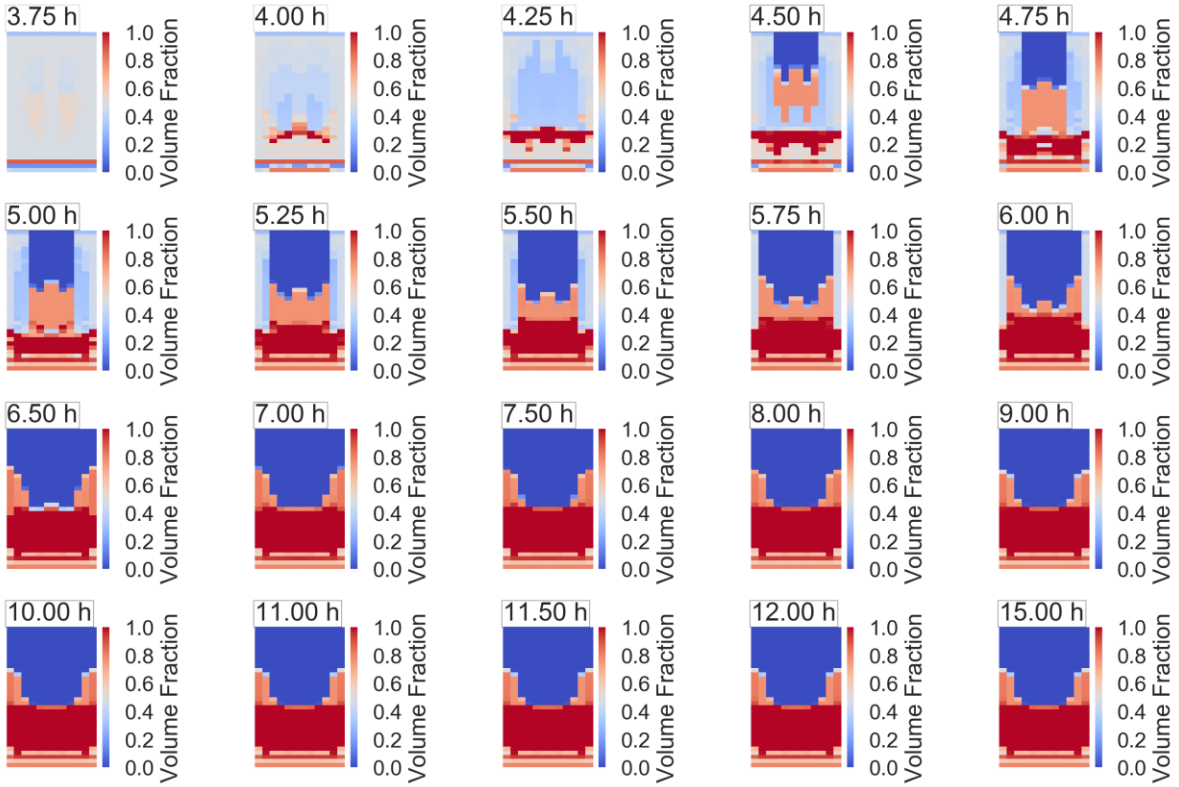

Figure 2-15. Nodalized core blockage fractions of reference case with injection delay of 1.0 hour and injection rate of 5.0 kg/s, MAAP

In the MELCOR simulation core blockage fraction increases first begin in the upper two thirds of the core due to candling and oxidation (3.75 hours); then this blockage spreads to the middle portion of the core as it heats up (4.0 hours). When fuel assemblies fail in the upper portion of rings one and two, the debris formed relocates to the core plate and creates a blockage in this area (4.5 hours). This blockage limits the ability of steam to cool this region, leading to the

failure of support structures for the innermost rings. When these rings fail, the inner portion of the core is made vacant, and it remains so until the end of the simulation.

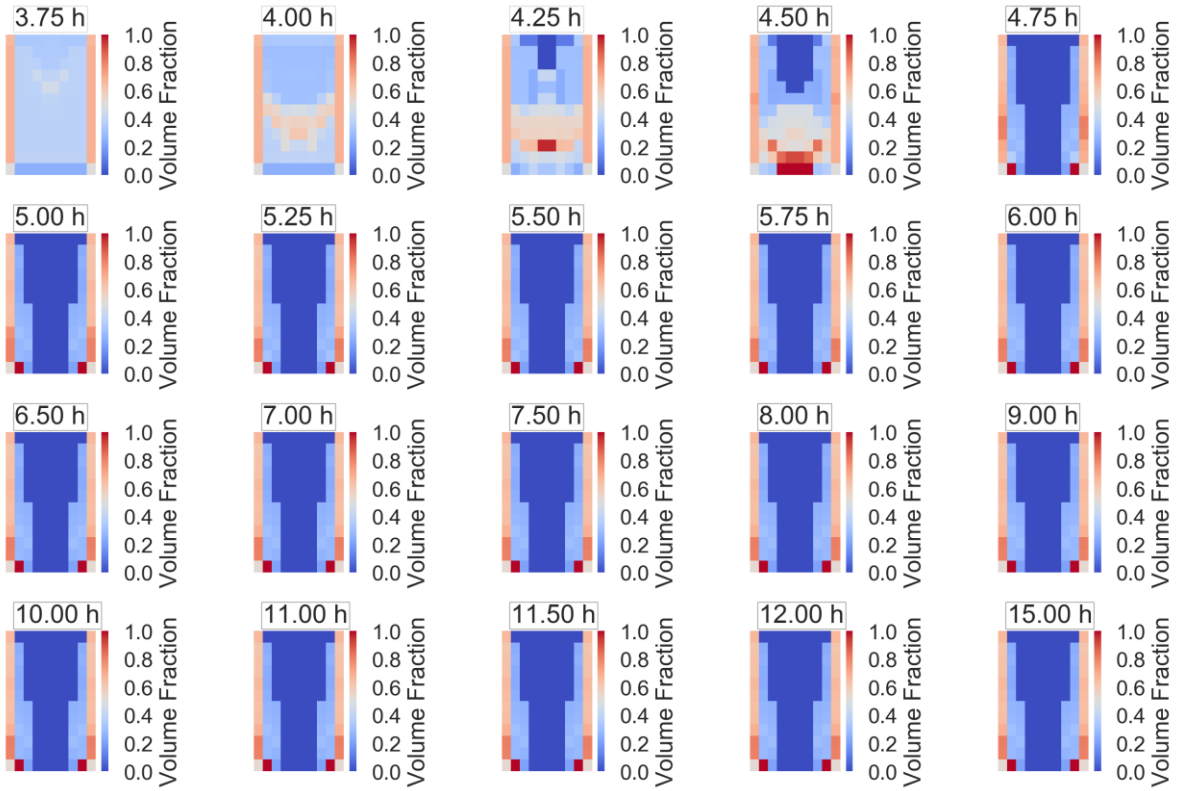

Figure 2-16. Nodalized core blockage fractions of reference case with injection delay of 1.0 hour and injection rate of 5.0 kg/s, MELCOR

3. CONSTANT INJECTION DELAY CASES

This chapter examines the six constant delay cases ran for this comparison. All of these cases have an injection delay of 1.0 hour after the onset of core damage (5.0 kg of H_2 total), meaning that injection began at 4.6 hours into the accident scenario. At 4.6 hours, differing injection rates were used spanning from no injection (Case 1) to 20 kg/s. The reference case (Case 4) is highlighted in Table 3-1, which includes all of the constant injection rate cases. For MAAP or MELCOR, the response of the system is identical until the point of injection.

Table 3-1. Case matrix for the MELCOR-MAAP Crosswalk, Phase II: constant injection delay cases

Case	Injection Rate (kg/s)	Injection Delay (hours)
1	0.0	1.0
2	1.0	1.0
3	2.5	1.0
4	5.0	1.0
5	15.0	1.0
6	20.0	1.0

3.1. Water Level

Water level for all of the constant injection delay cases is show in Figure 3-1 for both MAAP and MELCOR. For the first 4.6 hours of the accident scenario, the water level in MELCOR and MAAP track very closely. At 4.6 hours injection begins in both MELCOR and MAAP. At this point divergence between the two codes begins. For cases with reflooding, the MELCOR's water level is lower than MAAP's. This is due to the core plate in the MELCOR cases failing significantly faster than the core plate in MAAP. This leads damaged fuel material to relocate to the lower plenum. In the lower plenum, this fuel debris is quenched. As time progresses the decay heat of this debris continues to be cooled through the boiling of water in the lower plenum.

This divergent behavior can most easily be seen when the injection rate is less than 5.0 kg/s. For these cases, the injection rate in MELCOR is not high enough to makeup the boil-off caused by particulate debris in the lower plenum. Even in the highest injection cases of 15.0 kg/s and 20.0 kg/s the reflooding rate of the MELCOR cases is lower because of debris in the lower plenum.

For the case with no injection (Case 1) it can be seen that dryout occurs at 7.1 hours in MELCOR; this precedes the inevitable failure of the lower head that occurred at 9.6 hours for this case. In MAAP the failure of the lower head occurred at 10.8 hours. The root of the divergence in these unrecovered cases is not covered in-depth in the analysis, since this was the main topic explored in the first phase of this analysis. [1]

Lower head failure was also seen in Case 2 in MELCOR, which had an injection rate of 1.0 kg/s. In this case, the injection rate was not enough to remove all of the decay heat from debris that

eventually relocates to the lower plenum in both MAAP and MELCOR. In MELCOR, this lower head failure occurred at 15.4 hours while, in MAAP, it did not occur.

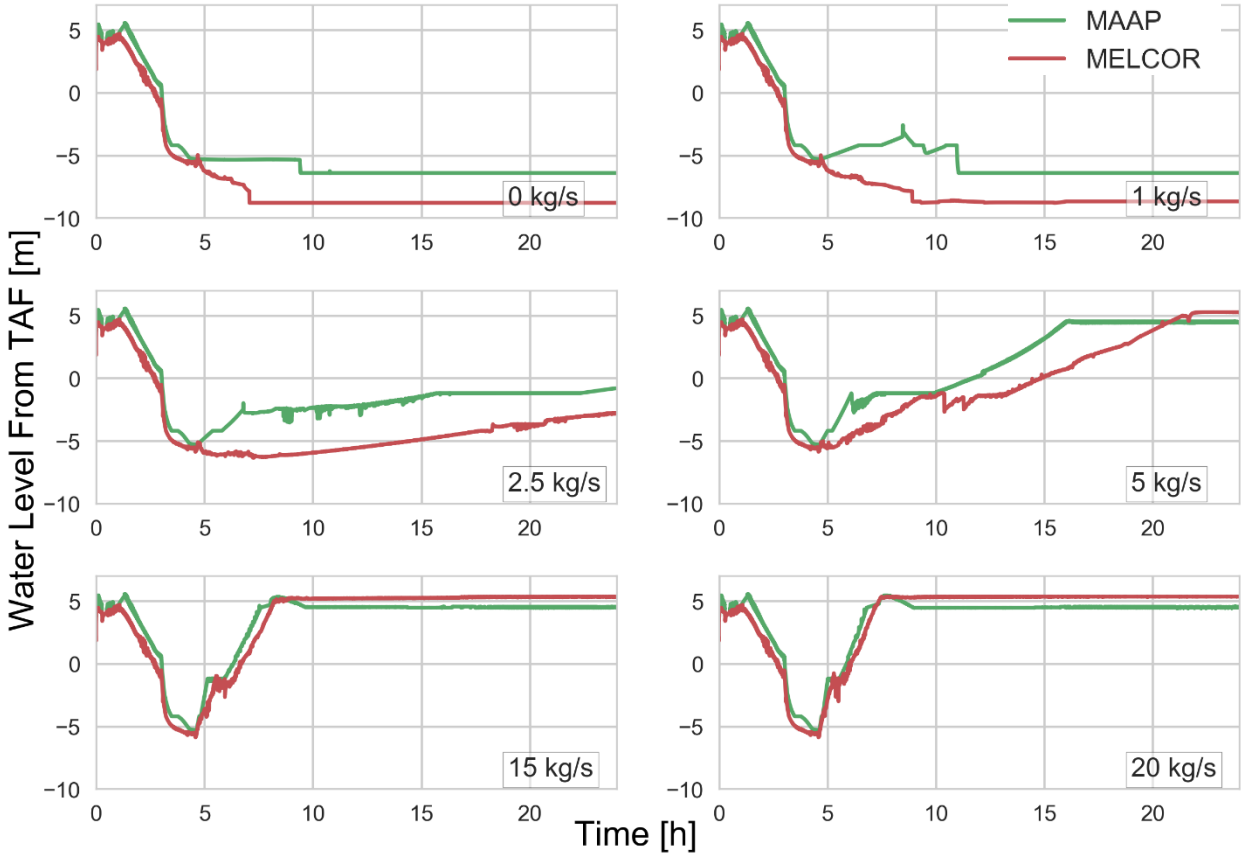

Figure 3-1. Collapsed water level for constant injection delay cases

3.2. Primary System Pressure

The pressure of the reactor pressure vessel for all constant injection delay cases shows very close agreement in both MAAP and MELCOR through the point of RPV depressurization. This can be seen in Figure 3-2. The first major divergence can be seen just after 4.5 hours into the transient when the first ring of the core relocates to the lower plenum in the MELCOR simulation. A spike in the primary system pressure can be seen in all cases to near 2.0 MPa. Subsequently there are several smaller relocations to the lower plenum in the MELCOR simulations of the no injection and 1.0 kg/s injection cases; these relocations result in minor spikes to near 1.0 MPa.

For the no injection case and the 1.0 kg/s case, there is a dramatic failure of the core plate in the MAAP simulation, relocating nearly all of the molten mass to the lower plenum. This can be seen in the nodalization diagrams found in Figures A-1 and A-2 in Appendix A. This large relocation causes a spike in the pressure to nearly 7.0 MPa. The small spikes in the MAAP simulations for non-zero injection rates is resultant from boiling that begins to occur when the water level increases to the point partial contact with melted fuel. These spikes occur progressively sooner in the simulation, with the latest in time for the lowest injection rate of 1.0 kg/s and the earliest in time with the highest injection rate of 20 kg/s (near 5.1 hours).

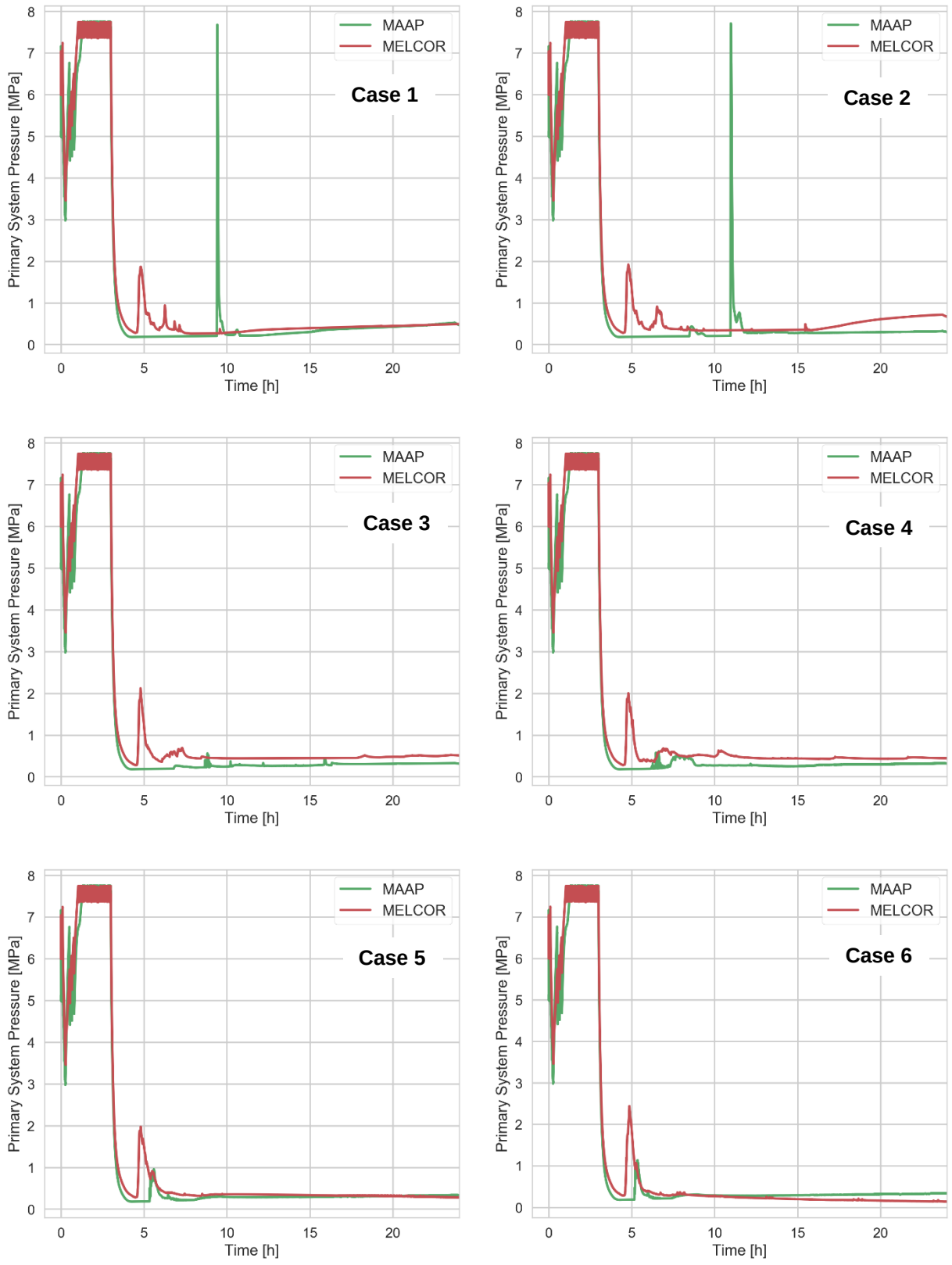

Figure 3-2. Primary system pressure for constant injection delay cases

3.3. Fuel Temperature

Clear differences can be seen comparing the fuel temperatures of each in-core nodal location for the constant injection delay cases. In general, it can be seen that the in the MELCOR cases that if the fuel remains intact then it will be quenched, assuming there is sufficient injection. This is clearly shown in Figure 3-3 and Figure 3-4, where injection rates over 2.5 kg/s show a decreasing fuel temperature trend as water enters the core region, for the MELCOR simulations. The MAAP simulations show that there is still a significant amount of high temperature, molten fuel at 24 hours into these same cases. This is due to the formation of a crust that allows minimal heat transfer out of the molten regions of the core.

All MELCOR and MAAP simulations show the failure and relocation of fuel before 5.0 hours into the transient. For the MELCOR simulations, there is minimal fuel relocation after 5.0 hours. This is due to the increased effectiveness of steam and water cooling, as well as the more favorable cooling geometry in MELCOR compared to MAAP.

In Case 5 and Case 6 (injection rates of 15 kg/s and 20 kg/s), it can be seen that a large molten pool has already developed in the MAAP simulations before injection commences. This indicates that even though there is a significant amount of injection, coolability of degraded fuel debris is less than in MELCOR. Figures A-5 and A-6 (in Appendix A) show that there is a large molten pool concentrated on top of the core plate at the end of the 24 hours for MAAP. Whereas for MELCOR, Figures B-5 and B-6 (in Appendix B) show that after 24 hours fuel remaining in the core region is near the temperature of the injected water.

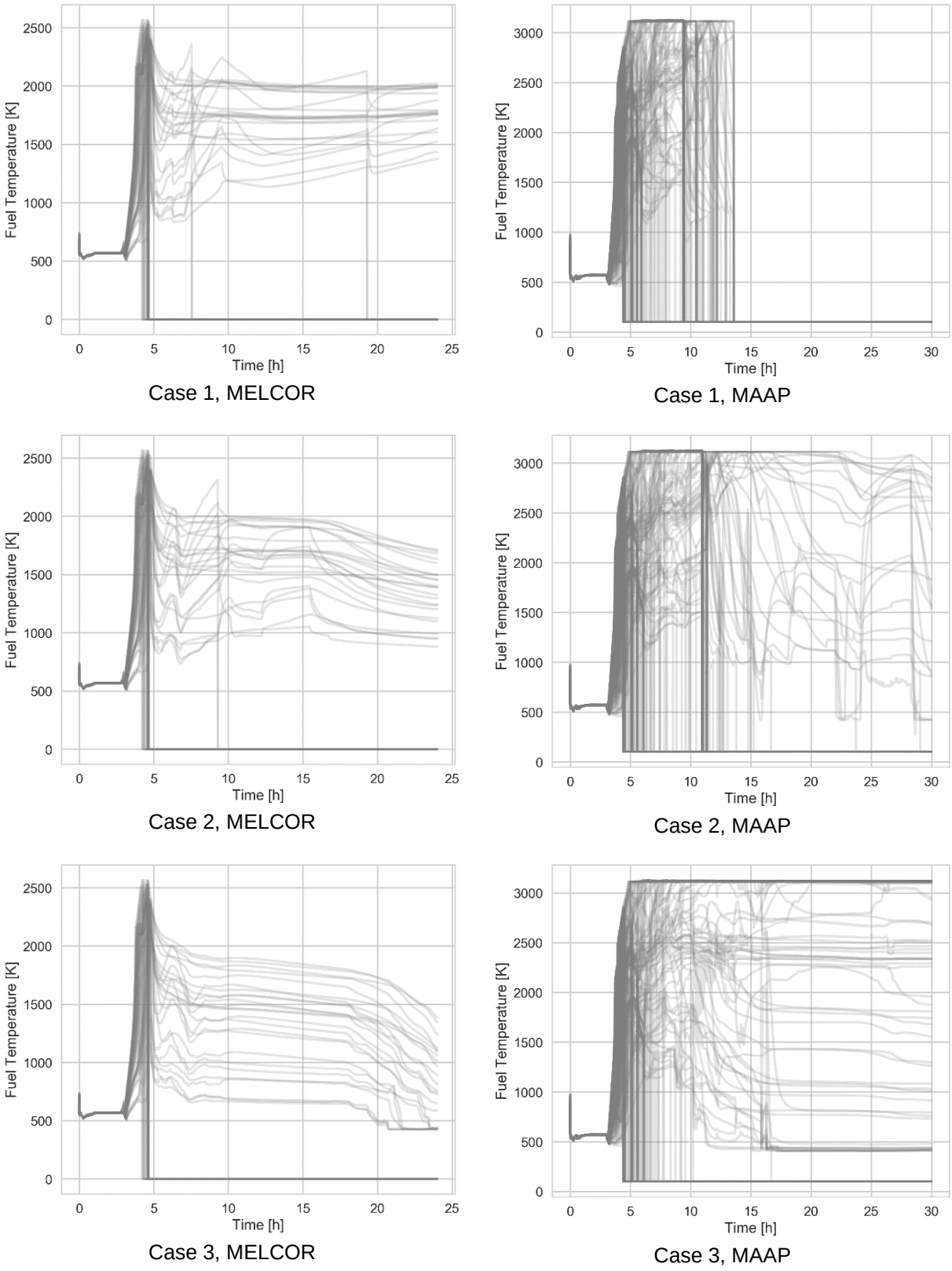

Figure 3-3. Fuel temperature for constant injection delay cases 1, 2 and 3

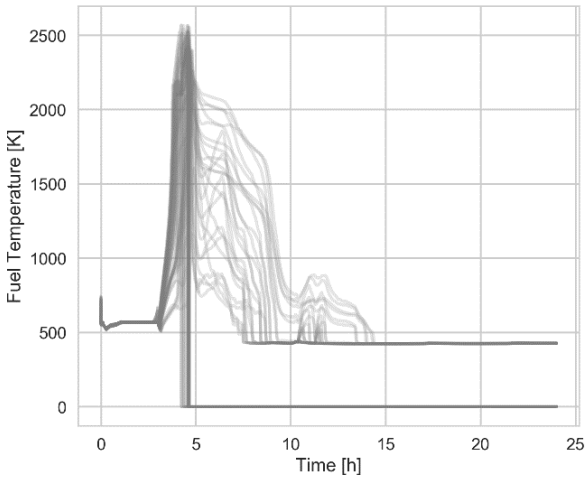

Case 4, MELCOR

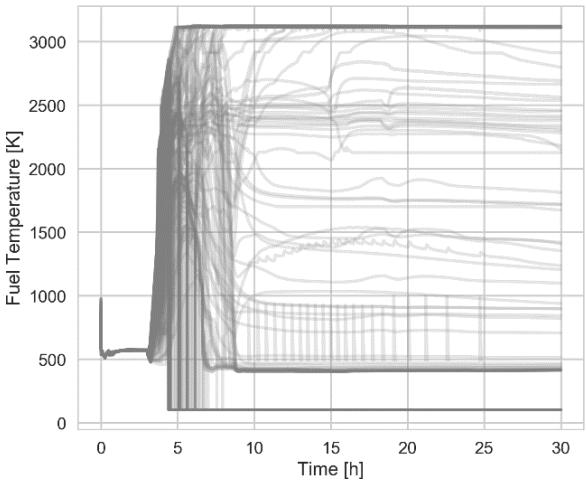

Case 4, MAAP

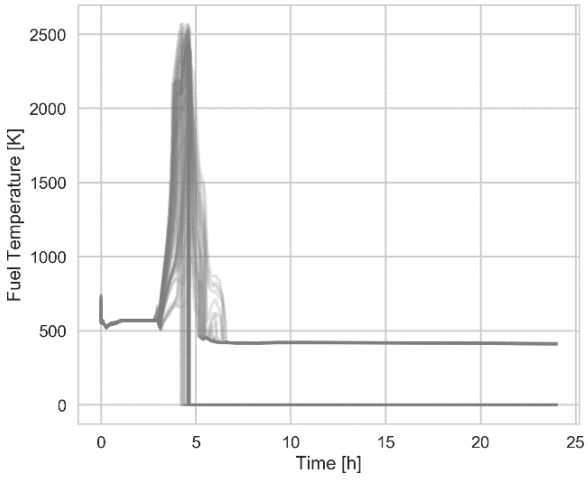

Case 5, MELCOR

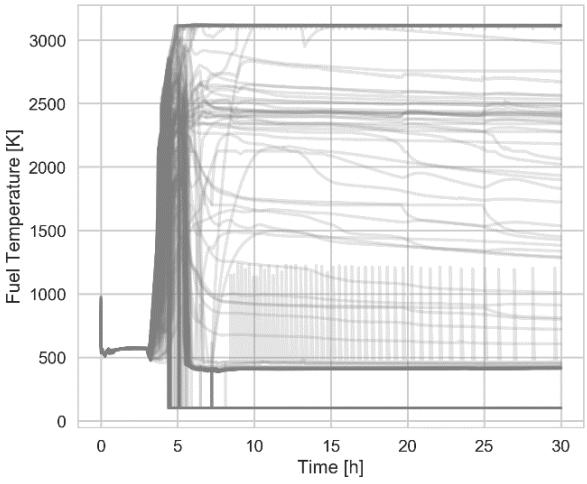

Case 5, MAAP

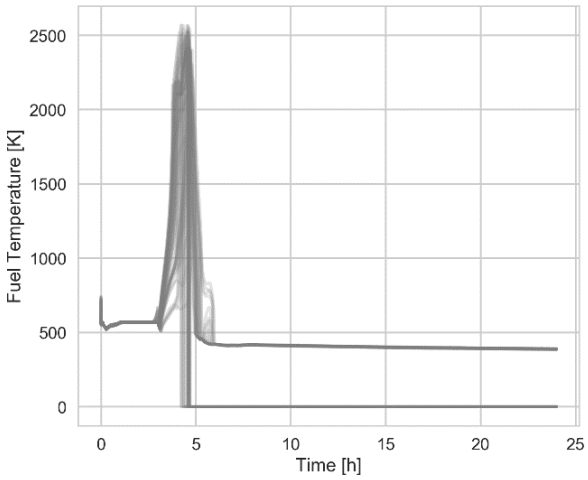

Case 6, MELCOR

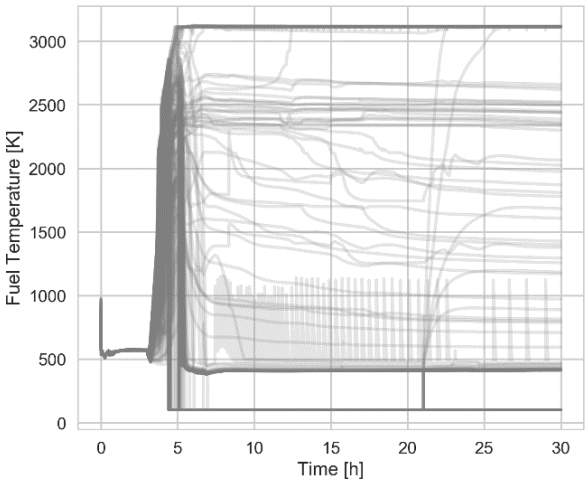

Case 6, MAAP

Figure 3-4. Fuel temperature for constant injection delay cases 4, 5 and 6

3.4. Steam Dome Temperature

Shown in Figure 3-5 is the maximum temperature achieved in the steam dome is higher in MELCOR than in MAAP. In all of the MELCOR simulations, there is a large spike in temperature to near 1050 K. This spike in temperature occurs just after the onset of core damage and continues until the water level in the RPV is recovered to the core region, allowing for cooling by water and low temperature steam.

Before the water level reaches BAF during the reflood phase, particulate debris that sits in the lower plenum generates steam, which is further heated as it passes through the core region. This heat transfer to steam in the core region is higher in MELCOR than in MAAP since MELCOR predicts a combination of an intact geometry and particulate debris, whereas MAAP predicts a crucible in the core region. This crucible has minimal open flow area, and its crust has poor heat transfer characteristics. Both contribute to steam that is less hot than MELCOR's as it exits the core region. This tendency of MELCOR to predict higher steam dome temperatures relative to MAAP when there is minimal injection is one of the contributing factors to the predictions of main steam line failures in the SOARCA and BSAF analysis. [4] [6]

In the MELCOR simulations, it can be seen that as the injection rate increases the temperature of the steam dome progressively decreases after 5.0 hours. For the zero injection analysis, Case 1, it can be seen that the steam dome temperature is well over 800 K after core degradation begins until the end of the simulation. Case 5, with 15 kg/s of injection, has a steam dome temperature below 500 K after nearly 7 hours into the simulation.

For cases with injection 5.0 kg/s or above, the steam dome temperature in MAAP after 10 hours is generally higher than that in MELCOR. At this point in the MELCOR simulations the core has been fully quenched, whereas in the MAAP simulations there is still a partially molten crucible within the core region that transfers heat to water in the RPV.

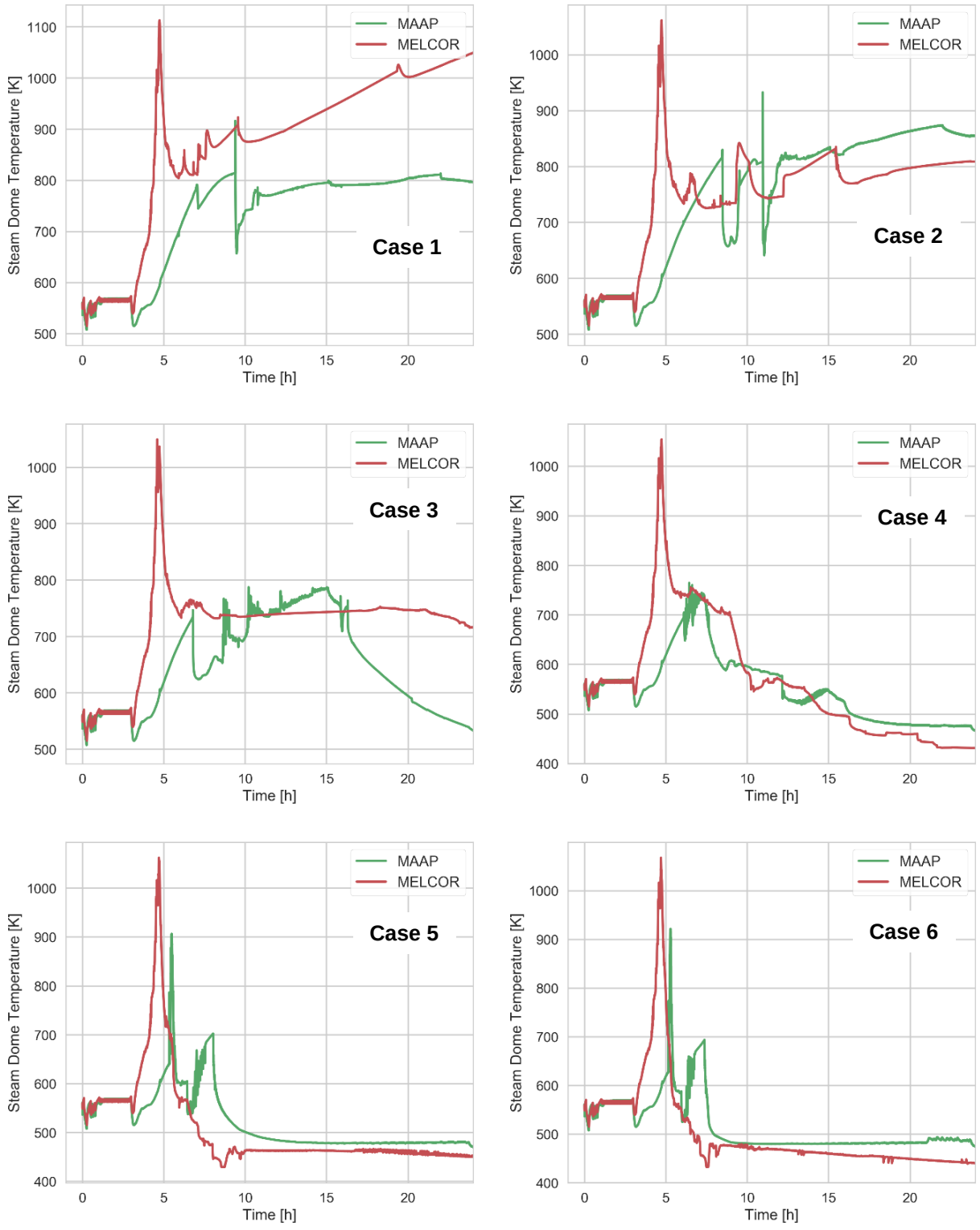

Figure 3-5. Steam dome temperature for constant injection delay cases

3.5. Containment Pressure

The containment pressure in for all of the cases show a higher pressure for MELCOR compared to MAAP. See Figure 3-6 for the drywell pressures of the constant injection delay cases; wetwell pressures are presented in Appendix E and follow drywell pressure with minimal differences. The containment pressures for MELCOR and MAAP track one another until the commencement of core damage. After this the increased hydrogen generation in MELCOR leads to an increased containment pressure relative to MAAP.

The period of run-away hydrogen generation in both MAAP and MELCOR lasts from 3.6 hours until roughly 5.0 hours in each of the cases. During this time, the difference between the MAAP and MELCOR containment pressures is established. This pressure difference then remains for the remainder of the simulation unless there is a lower head failure.

Lower head failure occurs for both codes in Case 1 and for MELCOR in Case 2. Following the lower head failure, drywell pressure increases due to gas generation from melt coolability concrete interactions (MCCI). For Case 1, which has no injection, MAAP predicts a more aggressive MCCI than MELCOR. An in-depth discussion of the differences in MCCI modeling is not included in this analysis since it is out of scope. It is likely that this will be examined in future code comparison activities.

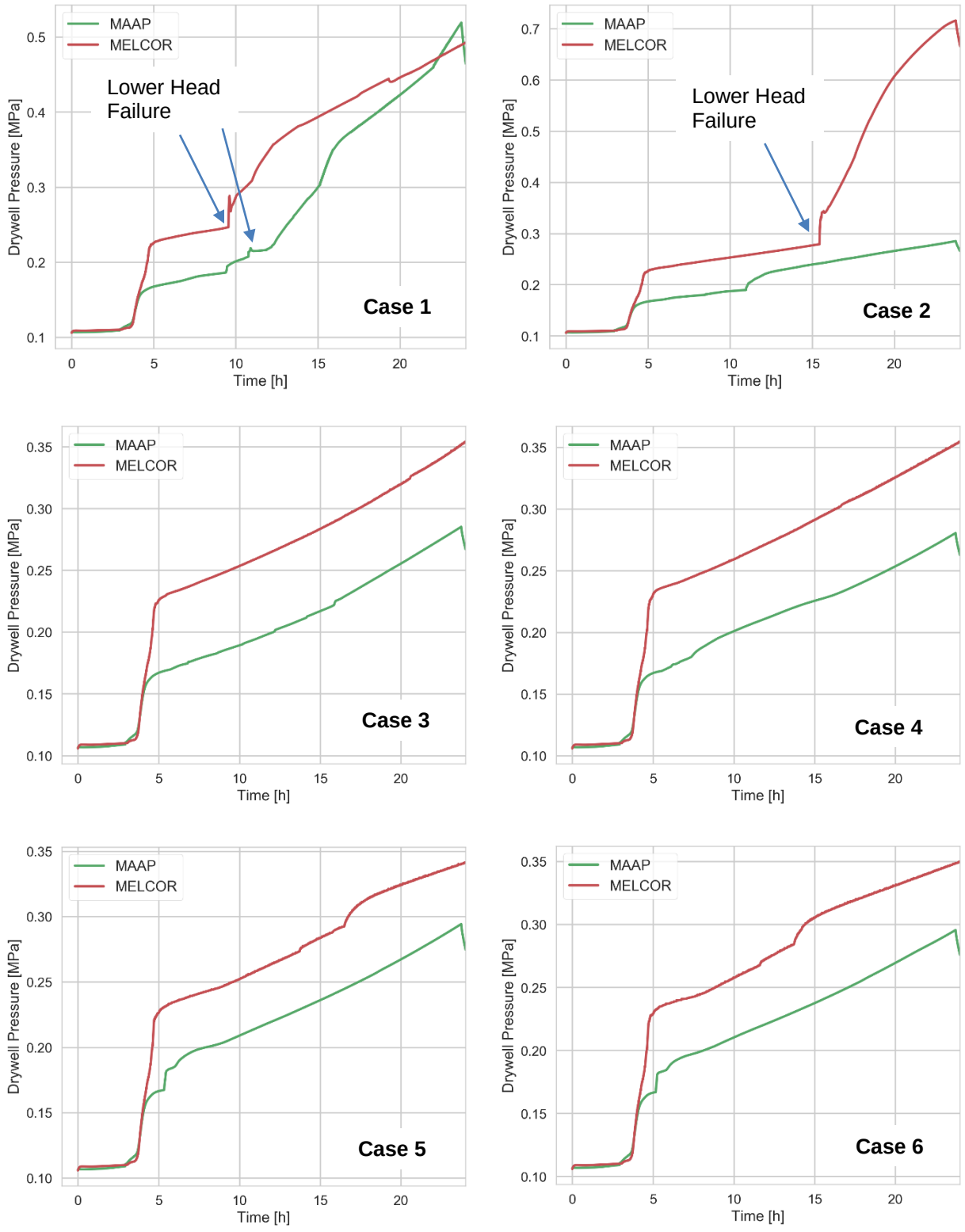

Figure 3-6. Drywell pressure for constant injection delay cases

3.6. Wetwell Temperature

The wetwell temperature for all constant injection delay cases can be seen in Figure 3-7. The MAAP cases without core plate failure are all very similar, showing a gradual increase to a temperature near 390 K at the end of 24 hours. After the core plate failure in Cases 1 and 2 of the MAAP simulations, there is a large increase in the wetwell temperature from the rapid boil-off of water in the lower plenum.

For the MELCOR cases, the wetwell temperature history increases with injection for the first three cases and decreases with the next three. For the first three cases, it takes more time to reflood the core and there is a significant amount of steam cooling. This energy imparted to the steam is then quenched in the wetwell. It can clearly be seen that the wetwell temperature tracks the steam dome temperature closely.

Long-term wetwell temperature for the high injection MELCOR cases is lower at 24 hours then the corresponding MAAP cases. In these cases MELCOR predicts the full quenching of the core and debris early into the scenario while MAAP still retains a molten crucible within the core region.

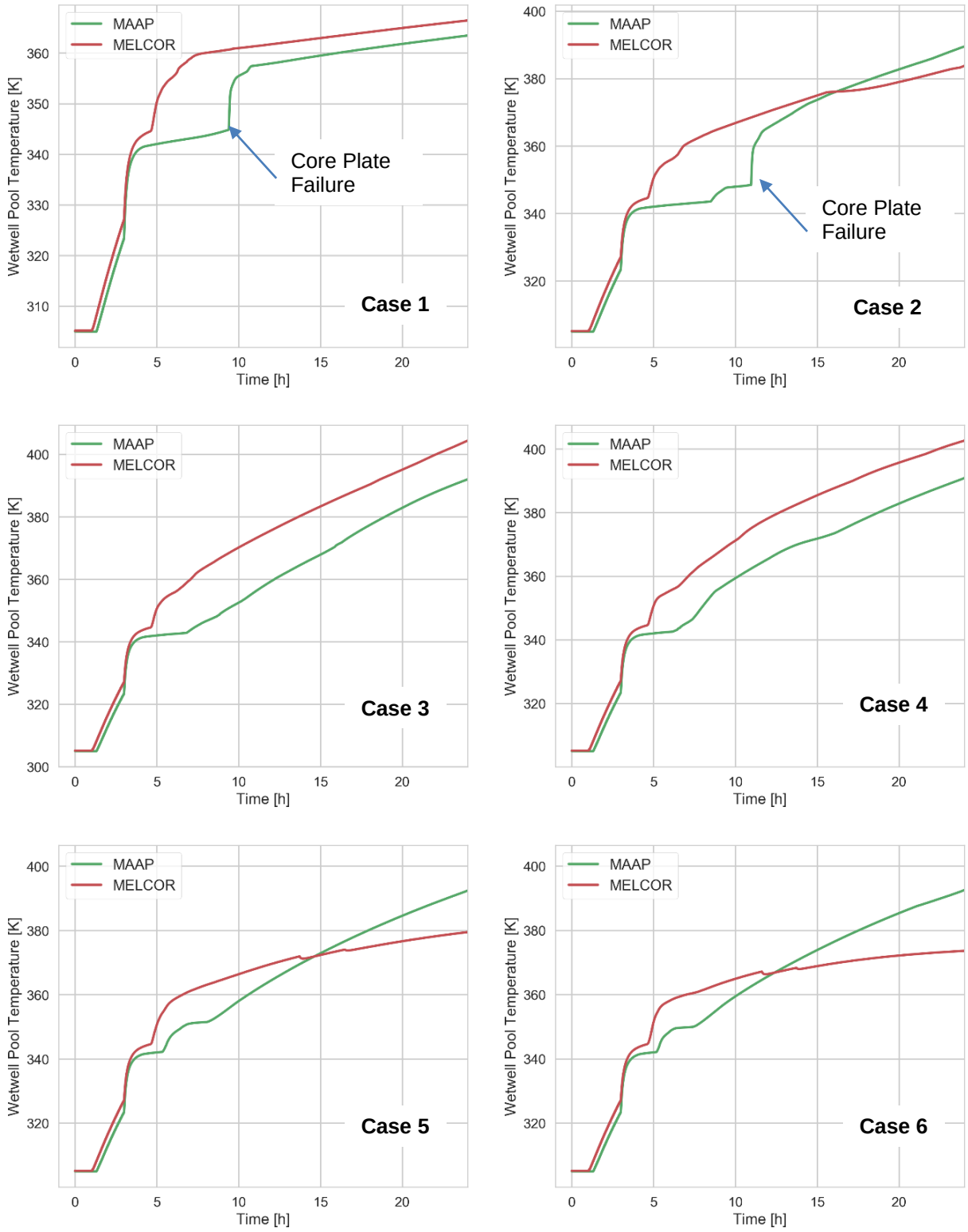

Figure 3-7. Wetwell temperature for constant injection delay cases

3.7. In-vessel Hydrogen Generation

It can be seen in Figure 3-8 that there is little difference between the constant injection delay cases in the hydrogen generation trends. For all MELCOR cases, it can be seen that there are roughly 450 kg of hydrogen generated by 5 hours into accident scenarios. From 5 hours to the end of the simulation, there is a minimal amount of additional hydrogen generated. In the MAAP simulations the total amount varied from between 200 kg and 260 kg. This difference in the total amount generated between the two codes was explored in-depth in Phase I of the crosswalk analysis. [1]

The molten crucible that is formed in all of the MAAP cases limits the flow of steam through the core and limits the amount of zirconium available for autocatalytic reactions. This leads to a lower amount of hydrogen generation. In MELCOR, there is additional steam generation compared to MAAP from debris relocating to the lower plenum and intact fuel in the outer core regions. This lead to additional generation compared to MELCOR. Additionally, when debris is present within the core region it is primarily particulate. This particulate debris allows more steam to flow through it and thus allows more zirconium available for reaction.

In the MAAP cases, it can be seen that when the water level increases to the bottom of the active core region during reflooding, there is a quick jump in hydrogen generation. When the water reached with bottom of the core, additional steam is generated which oxidizes any remaining available hydrogen. This is most apparent in Case 5 and Case 6, which reflood the RPV rapidly.

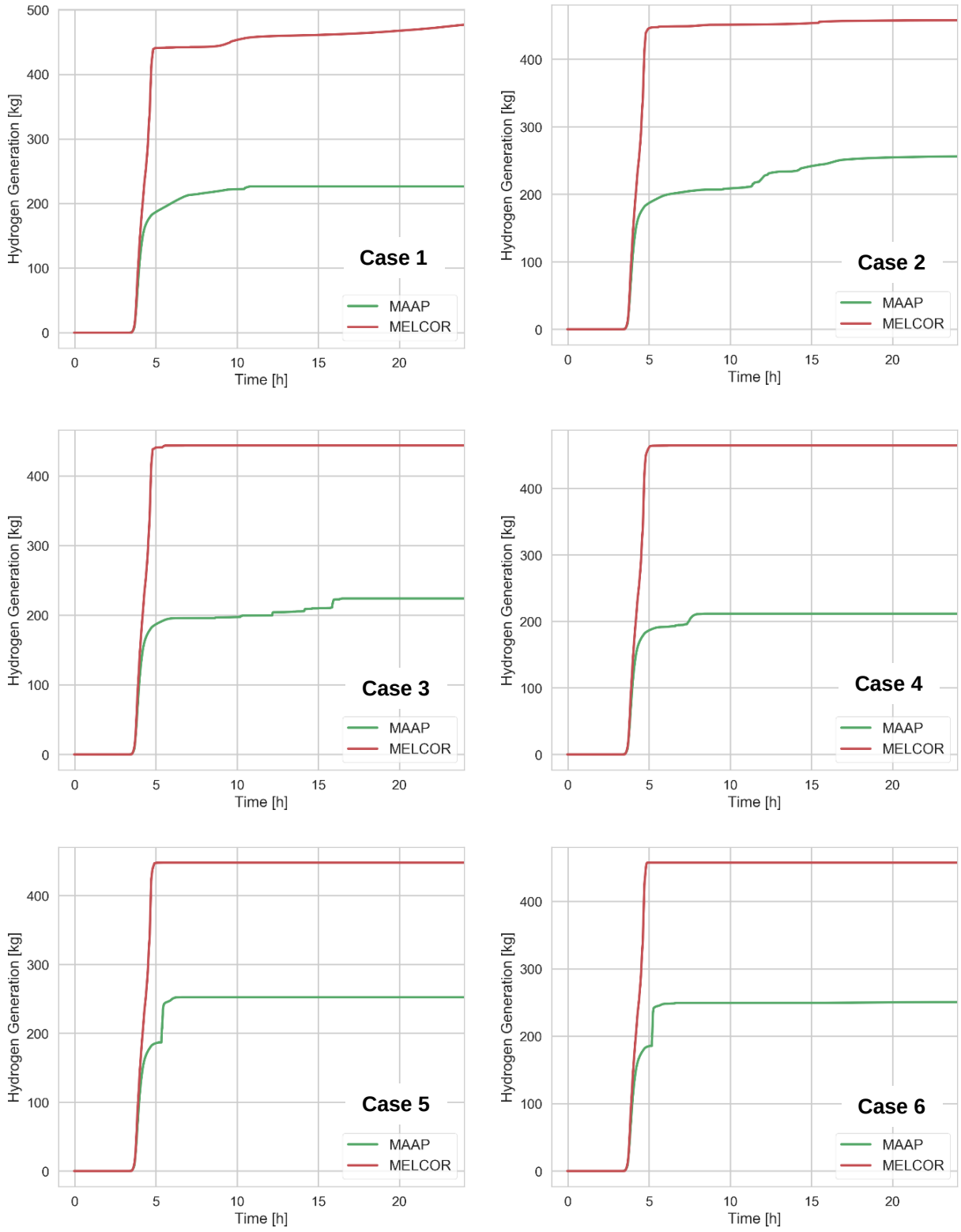

Figure 3-8. Hydrogen generation for constant injection delay cases

4. CONSTANT INJECTION RATE CASES

This chapter examines six different MELCOR and MAAP simulations with a constant injection rate of 5.0 kg/s. These cases explore different timing delays in injection into the downcomer following the onset of core damage, which is taken to be 5.0 kg of H_2 total. The delays range from zero to 5.0 hours, or 3.6 hours (Case 1) to 8.6 hours (Case 6) into the accident scenario. The reference case is presented here as Case 9. The cases are all presented in Table 4-1.

Table 4-1. Case matrix for the MELCOR-MAAP Crosswalk, Phase II: constant injection rate cases with the timings of injection commencement (relative to core damage time with net simulation time in parentheses).

Case	Injection Rate (kg/s)	Injection Delay (hours)
7	5.0	0.00 (3.6 hours)
8	5.0	0.25 (3.9 hours)
9	5.0	1.0 (4.6 hours)
10	5.0	2.0 (5.6 hours)
11	5.0	3.0 (6.6 hours)
12	5.0	5.0 (8.6 hours)

4.1. Water Level

The collapsed water levels for the constant injection rate cases can be seen in Figure 4-1. For the first 3.6 hours of the accident scenario until the onset of core damage, the MAAP and MELCOR water levels track very closely. After this point differences in the water level begin to emerge.

In MAAP, the water level remains essentially constant until injection into the downcomer begins. The water level remains constant because all of the fuel debris in the MAAP calculations remains held up within the core region in a molten crucible. There is minimal radial heat transfer to water below the core plate, and thus RPV water level does not significantly decrease.

However, for MELCOR the relocation of fuel into the lower plenum early in the transient leads to continued boil-off and a decreasing water level until the start of water injection. This is most clearly illustrated in Case 11 and Case 12, which have the longest delays before injection commences. Reflooding occurs slower in the MELCOR cases than in MAAP for the same reason.

As the reflooding progresses and reaches the core region, both MAAP and MELCOR simulations show a leveling off when the water level near 1.0 m below TAF. During this period of leveling off, a portion of the core is filled with steam generated by the transfer of heat out of hot fuel material in the core region, both intact and molten/crust. As the built-up internal energy of this fuel is removed and decay heat decreases, an increasing portion of the heat is able to be removed by liquid water. At this point it is possible for all of the decay heat to be removed through convective cooling by liquid as opposed to boiling heat transfer. For the MELCOR

simulations, the fuel node temperatures converge to the water injection temperature when cooling is all done through sensible energy and the collapsed water level increase above TAF.

Another contributing factor to the more rapid reflood to TAF in the MAAP simulations is the less effective heat transfer out of the molten crucible that is formed in all MAAP simulations. The crust of the crucible is composed of oxides, and subsequently there is less conductive heat transfer to the outer surface, compared to both the particulate debris and nominally intact geometry (candling has still occurred) found in the MELCOR simulations.

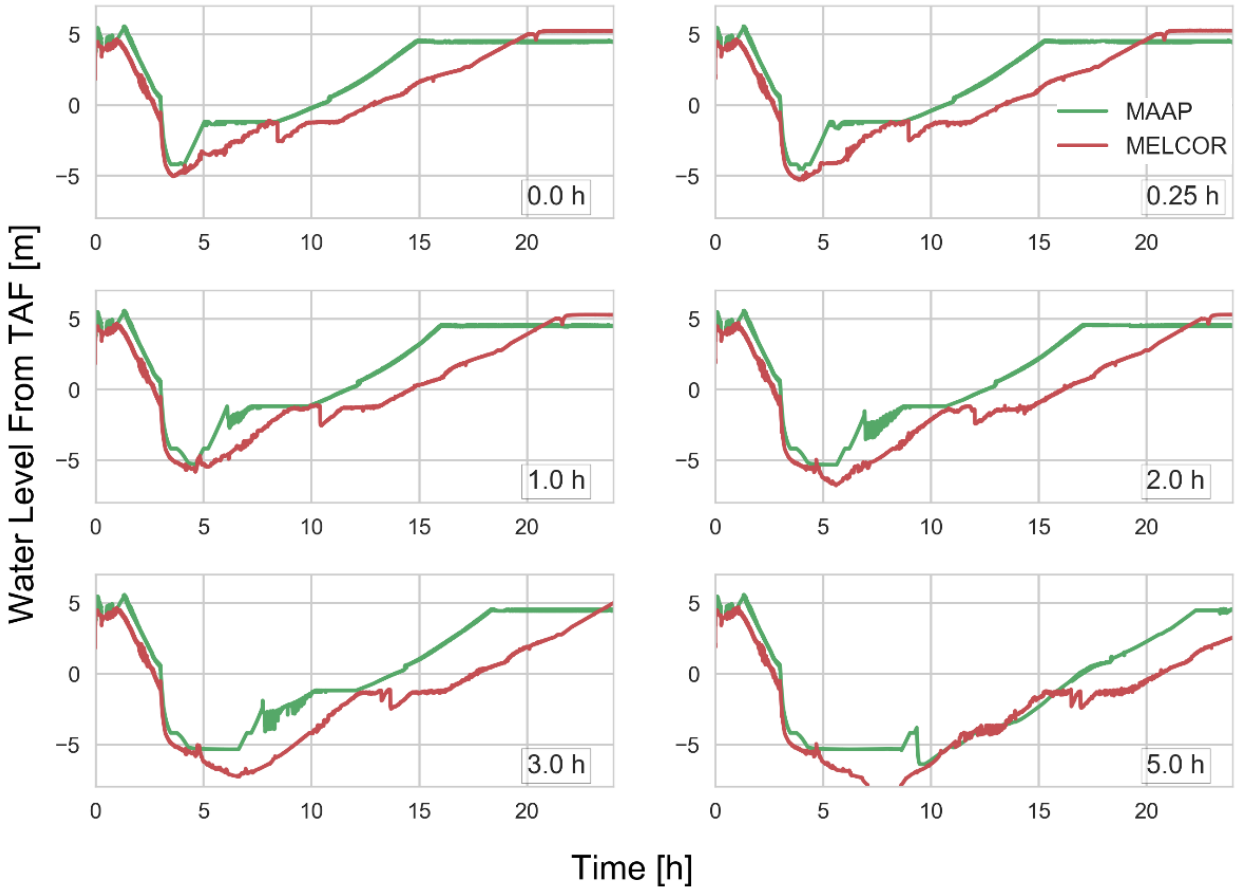

Figure 4-1. Collapsed water level for constant injection rate cases

4.2. Primary System Pressure

Similar to the constant injection delay cases, it can be seen that there is a high level of agreement between MAAP and MELCOR from the onset of the accident to the point of depressurization. This can be seen in Figure 4-2. After depressurization, the MELCOR simulations have several small spikes to near 1.0 MPa or above when failed fuel relocates to the lower plenum. For the MAAP simulations, only Case 12 (5 hours delay), sees a large relocation of fuel to the lower plenum near 9 hours. Oscillatory pressure increases can be seen in both MAAP and MELCOR simulations as the water level in the reactor pressure vessel begins to reflood the core region.

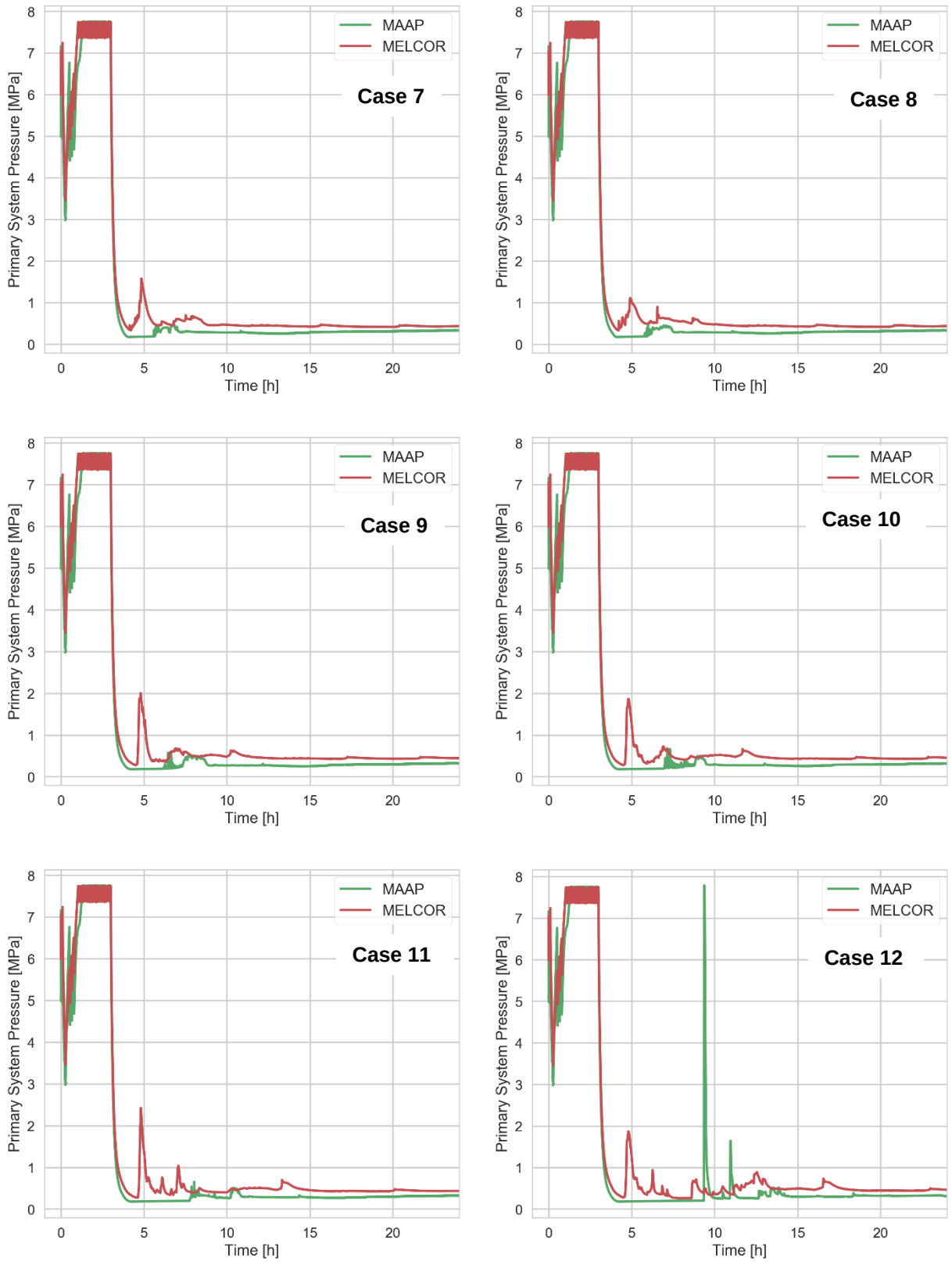

Figure 4-2. Primary system pressure for constant injection rate cases

4.3. Fuel Temperature

Fuel failures in MELCOR generally occur between 4.0 and 5.0 hours of the simulations. Remaining fuel is progressively quenched as the core refloods; this quenching lasts 10 to 15 hours after the quenching begins until the fuel temperature equalizes with the coolant injection temperature. Fuel temperatures for Cases 7 to 9 (0.25 hours to 1 hour injection delay) are shown in Figure 4-3 and Cases 10 to 12 are shown in Figure 4-4 (2 hours to 5 hours delay).

In Case 7 and Case 8, it can be seen that there are two separate spikes of fuel temperatures. The first is an initial spike centered near 4.5 hours into the simulations. This corresponds to the initial oxidation phase of the accident. The second spike is centered at 7 hours. This spike is from a decrease in the total amount of steam cooling in the upper region of the core. As the lower portions of the core become quenched by early injection, eventually there is not enough steam to cool the upper, central regions of the core. This contributes to heatup and may lead to fuel failures.

All of the six MAAP simulations exhibit the formation of a molten pool surrounded by an external, low conductivity crust. It can be seen that following the recovery of water to the height of BAF, portions of the core are quickly quenched, achieving a temperature corresponding to the injection. However, for the majority of MAAP fuel nodes, the temperature remains over 3000 K until relocation to a lower region in the core or lower plenum.

The nodalized fuel temperature figures contained within Appendix A and Appendix B (Figure A-7 to A-12 and B-7 to B-12) clear illustrate the different phenomenological assumptions in MAAP and MELCOR in the abstraction of core damage progression. In all cases, MAAP forms a crucible while MELCOR remains in a more intact geometry until fuel becomes particulate debris and relocates to the lower plenum. This is the same phenomenological difference that was indicated the first phase of the crosswalk analysis. [1]

Additionally, examining the core blockage plots for the corresponding cases in Appendix C and Appendix D in the MAAP analyses, a large blockage appears in the core region by 4.0 hours. This leads to decreased cooling, rapid melt and the formation of a molten pool with a crust.

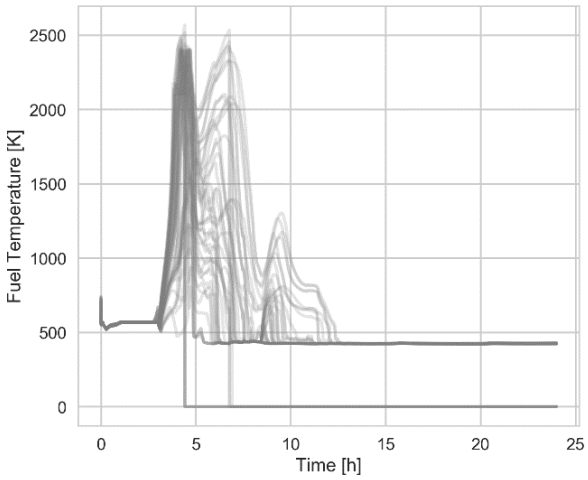

Case 7, MELCOR

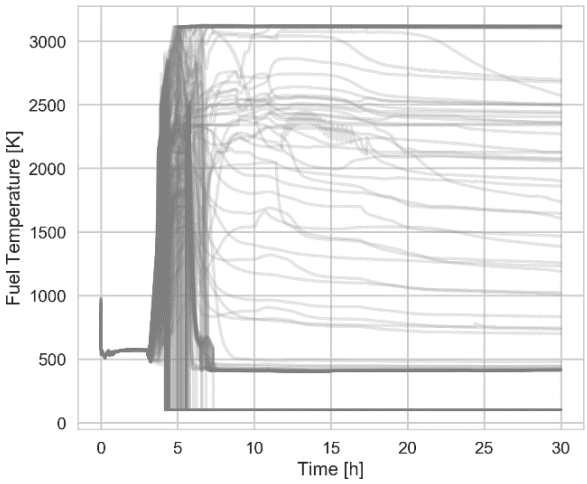

Case 7, MAAP

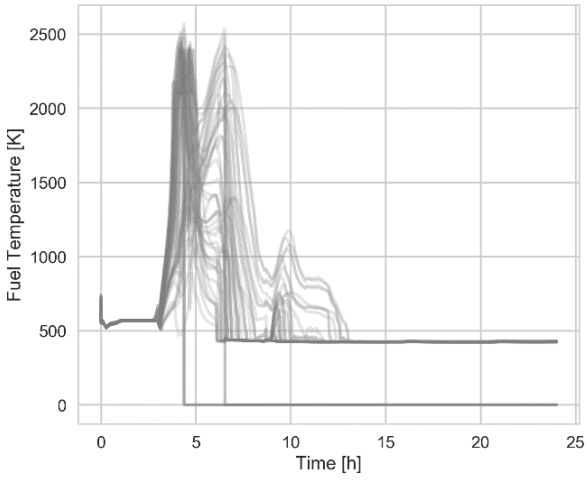

Case 8, MELCOR

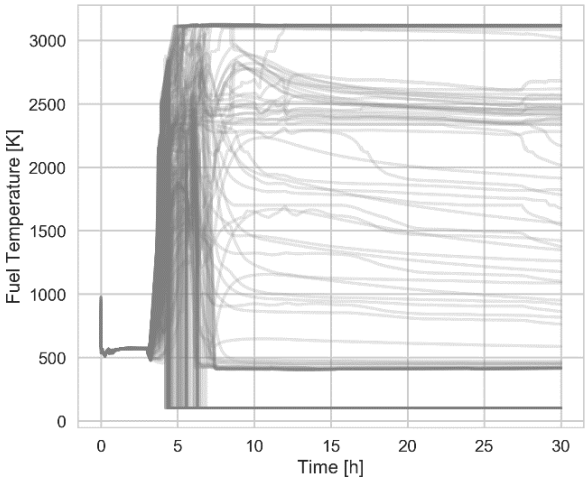

Case 8, MAAP

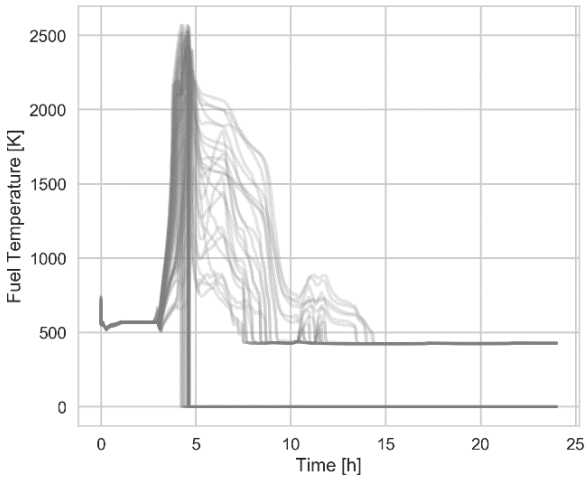

Case 9, MELCOR

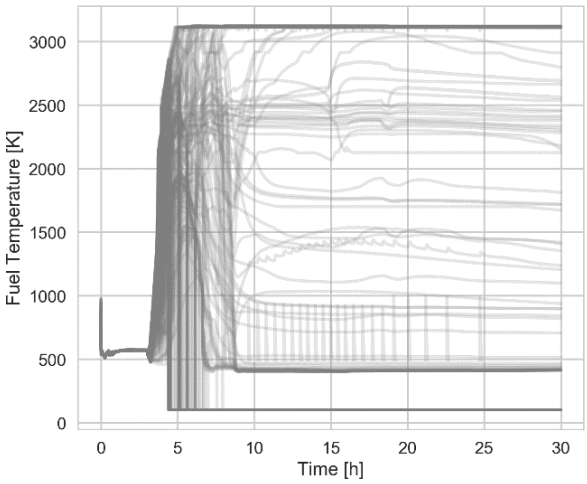

Case 9, MAAP

Figure 4-3. Fuel temperature for constant injection rate cases 7, 8 and 9

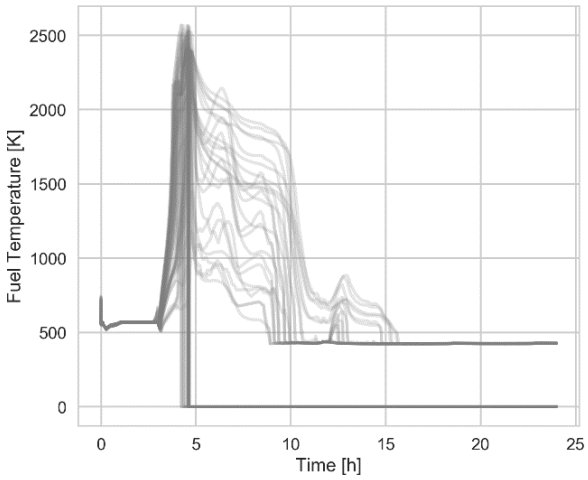

Case 10, MELCOR

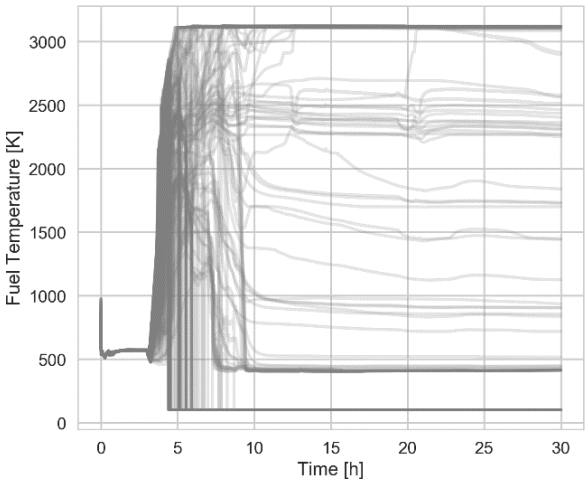

Case 10, MAAP

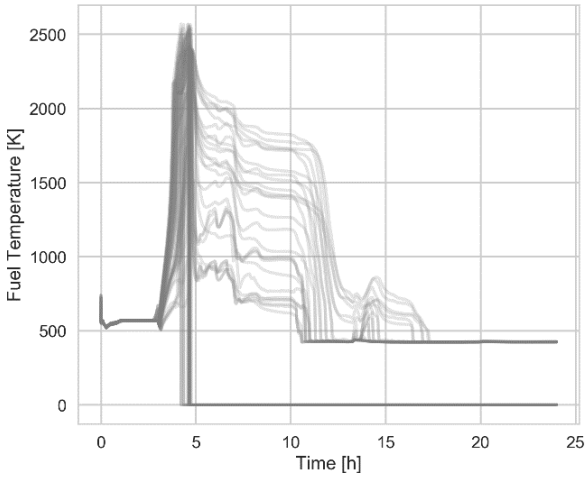

Case 11, MELCOR

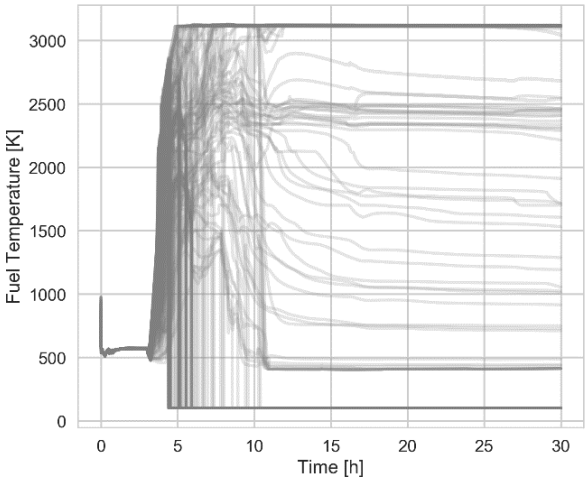

Case 11, MAAP

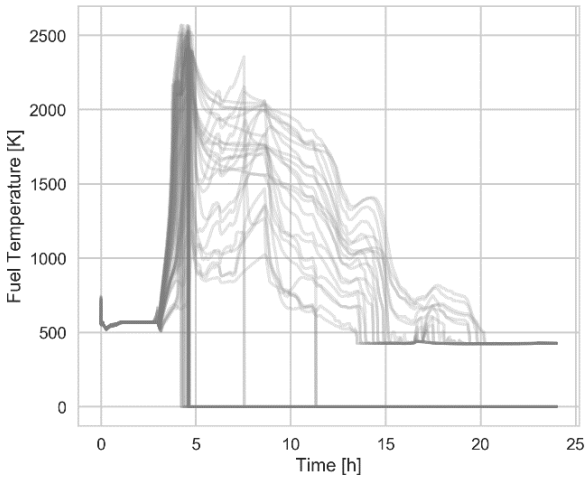

Case 12, MELCOR

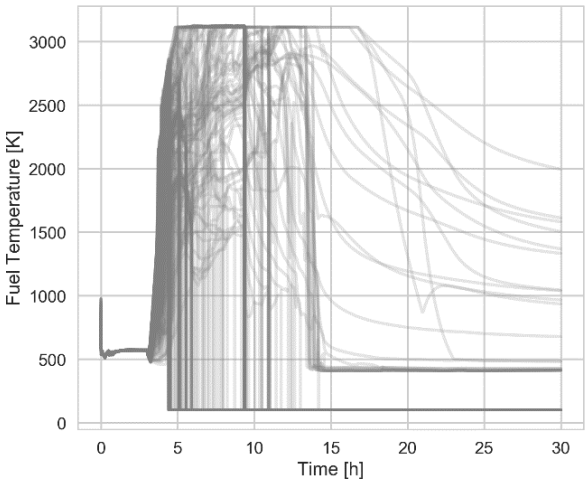

Case 12, MAAP

Figure 4-4. Fuel temperature for constant injection rate cases 10, 11 and 12

4.4. Steam Dome Temperature

The steam dome temperatures of both MAAP and MELCOR, shown in Figure 4-5, follow one another for the first 3.6 hours of the simulations until the onset of core damage at 3.6 hours. After this there is a sharp divergence. The MELCOR steam dome temperature increases rapidly while the MAAP steam dome temperature briefly drops in temperature and then gradually increases until the point of reflooding to BAF, at which point the quenching eventually leads to a decrease in steam dome temperature.

The large initial spike in the MELCOR simulation can mainly be attributed to two factors: steam generation in the lower plenum and differing oxidation behavior. There is a change in the rate of steam dome temperature increase when a significant amount of fuel debris begins to relocate to the lower plenum in MELCOR, between 4.0 and 4.25 hours in all simulations. Steam generated in the lower plenum that increases in temperature as it passes through the core, which fuels more oxidation.

During the initial oxidation phase, before core relocation, differing oxidation rates contribute to a higher steam dome temperature in MELCOR compared to MAAP. MELCOR generates nearly twice as much in-vessel hydrogen by 5 hours into the simulation for each case. This additional autocatalytic hydrogen formation reactions release more heat to the system. This can be attributed to differing oxidation models and differences in how core degradation is represented within the program. Core blockages in MAAP already begin to form by only 4.0 hours into the accident scenarios. In MELCOR, the blockages begin to appear at 4.25 hours.

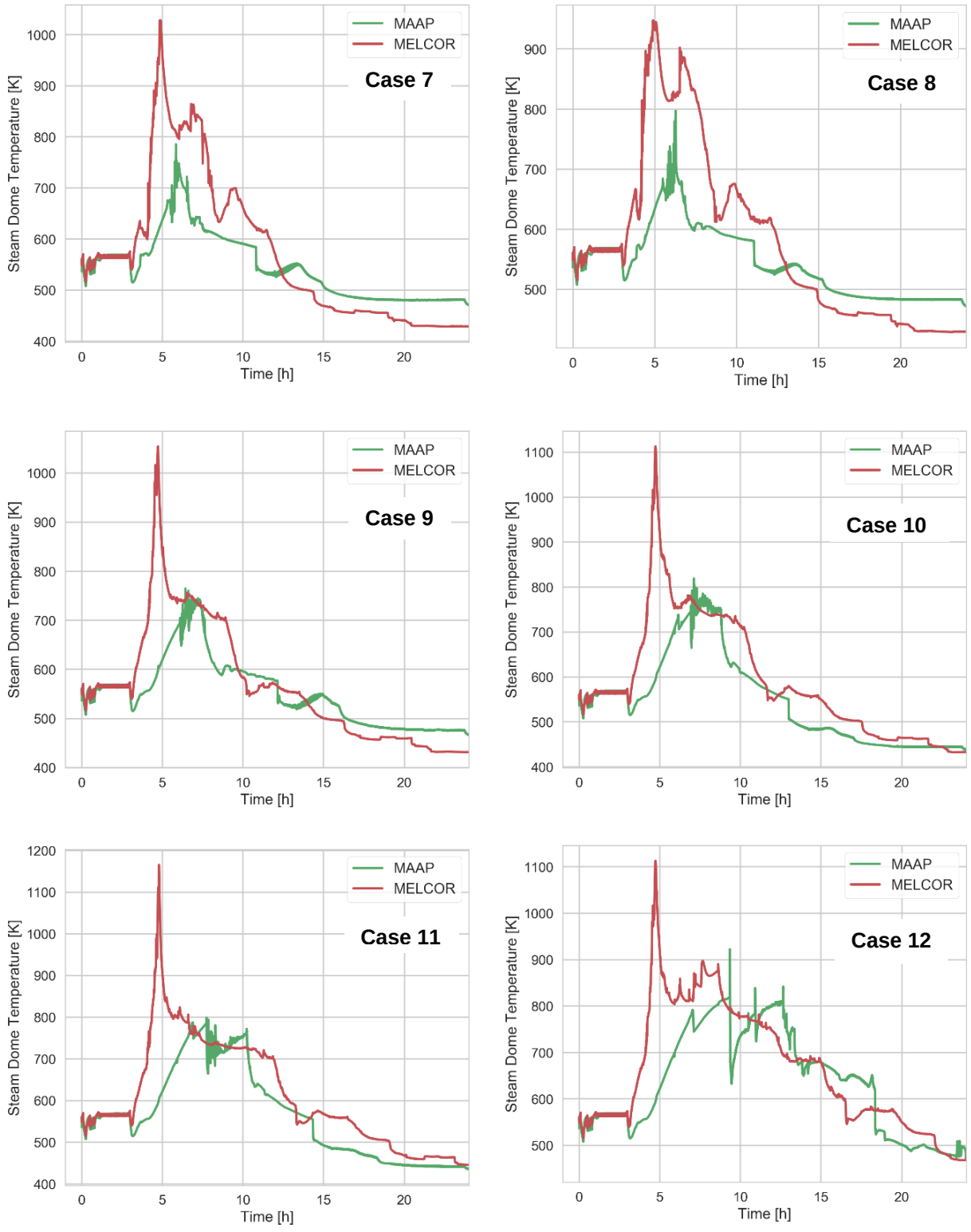

Figure 4-5. Steam dome temperature for constant injection rate cases

4.5. Containment Pressure

MELCOR consistently predicts a higher containment pressure relative to MAAP for all partially recovered severe accident cases presented in this analysis; this trend can clearly be seen in Figure 4-6, which shows MELCOR's drywell pressure diverging from that of MAAP after the onset of core damage.

The difference in containment pressure is directly related to the relative amount of hydrogen generated in-vessel, with MELCOR generally generating approximately twice as much as MAAP. Additionally, the early phase of hydrogen generation is the point when the containment pressure differences between MAAP and MELCOR are established (see Figure 4-8).

The closer agreement in Case 7 and Case 8 containment pressure is due to increased hydrogen generation in MAAP early in the accident scenario. This increased hydrogen generation is due to the minimal injection delay in these cases. The jump immediately after 5.0 hours is due to the reflood water height reaching BAF and subsequent steam generation.

The late-in-time jump of the containment pressure in the MAAP Case 12 simulation is due to a failure of the core plate. When this happens, there is a large spike in the RPV pressure followed by the transmission of a significant amount of steam to the wetwell. This increases the pressure and temperature of the wetwell.

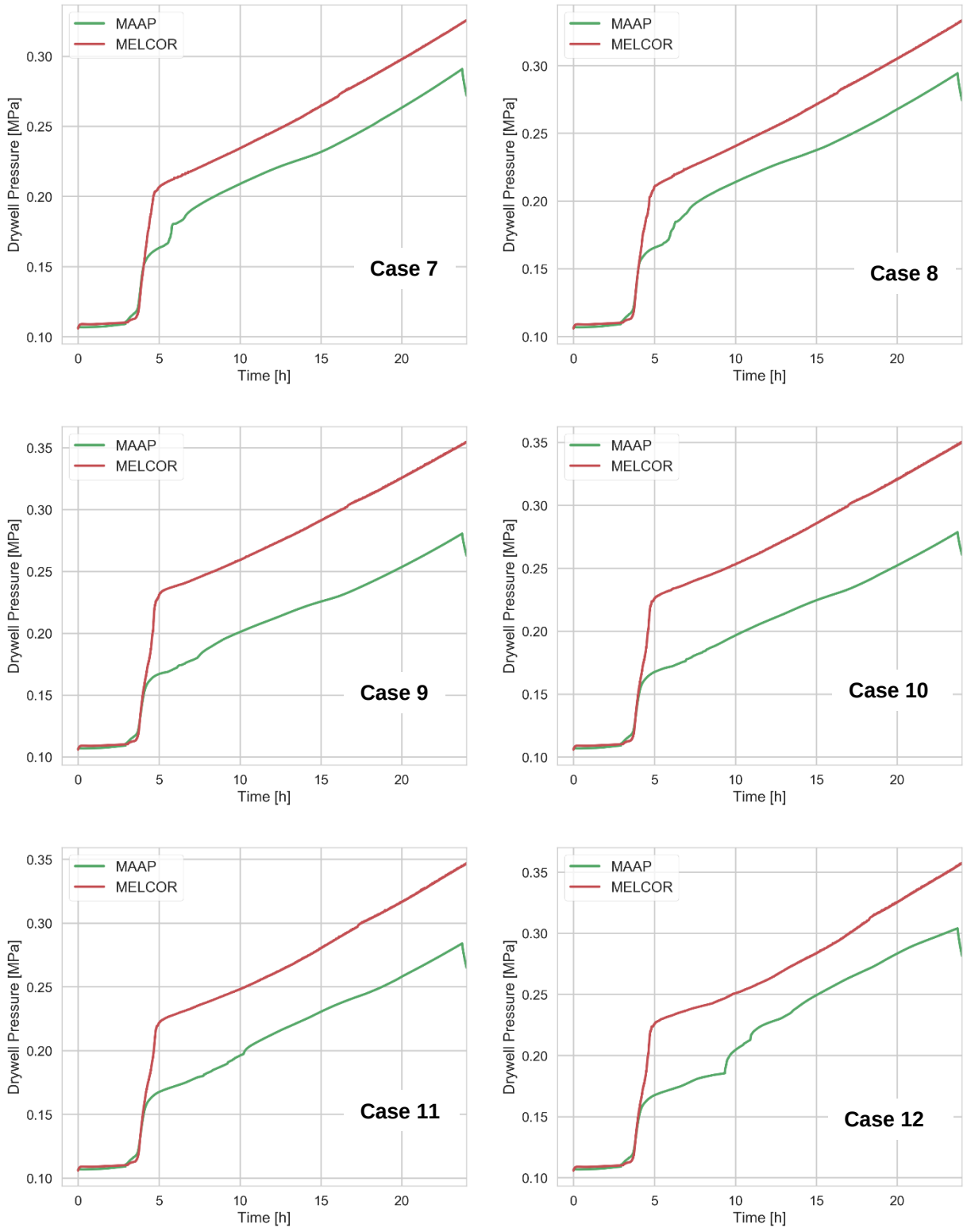

Figure 4-6. Drywell pressure for constant injection rate

4.6. Wetwell Temperature

The increased steam generation rate in the lower plenum and the core region in MELCOR realizations leads to a higher steam dome temperature. This higher energy steam eventually increases the temperature of the wetwell relative to MAAP. This phenomena can be seen in Figure 4-7, which show the wetwell temperatures of the constant injection rate cases.

In the MAAP cases, after the initial boil-off transient there is a flattening of the rate of increase of wetwell temperature. This flattening can be attributed to a decreased steam generation in MAAP. At this point no portion of the core or degraded fuel debris is in contact with water. This leads to minimal H_2 generation and therefore little increase in wetwell pressure. After reflooding of the RPV begins and steam in once again generated when the water level reached BAF, the wetwell temperature begins to increase once again.

The large spike in the MAAP realization of Case 12 is due to the failure of the core plate and ensuing relocation of fuel debris to the lower plenum. When this debris reaches the lower plenum it is quenched, caused a spike in steam generation and a jump in the temperature of the wetwell as this steam is discharged.

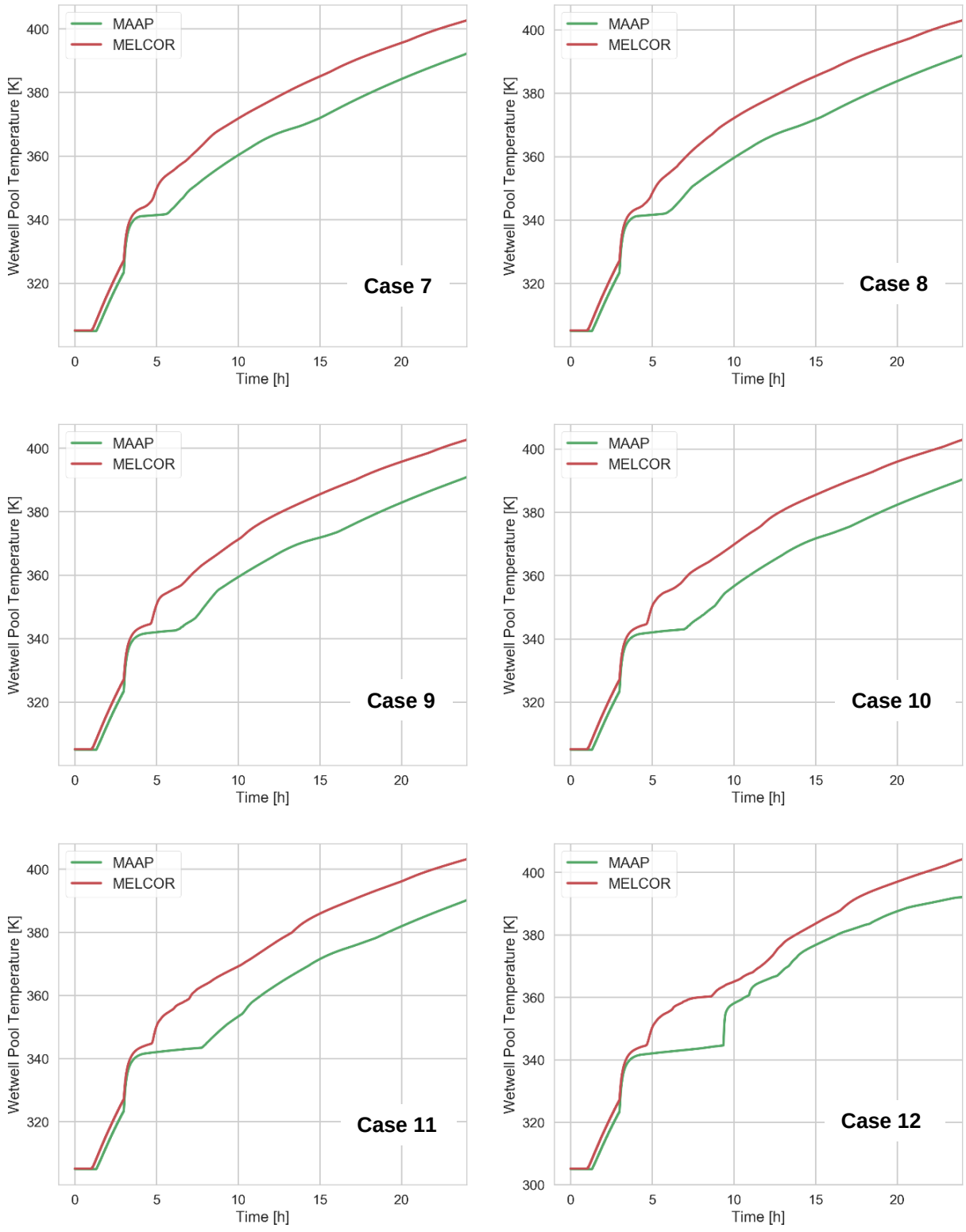

Figure 4-7. Wetwell temperature for constant injection rate cases

4.7. In-vessel Hydrogen Generation

The total in-vessel hydrogen generation mass for this injection timing study can be seen in Figure 4-8. In all cases examined, MELCOR produced significantly more hydrogen than MAAP (~400 kg compared to ~220 kg). A discussion as to why MELCOR generates more hydrogen is provided in Section 3.7 and Section 2.2.4, and is not discussed here.

Cases 9 to 12 (injection delays of 1.0 hour or more) MELCOR realizations generated over twice as much total hydrogen as the MAAP realizations. However, this difference is smaller when injection occurs earlier in the accident transient, such as in Case 7 and Case 8. In those cases, MELCOR roughly generates 10 to 15% less hydrogen while MAAP generates roughly 10 to 15% more.

The reduced generation in these two MELCOR cases, Case 7 and Case 8, is likely due to the rapid reflood of the core region and the prevention of several early stage fuel assembly collapses, relative to cases with no injection for an hour or more. The increased generation in MAAP in the early injection cases is from early injection and subsequent boil-off when the reflood height reaches BAF. This leads to increased steam availability early in the accident transient before the core forms a complete blockage of flow. Additionally more materials are available for oxidation, as they have not fully been incorporated into a molten crucible yet.

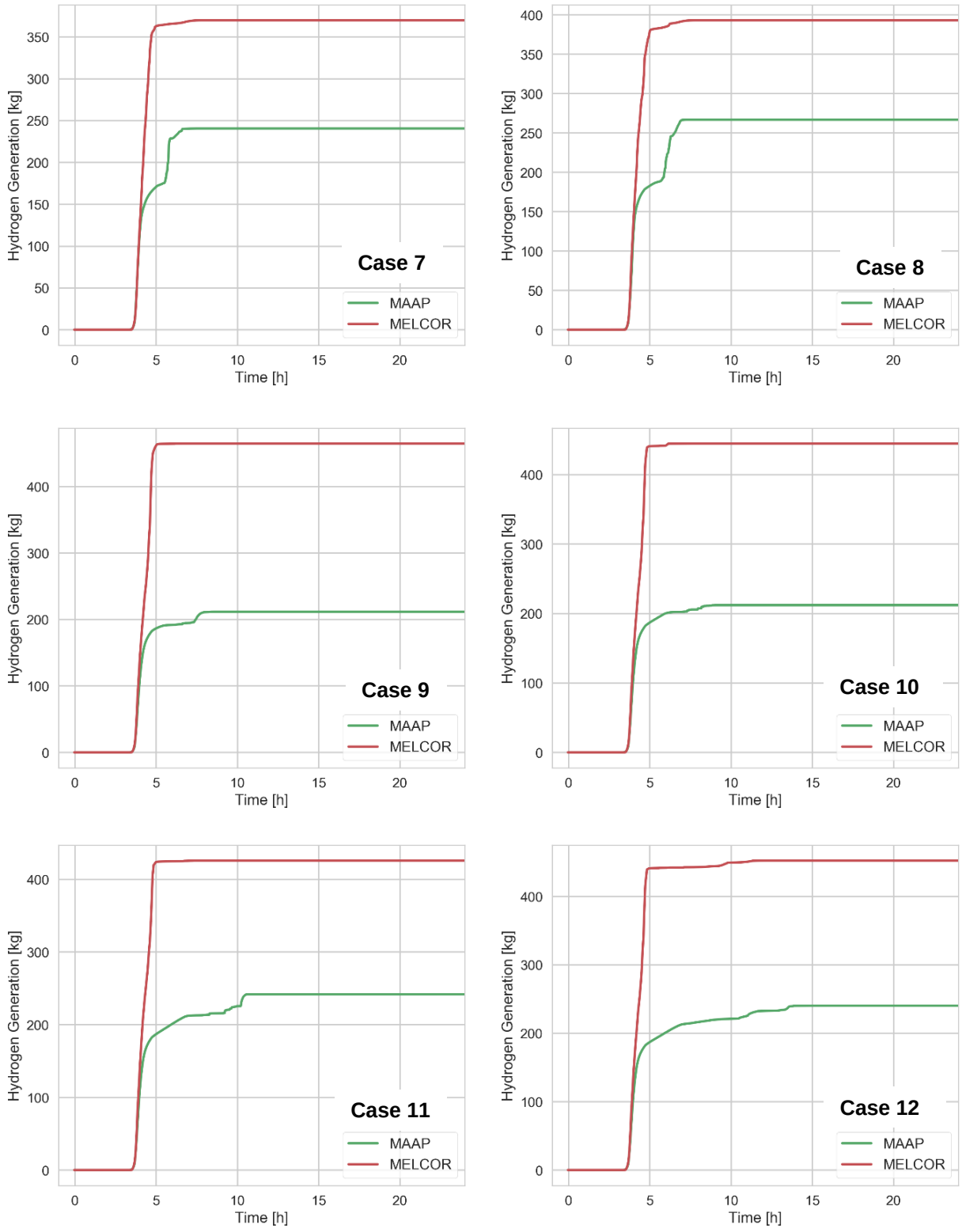

Figure 4-8. Hydrogen generation for constant injection rate cases

5. COMPARISON OF MELCOR ANALYSIS TO STATE-OF-THE-ART REACTOR CONSEQUENCE ANALYSIS ASSUMPTIONS

Since the first phase of the MAAP-MELCOR Crosswalk activity, there have been changes in the default, recommended assumptions that are used in MELCOR inputs. The main difference, impacting core damage progression is a change in the recommended melting point for UO_2, fuel material, and ZrO_2, oxidized clad. These materials form a eutectic, which depresses the melting temperature. This analysis used the 2800 K melting temperature for both UO_2 and ZrO_2 to remain consistent with the first phase of the crosswalk. However, in the most recent SOARCA analyses this melting point has been changed to 2500 K. This chapter presents an analysis compares the reference case, which used a melting temperature of 2800K, to one using 2500K and examining the impact on the main accident signatures. [6]

5.1. Core Degradation Transient

A comparison of the core degradation transients of the two different melting temperatures can be seen in Figure 5-1. The degradation is similar until 4.0 hours, after which core damage begins.

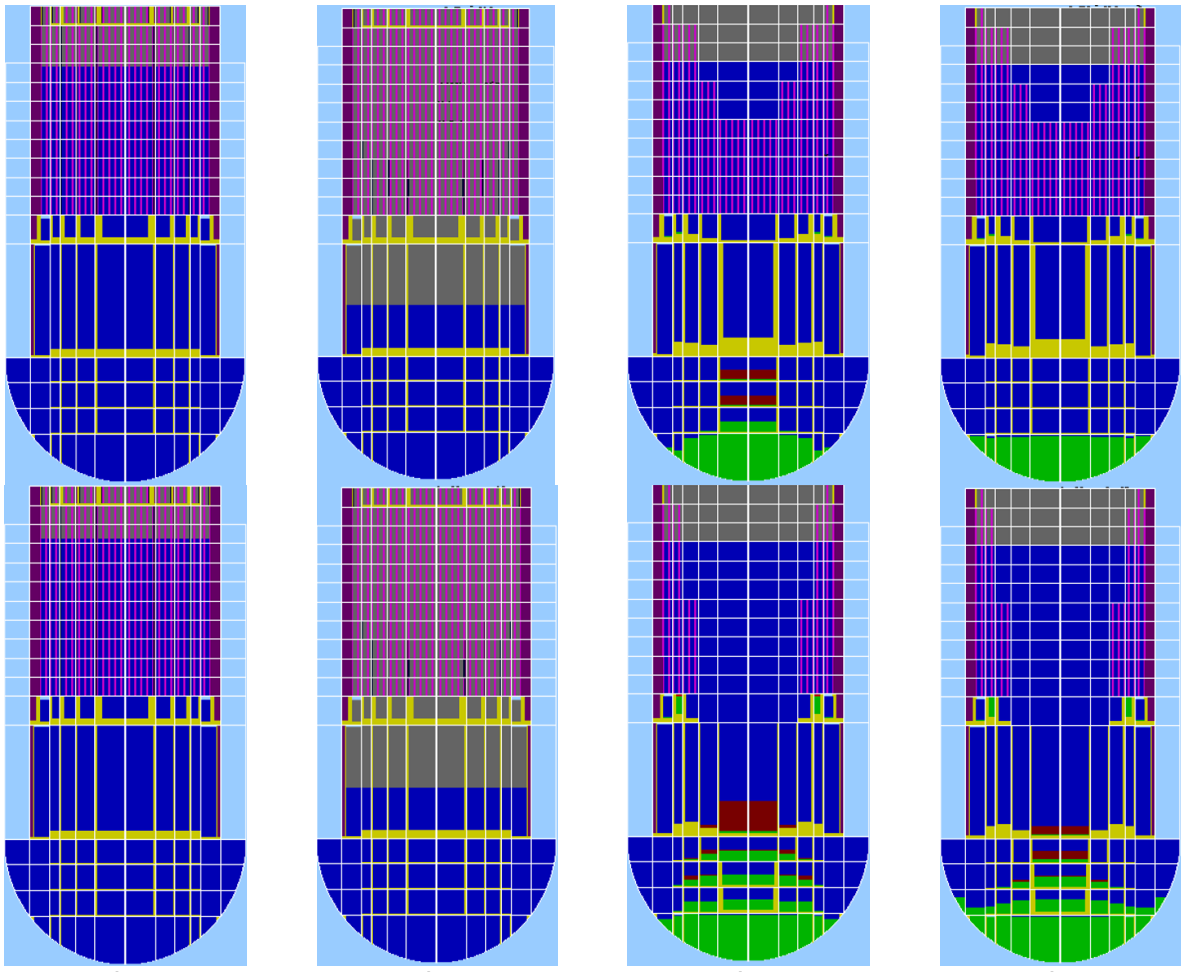

Figure 5-1. Core degradation transient, for 2500 K melting temperature (top) and 2800 K melting temperature (bottom)

The lower melting temperature case does not see the complete failure rings one and two. This is because the lower melting temperature allows the fuel to relocate sooner. This faster relocation prevents the heatup and failure of fuel and support structures associated with the innermost rings. The 2800 K simulation sees a further increase in the temperature in the lower third of the interior core region prior to the failure of associated the rings. This can be seen in the 4.5 hours snapshot in Figure 2-2.

5.2. Water Level

The water level for the melting temperature comparison is shown in Figure 5-2. The water level for the two different realizations is nearly identical over the whole course of the simulation. Differences are likely attributable to the differing amount of relocation behavior in the innermost rings.

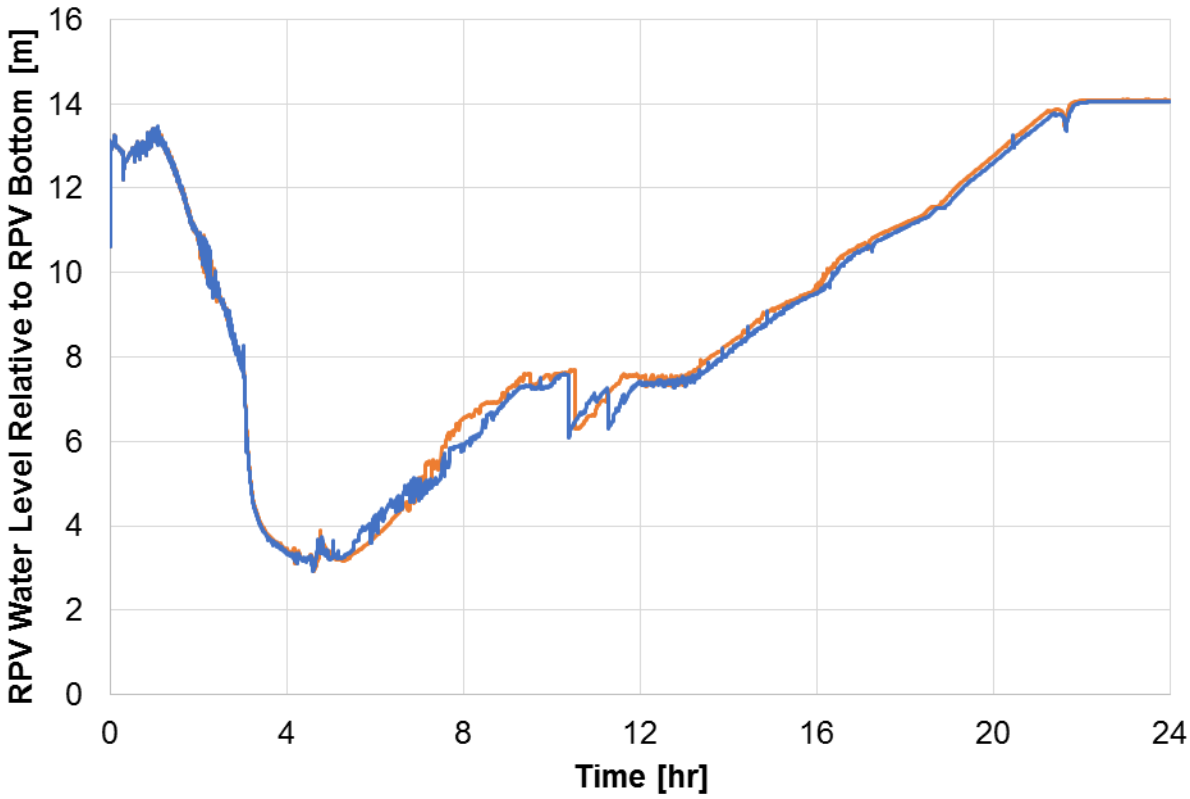

Figure 5-2. Reactor pressure vessel water level, for 2500 K melting temperature (orange) and 2800 K melting temperature (blue)

5.3. Primary System Pressure

The primary system pressure is shown in Figure 5-3. Both simulations show the same signatures: depressurization behavior, a spike following the quenching of fuel relocation and long-term equalization with drywell pressure.

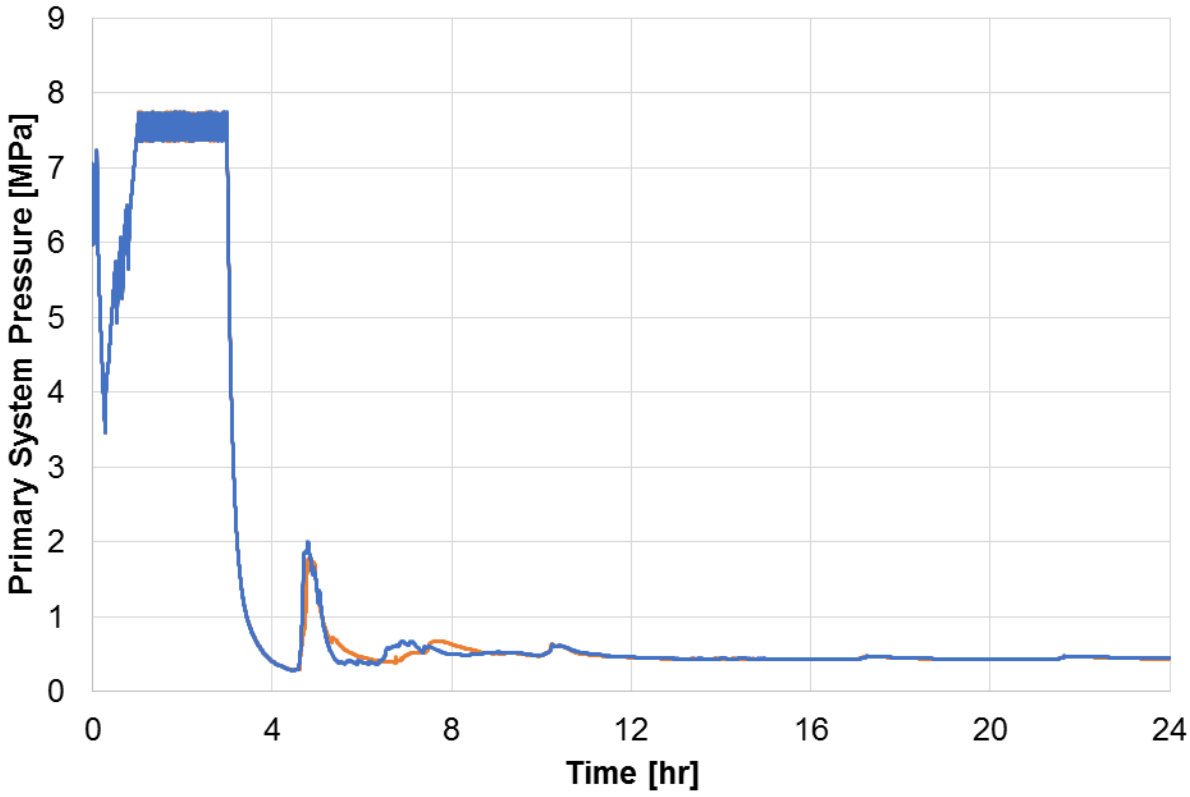

Figure 5-3. Primary system pressure, for 2500 K melting temperature (orange) and 2800 K melting temperature (blue)

5.4. Steam Dome Temperature

The difference in steam dome temperature, shown in Figure 5-4, can be attributed to increased steam cooling in the 2500 K simulation. In the 2500 K simulation the central two rings of the core region do not fully relocate to the lower plenum. As steam passes through this core region, it is heated, leading to the increased temperature of the steam dome. The 2800 K simulation does not have this central region, so a large amount of steam is able to pass directly through the core without being heated by fuel in a near-intact geometry.

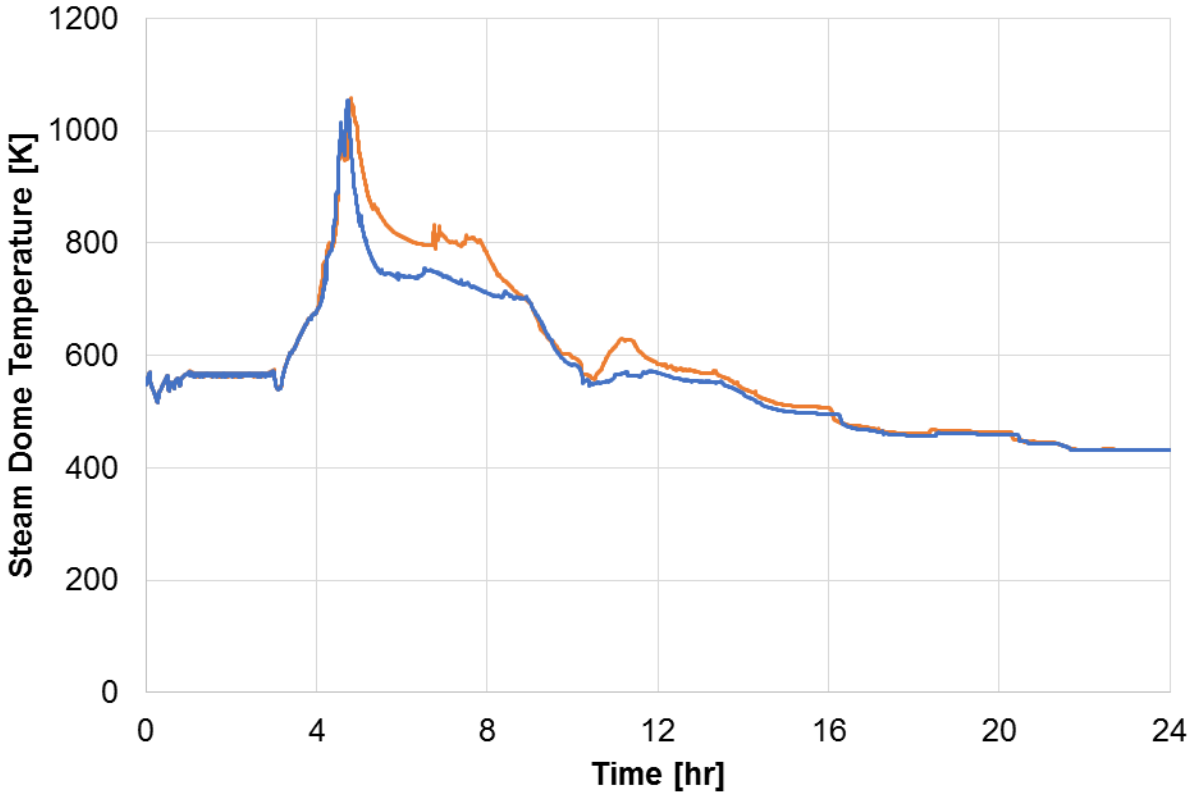

Figure 5-4. Steam dome temperature, for 2500 K melting temperature (orange) and 2800 K melting temperature (blue)

5.5. Drywell Pressure

The drywell pressure of the two simulation can be seen in Figure 5-5. It can be seen that there is only a slight difference in the long-term pressure of the two simulations. This small difference is attributable to the fact that the 2800 K case produces a slightly more hydrogen than the 2500 K case.

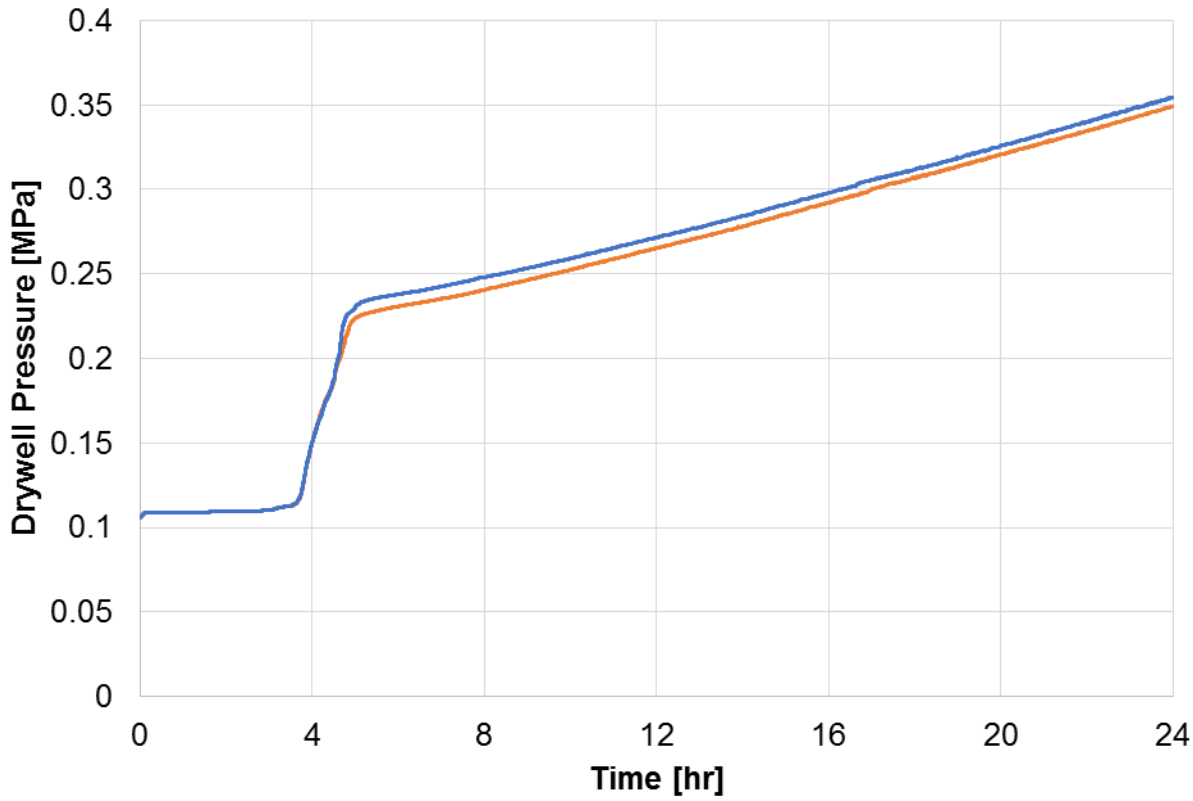

Figure 5-5. Reactor pressure vessel water level, for 2500 K melting temperature (orange) and 2800 K melting temperature (blue)

5.6. Hydrogen Generation

Compared to the 2500 K case, the 2800 K case generated more hydrogen during the initial phase of core degradation. Once this difference in total amount of hydrogen generated is established, it does not change for the remainder of the simulation. The difference in the hydrogen generation can be attributed to the difference in the core degradation in the central two rings of the core. In the 2800 K simulation, these rings achieve a hotter temperature before they fail, leading to an increase in hydrogen created.

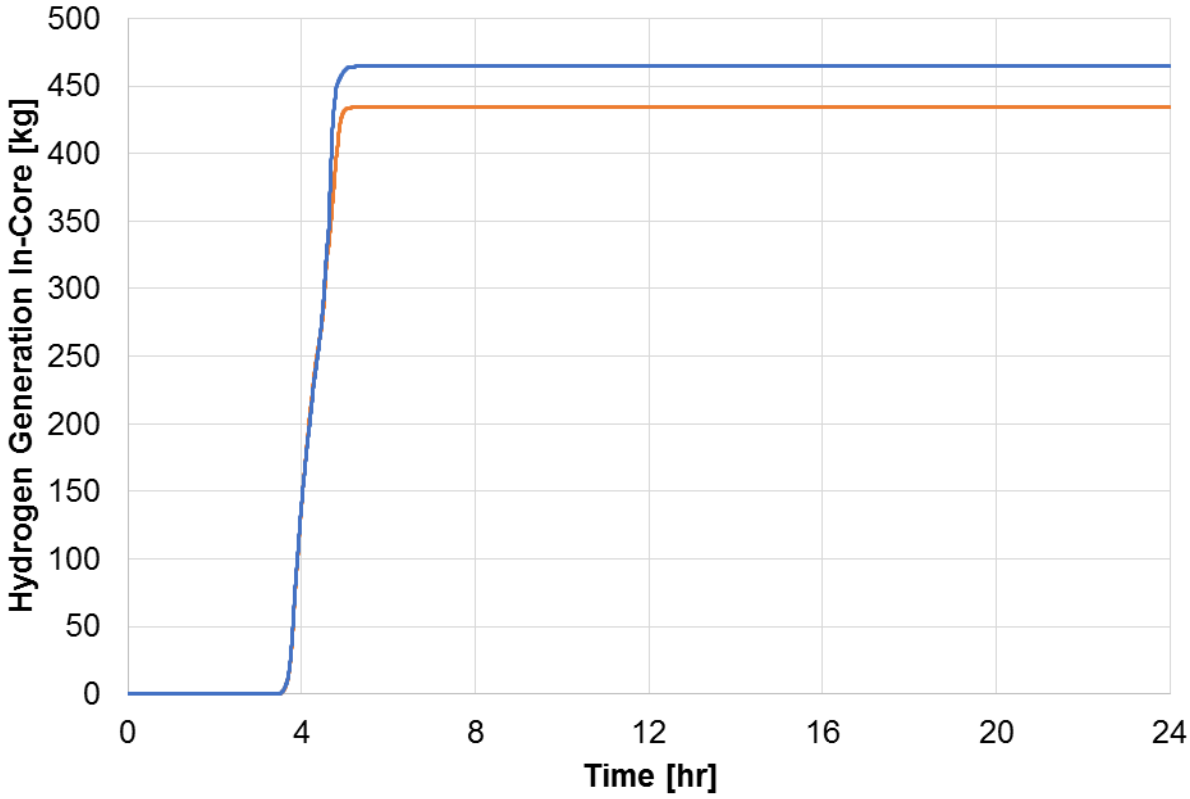

Figure 5-6. Reactor pressure vessel water level, for 2500 K melting temperature (orange) and 2800 K melting temperature (blue)

6. SUMMARY AND CONCLUSIONS

6.1. Plant and System Behavior

Significant differences were seen in the plant responses in the MAAP and MELCOR simulations. Both programs showed very close agreement in predictions of system level behavior until the onset of core damage at 3.6 hours. After this point the following characteristic differences were found the analysis.

- *Water level:* After core plate failure in the MELCOR simulations, fuel debris relocates to the lower plenum. In the lower plenum, this fuel debris is quenched, producing a source of steam at the bottom of the vessel. This leads to a slower reflooding in MELCOR relative to MAAP. Another contributing factor to the more rapid reflood to TAF in the MAAP simulations is the less effective heat transfer out of the molten crucible that is formed in all MAAP simulations.

- *Primary system pressure*: Following the onset of core damage, differences emerge in primary system pressure. Relocations of fuel to the lower plenum in MELCOR simulation result in less severe spikes in pressure. This is because MAAP fuel relocations, when they do occur, involved the complete failure of the core plate. This leads to nearly the entire core mass relocating to the lower plenum.

- *Steam dome temperature*: Relative to MAAP, MELCOR has an increased steam dome temperature during accident scenarios in which there is injection. This increase in temperature is resultant from increased steam cooling in MELCOR relative to MAAP. This steam cooling is enhanced by the generation of steam from fuel that relocates to the lower plenum near 4.0 hours in the MELCOR predictions.

- *Containment pressure:* Containment pressure in MELCOR scenarios is higher than in MAAP scenarios. This increase in pressure is directly resultant from the increased hydrogen in MELCOR relative to MAAP. This increased hydrogen generation originates from the different models of core degradation phenomena. The in-core crucible that forms in MAAP simulations limits the amount of zirconium and other materials available for interaction.

- *Wetwell temperature*: Additional steam generated in the lower plenum as well as increased steam cooling in the MELCOR simulations leads to an increased wetwell temperature relative to MAAP.

- *In-vessel hydrogen generation*: Relative to MAAP, MELCOR sees nearly twice as much in-core hydrogen generation. This difference in mass generation can be linked to the in-core crucible that forms in MAAP simulations. This crucible both blocks the flow of steam, which is necessary for oxidation, and decreases the total surface area of fuel debris that is available for interaction.

6.2. Core Degradation Behavior

As highlighted in the first phase of the MAAP-MELCOR Crosswalk analysis, MAAP and MELCOR inherently contain different abstractions of core degradation. Key core degradation behavior differences are highlighted. [1]

- *Degradation phenomena*:
    - In all cases contained in this analysis, MAAP predicted the formation of a molten pool with an exterior oxidic crust. This insulated crucible eventually agglomerates nearly all fuel and metallic material in the core region. If this crucible relocates to the lower plenum, it does so all at once when support structures are degraded.
    - Conversely MELCOR predicts the formation of primarily particulate debris after the failure of fuel assemblies. This debris relocates to the core plate, causing a flow blockage in the region. The core plate is eventually failed and the debris it supported relocates to the lower plenum, where it is quenched and generates steam.
- *Fuel temperatures*: Fuel temperatures in MAAP and MELCOR begin to drastically rise after the onset of core damage, leading to the failure of fuel and other core structures. Fuel that does not relocate in MAAP is agglomerated into a molten crucible, which retains a center over 3000 K until the end of the 24 hours simulation. MELCOR does not predict this behavior. Remaining fuel in the core region is fully quenched during the reflooding of the core, equalizing with the injection temperature.
- *Recovery progression*: MAAP predicts that at the end of the simulation a crucible still exists within the core region. At this point the crucible has not been fully quenched; however, core damage progression has been halted and the crucible has been arrested in the core region. MELCOR predicts the full quenching of the core at the time when the reflood water level reached TAF. This is due to the relatively “intact” geometry of MELCOR during reflood. The outer layers of the MAAP crucible insulate the interior, molten region.
- *Lower plenum characteristics*: In every MELCOR simulation fuel relocated to the lower plenum after failing. This relocated fuel is eventually fully quenched, forming non-molten particulate debris. This fuel material in the lower plenum generates steam, which contributes to the steam cooling of the core region. In the MAAP simulations, only those with no or minimal injection resulted in fuel relocation to the lower plenum. When the relocation occurs in MAAP a large spike in the primary system to near 7 MPa occurs, which is higher than the MELCOR spikes of 1 to 2 MPa.

6.3. Core Coolability and Recoverability

Differences in the long-term coolability and recoverability of damaged cores can be traced back to the representation and progression of fuel degradation in the early stages of the core degradation.

- *Convective heat losses*: Throughout the accident scenario MELCOR predicts that significantly more heat is removed through convection heat transfer compared to MAAP. In the late stages of the simulation, this heat removal rate is over ten times as much. The crucible that forms in MAAP limits the amount of heat that can be removed through convection.
- *Core blockage fraction*: In MAAP simulations the entire core region is eventually blocked by the formation of a crucible. In MELCOR, a short-lived blockage forms on top of the core plate, preventing flow to the area. However, the majority of the core is able to be convectively cooled during the accident.

6.4. Overall Conclusions

As highlighted in the first phase of the MAAP-MELCOR Crosswalk analysis, MAAP and MELCOR inherently contain different abstractions of core degradation. In all cases contained in this analysis, MAAP predicted the formation of a molten pool with an exterior oxidic crust. This insulated crucible eventually agglomerates nearly all fuel and metallic material in the core region. If this crucible relocates to the lower plenum, it does so all at once when support structures are degraded. Conversely MELCOR predicts the formation of primarily particulate debris after the failure of fuel assemblies. This debris relocates to the core plate, causing a flow blockage in the region. The core plate eventually fails and the debris it supported relocates to the lower plenum, where it is quenched and generates steam.

Differences in the long-term coolability and recoverability of damaged cores can be traced back to the representation and progression of fuel degradation in the early stages of the core degradation. MELCOR removes the majority of heat generated in the core region through convective cooling by steam and water. MAAP, conversely, sees significantly less removal from convection. In MAAP the majority of heat generated remains in the in-core crucible that is formed. This contributed to the crucible's high temperature, extending to the end of the simulation.

These differences in core degradation representation can have real consequences for operators developing drills that are made to represent the plant behavior during a severe accident.

REFERENCES

[1] Luxat D., Hanophy J. & Kalinich D., "Modular Accident Analysis Program (MAAP) - MELCOR Crosswalk Study Phase 1," EPRI Technical Report, Report 3002004449, (2014).

[2] "MELCOR Computer Code Manuals, Vol. 2: Reference Manual, Version 2.2.9541," SAND 2017-0876 O, Sandia National Laboratories, January 2017 (ADAMS Accession No. ML17040A420)

[3] "MAAP5 – Modular Accident Analysis Program for LWR Power Plants: Transmittal Document for MAAP5 Code Revision MAAP 5.04" prepared by Fauske and Associates, FAI/16-0951, Rev. 0, 2016.

[4] OECD Nuclear Energy Agency (NEA), "Benchmark Study of the Accident at the Fukushima Daiichi Nuclear Power Plant - (BSAF Project) - Phase 1 Summary Report," *NEA Technical Report*, NEA/CSNI/R(2015)18, (2015).

[5] Humpries, L. L., "Quicklook overview of model changes in MELCOR 2.2: Rev 6342 to Rev 9496," SAND2017-5599, May, 2017

[6] Cardoni, J., "Radionuclide Inventory and Decay Heat Quantification Methodology for Severe Accident Simulations," Unclassified Unlimited Release, SAND2014-17667, September, 2014.

APPENDIX A. NODALIZED CORE TEMPERATURES, MAAP

This appendix contains nodalized core temperature diagrams for MAAP.

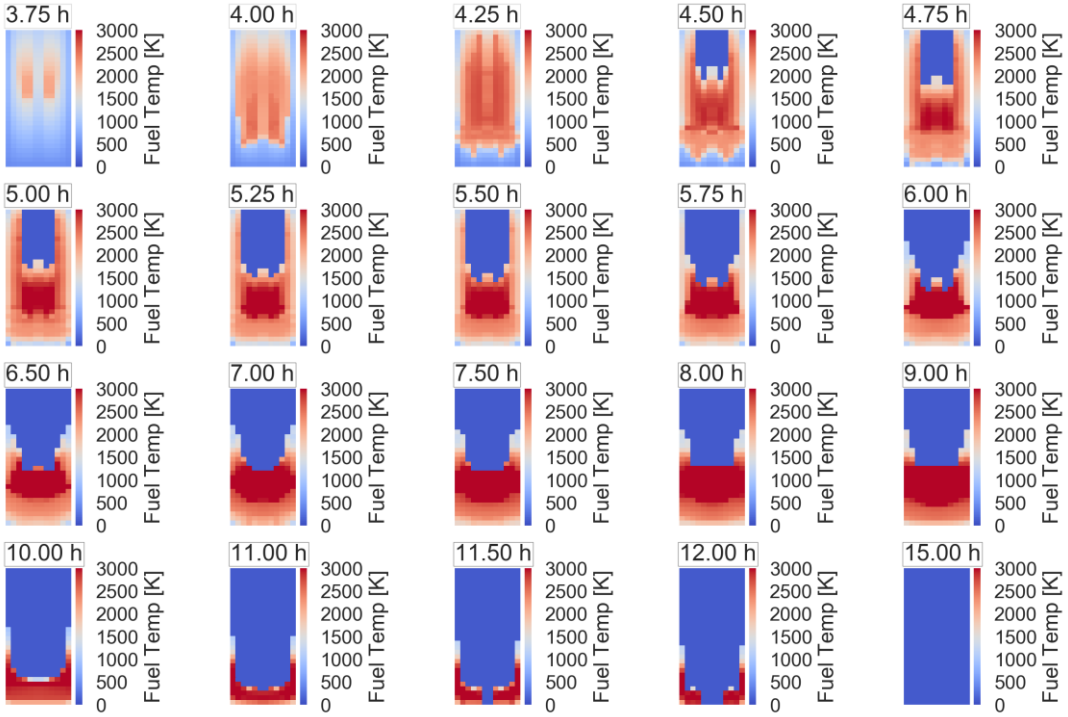

Figure A-1. Nodalized Core Temperature for Case 1, MAAP

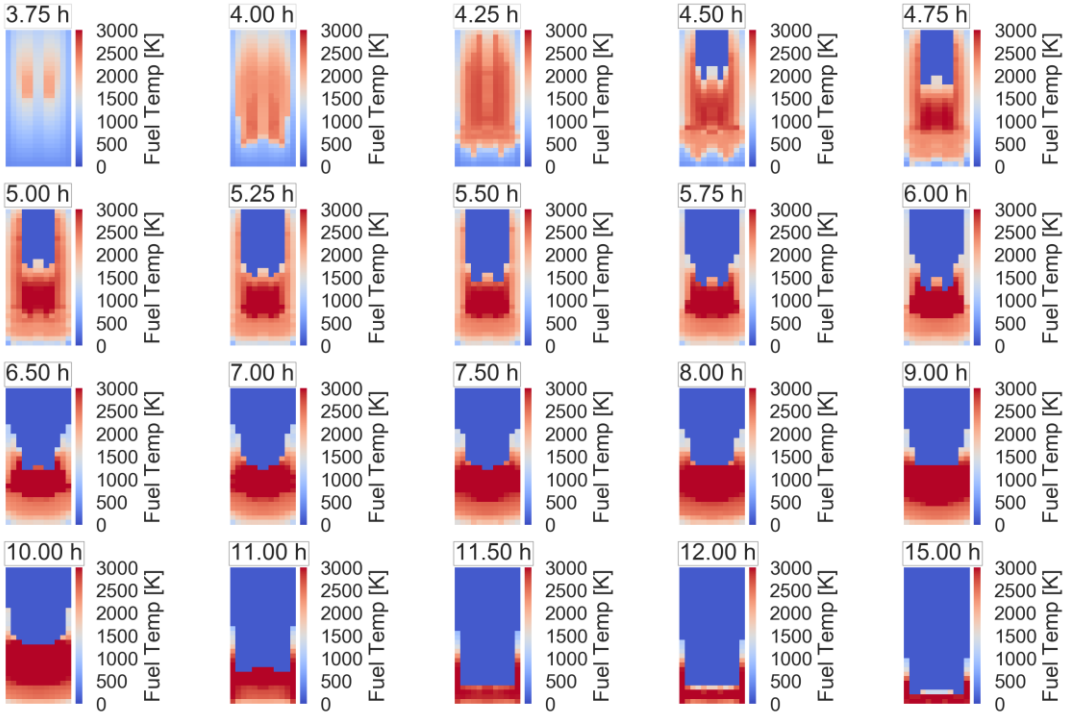

Figure A-2. Nodalized Core Temperature for Case 2, MAAP

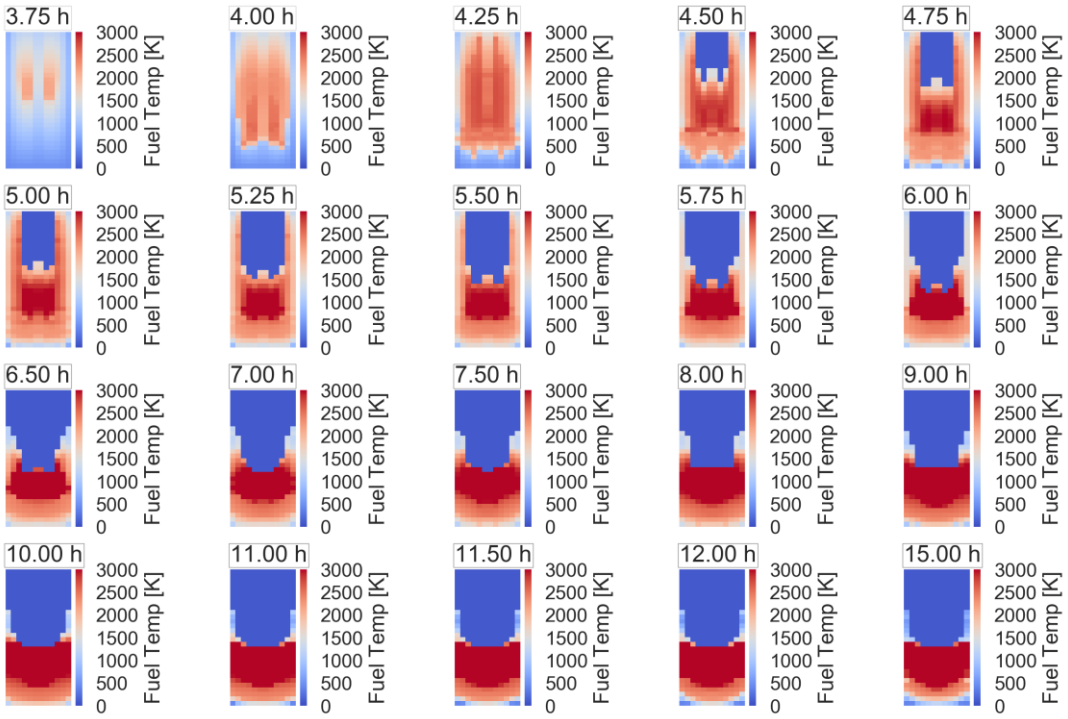

Figure A-3. Nodalized Core Temperature for Case 3, MAAP

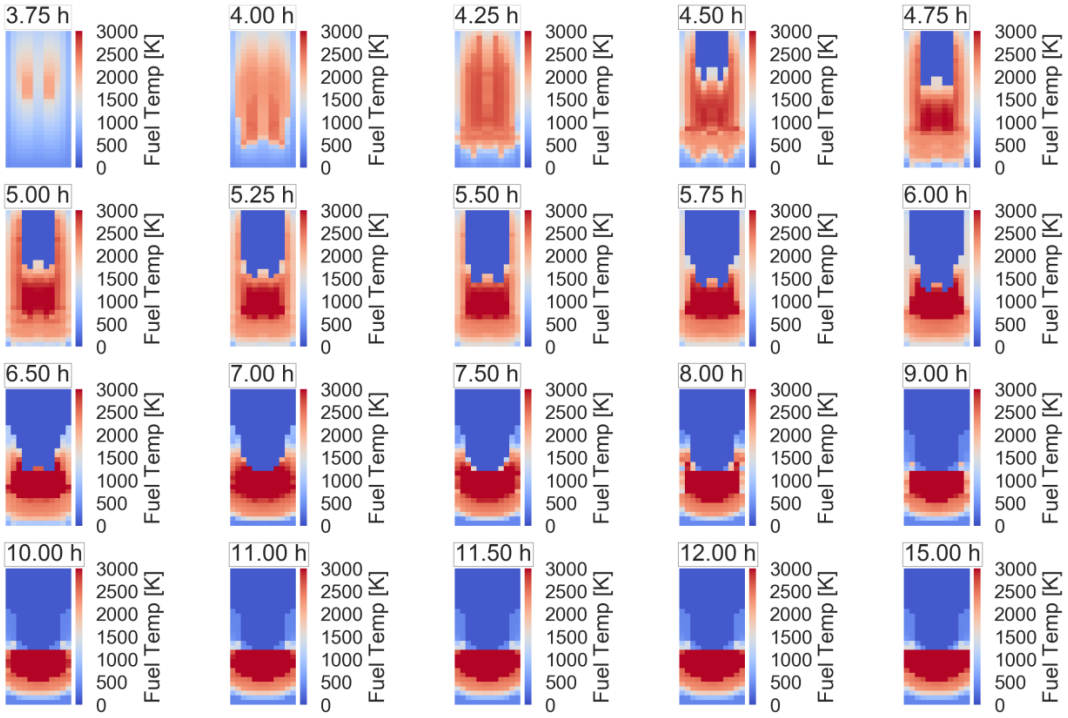

Figure A-4. Nodalized Core Temperature for Case 4, MAAP

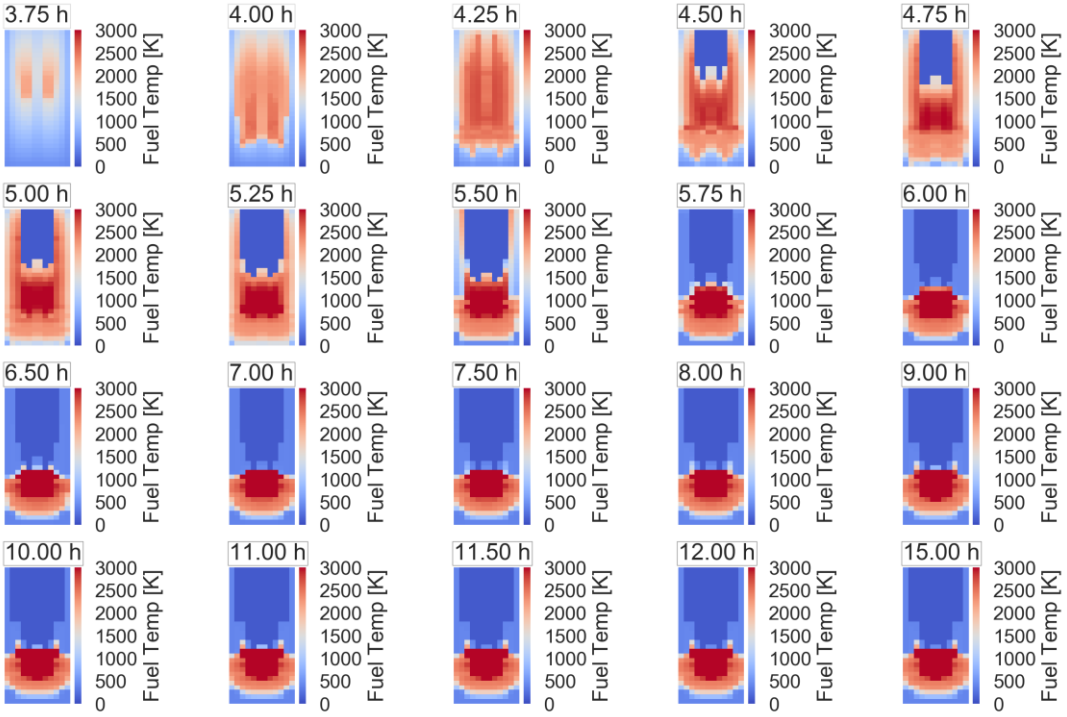

Figure A-5. Nodalized Core Temperature for Case 5, MAAP

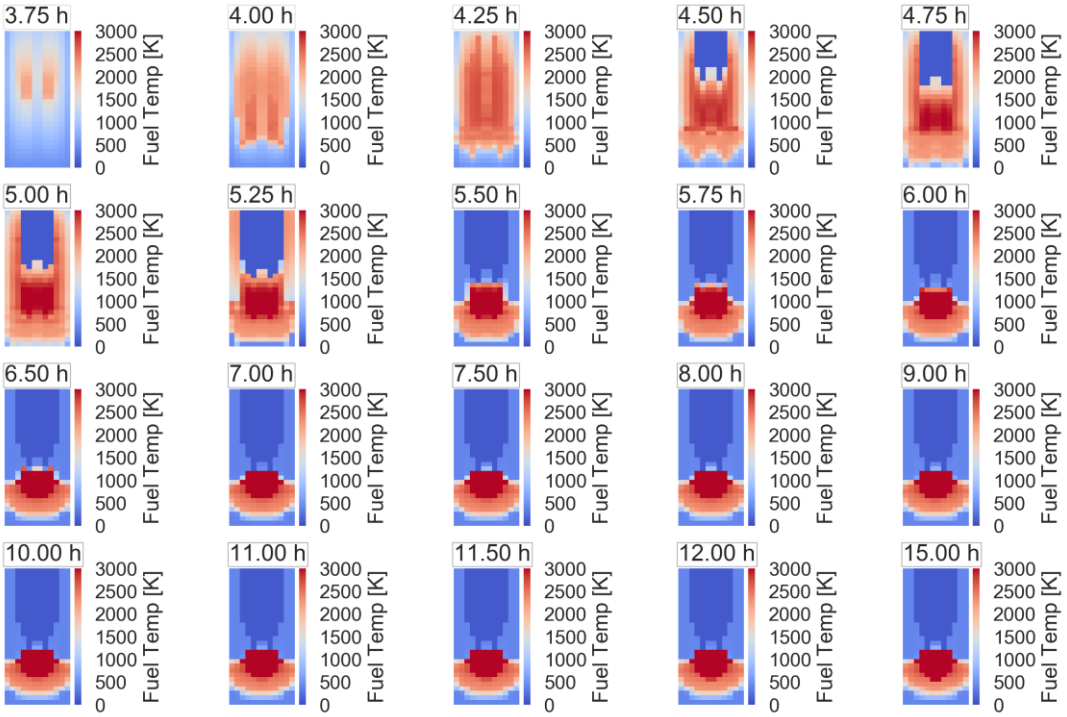

Figure A-6. Nodalized Core Temperature for Case 6, MAAP

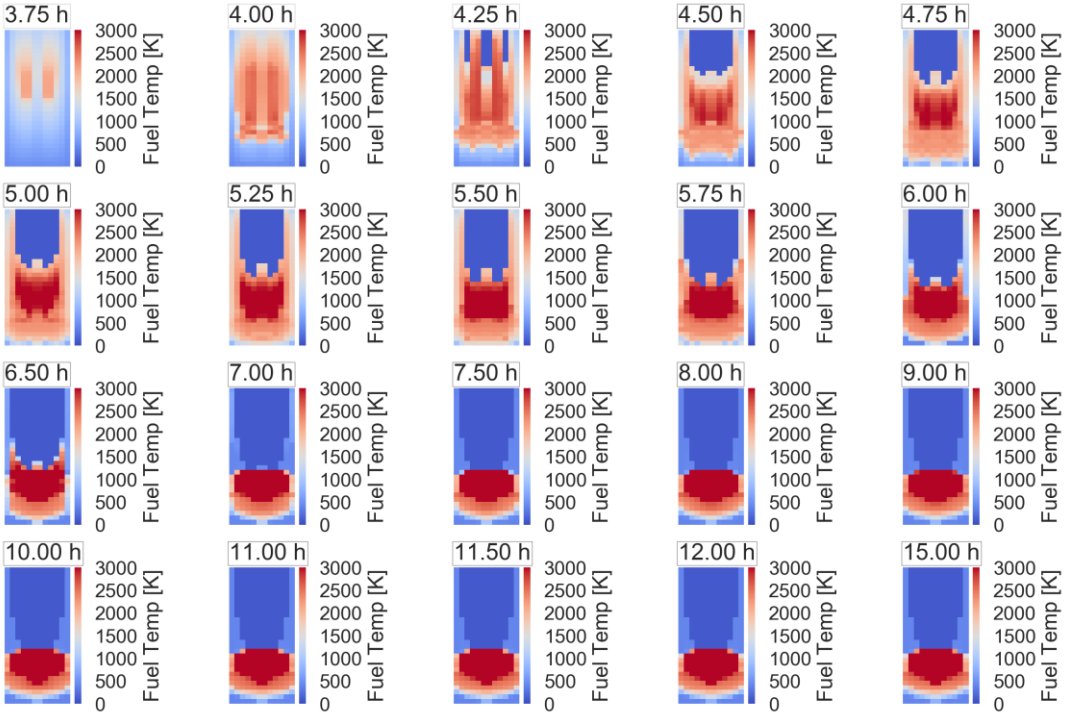

Figure A-7. Nodalized Core Temperature for Case 7, MAAP

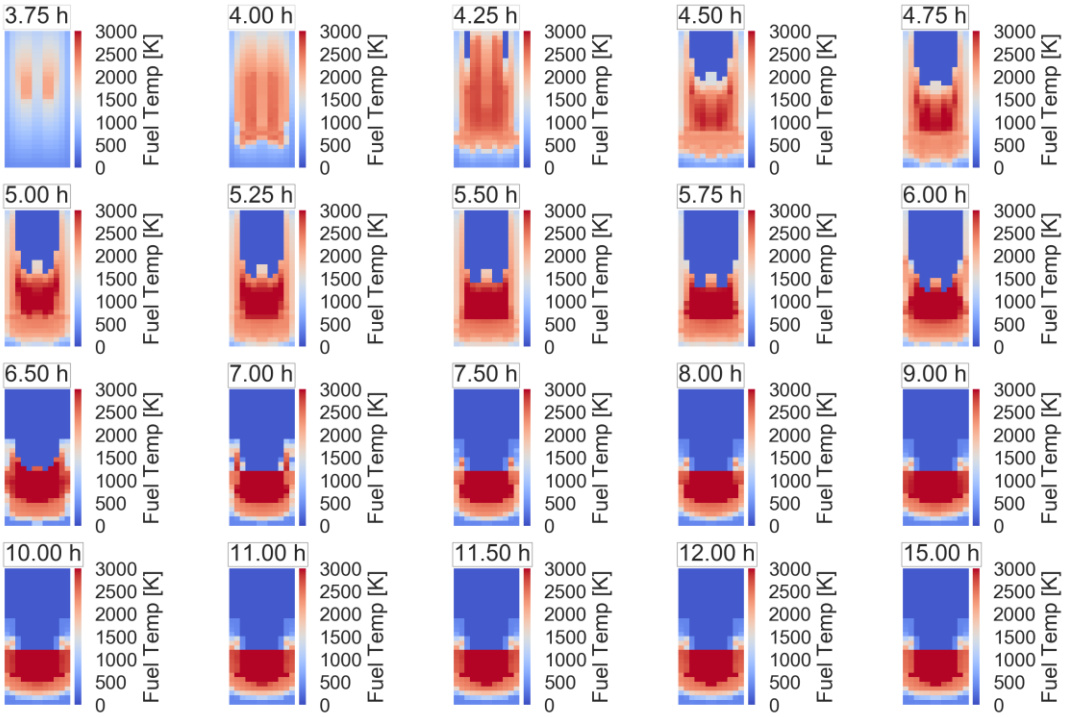

Figure A-8. Nodalized Core Temperature for Case 8, MAAP

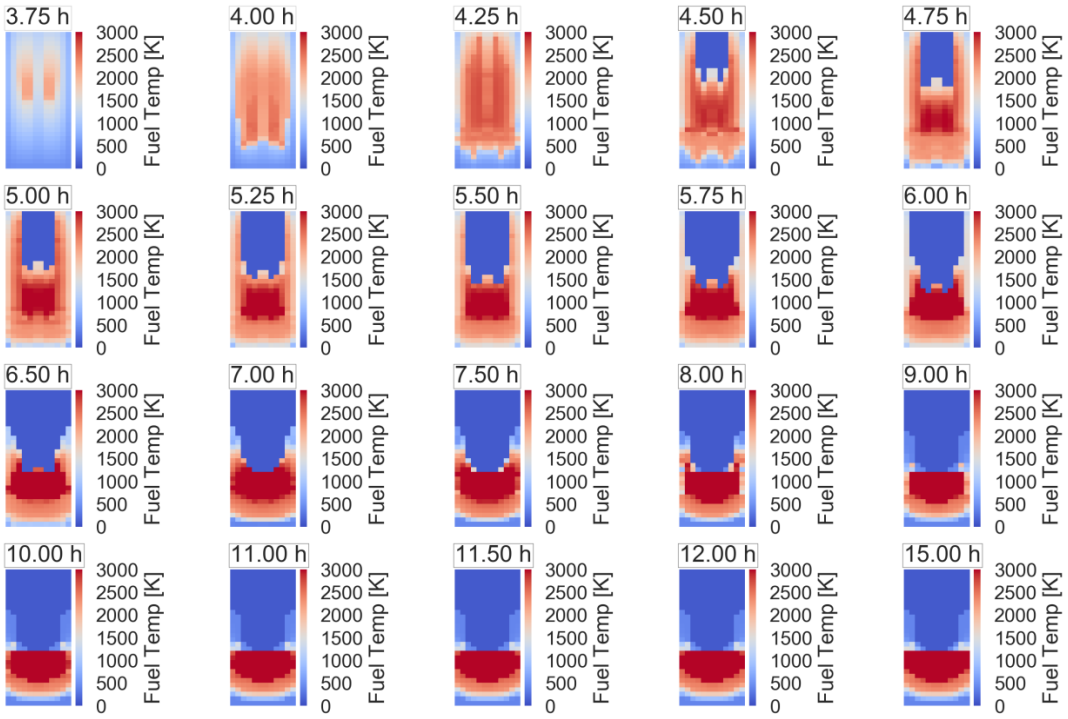

Figure A-9. Nodalized Core Temperature for Case 9, MAAP

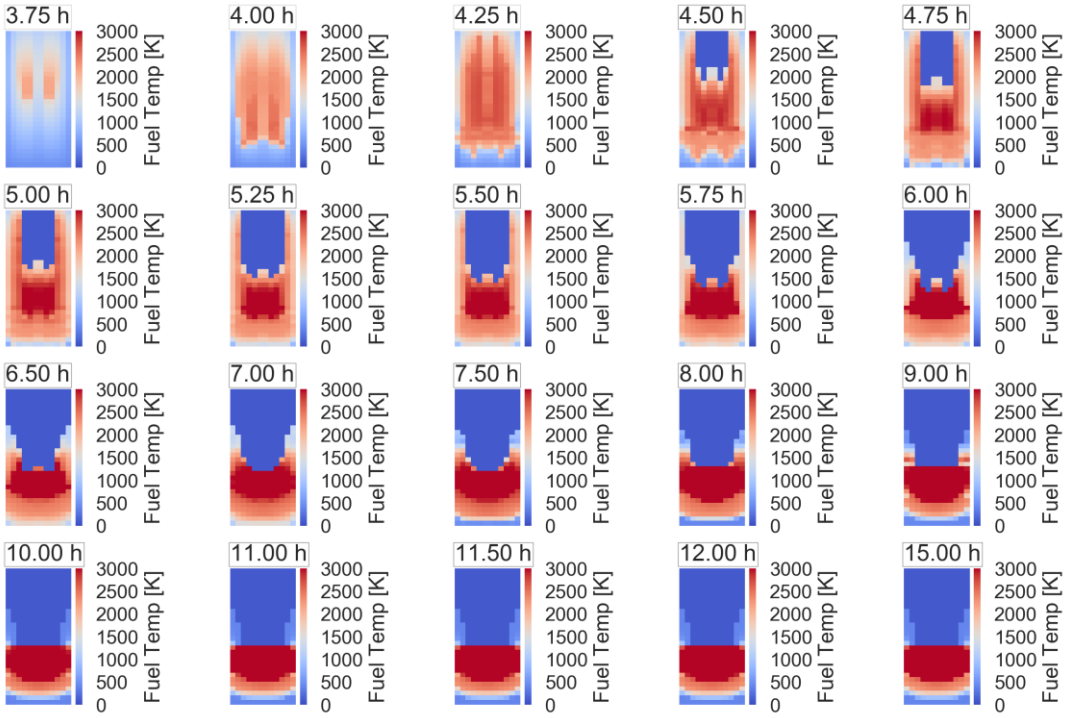

Figure A-10. Nodalized Core Temperature for Case 10, MAAP

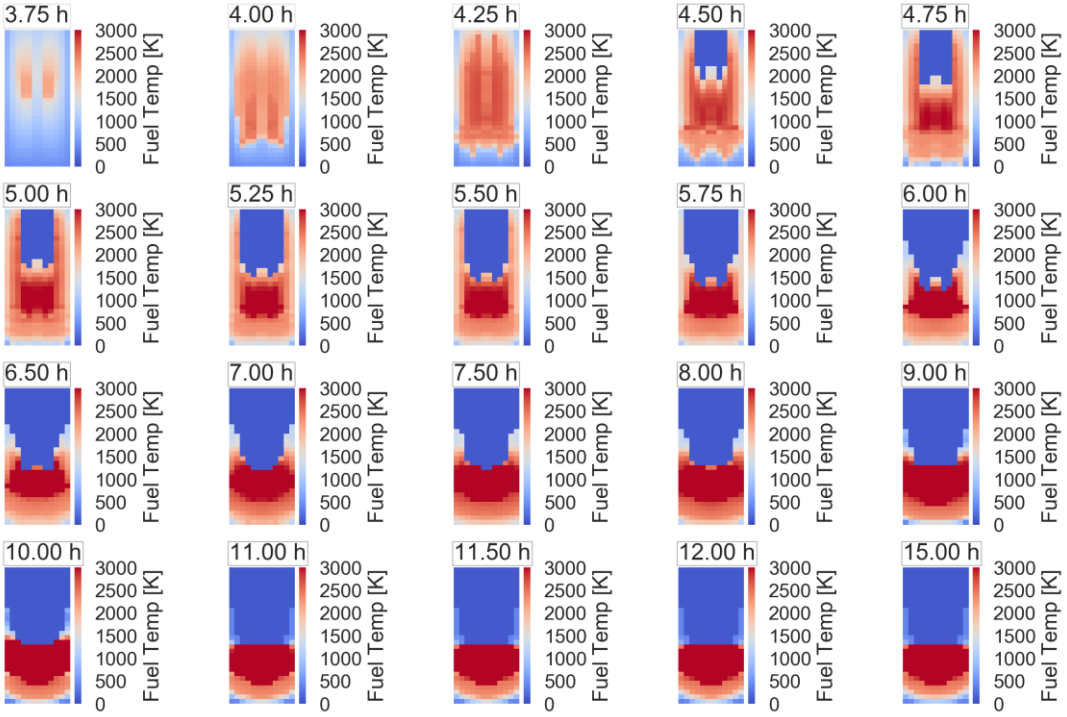

Figure A-11. Nodalized Core Temperature for Case 11, MAAP

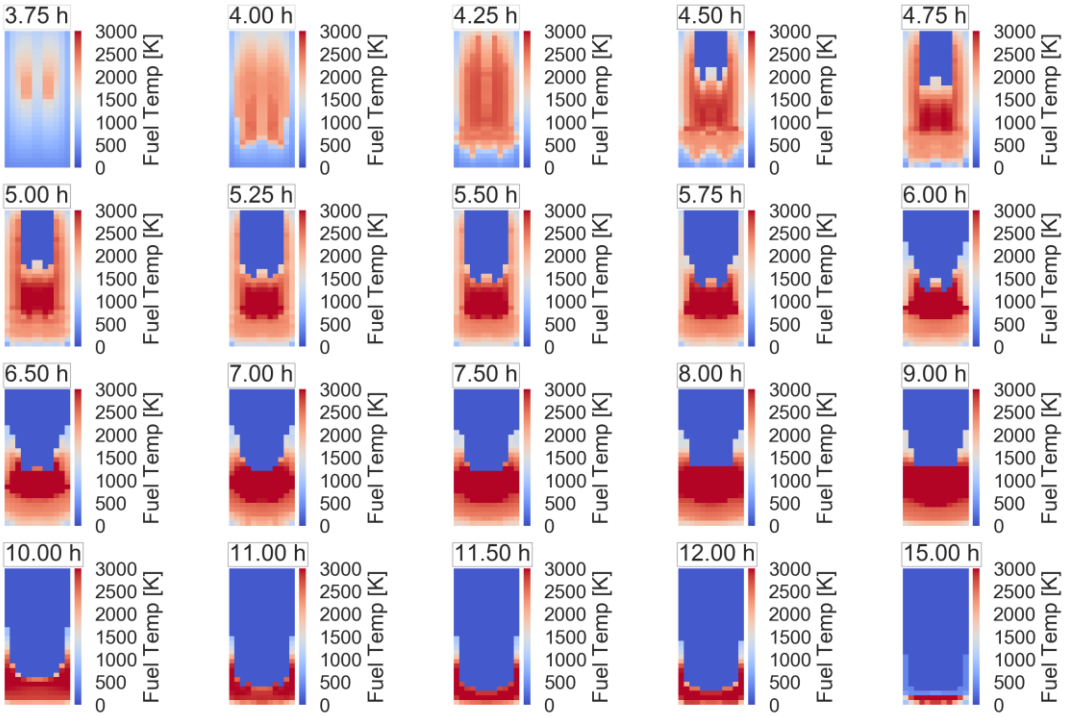

Figure A-12. Nodalized Core Temperature for Case 12, MAAP

APPENDIX B. NODALIZED CORE TEMPERATURES, MELCOR

This appendix contains nodalized core temperature diagrams for MELCOR.

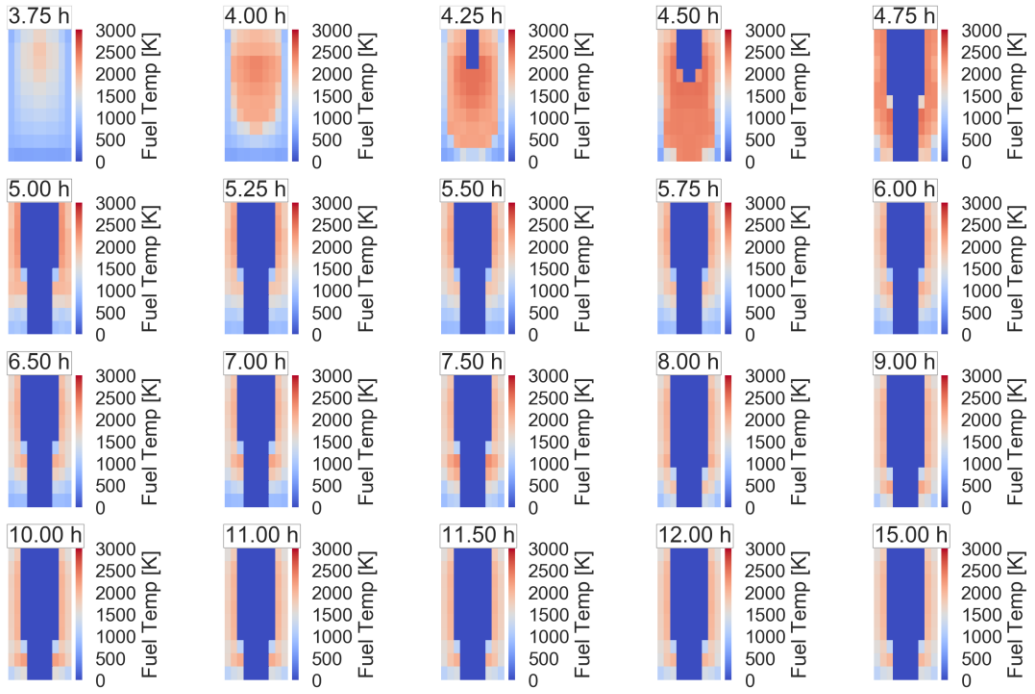

Figure B-1. Nodalized Core Temperature for Case 1, MELCOR

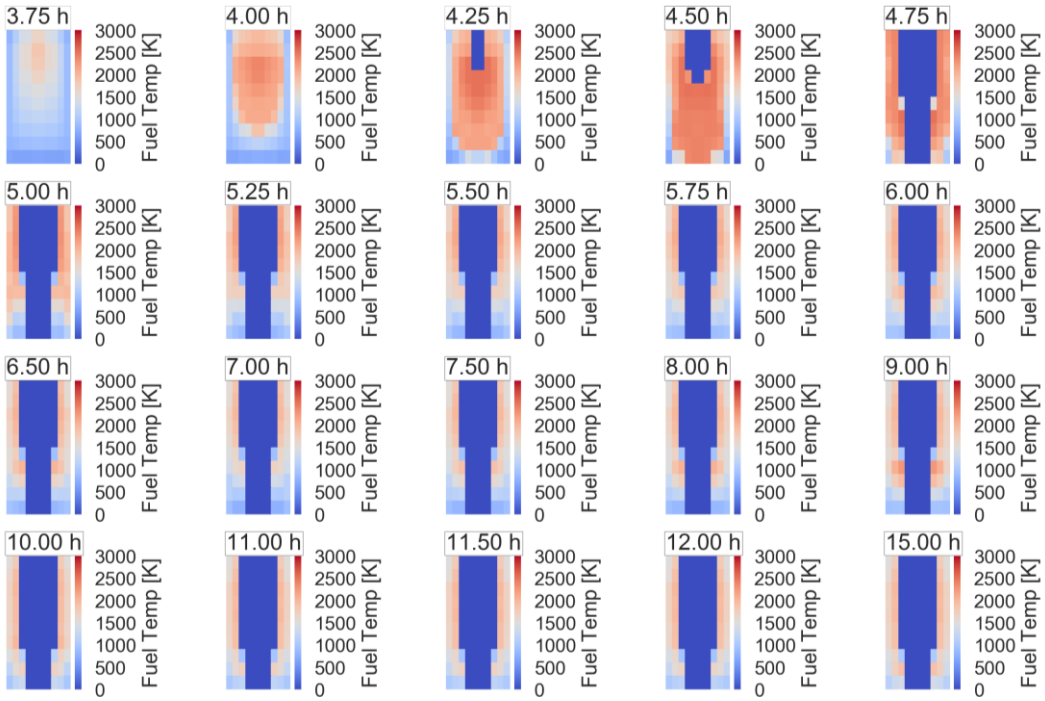

Figure B-2. Nodalized Core Temperature for Case 2, MELCOR

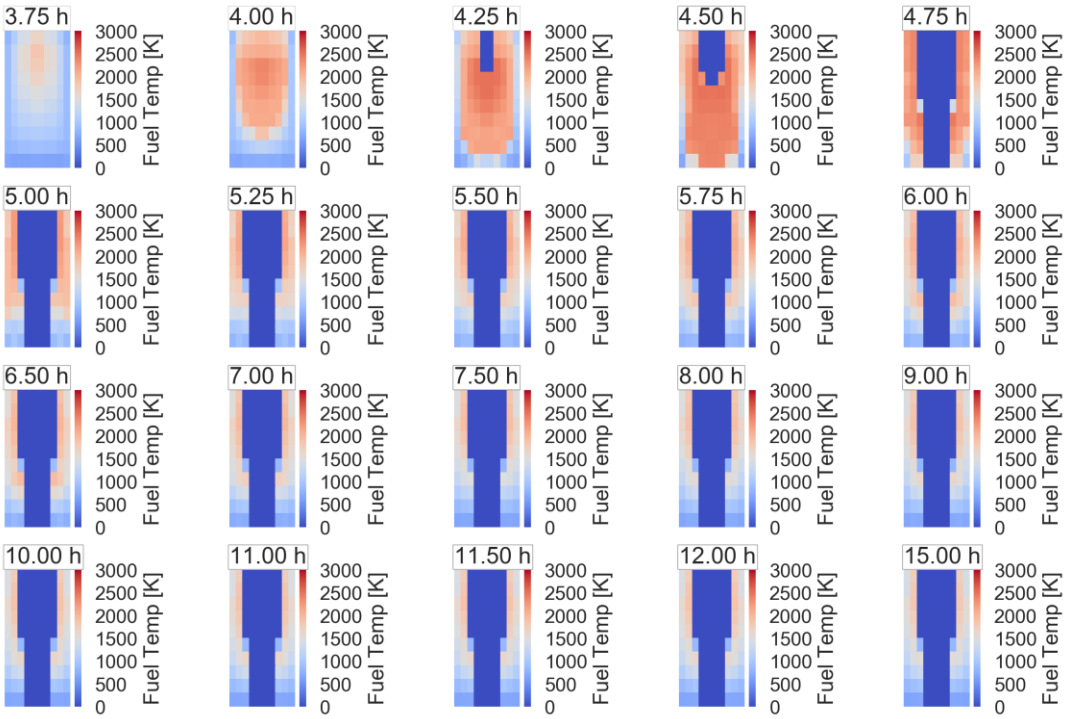

Figure B-3. Nodalized Core Temperature for Case 3, MELCOR

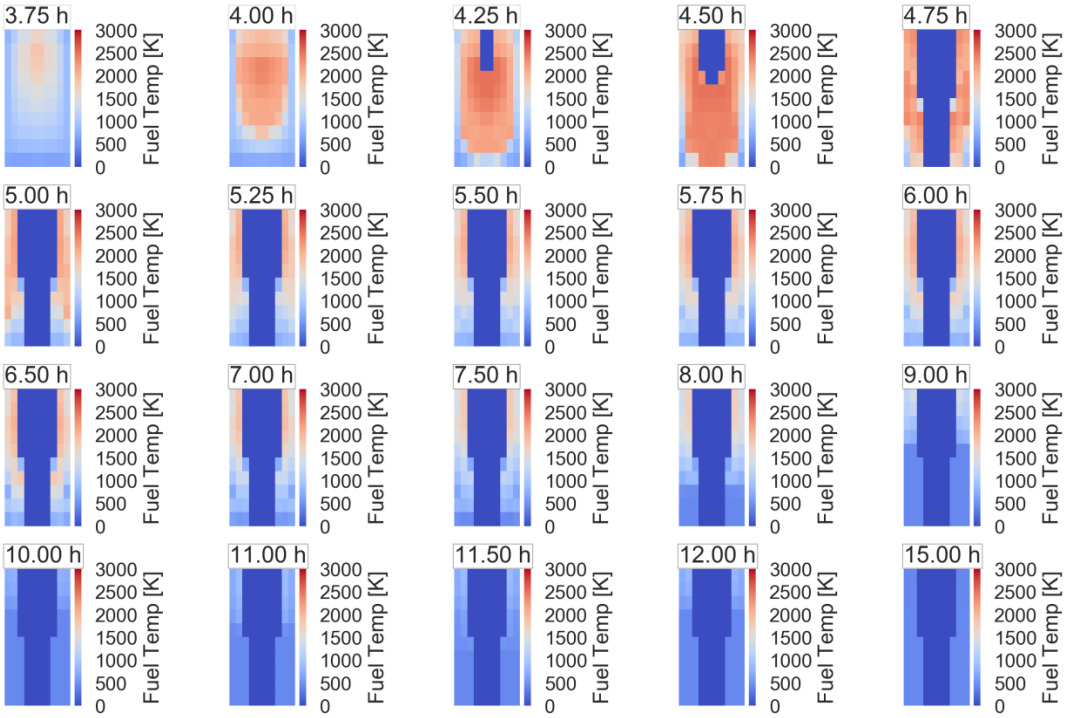

Figure B-4. Nodalized Core Temperature for Case 4, MELCOR

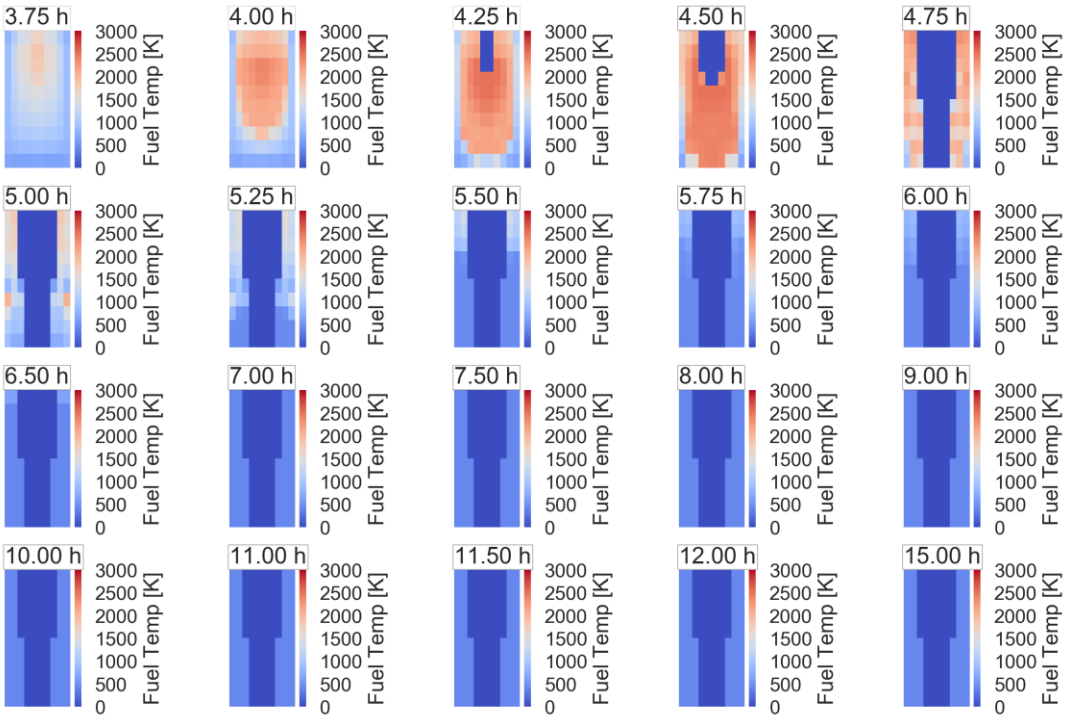

Figure B-5. Nodalized Core Temperature for Case 5, MELCOR

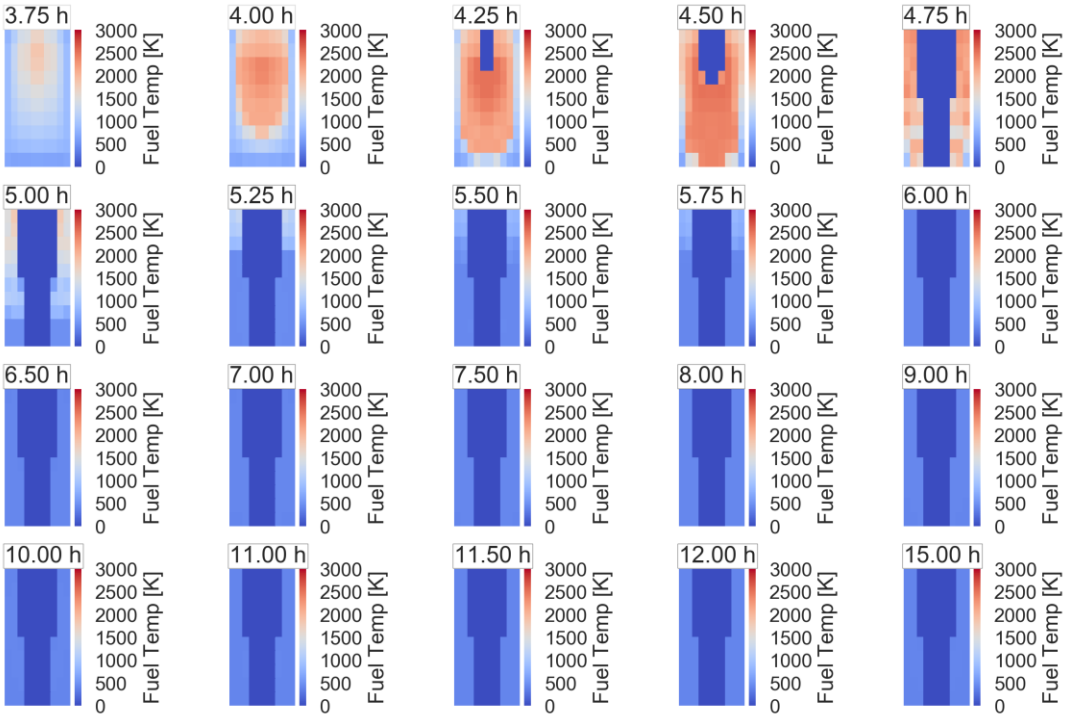

Figure B-6. Nodalized Core Temperature for Case 6, MELCOR

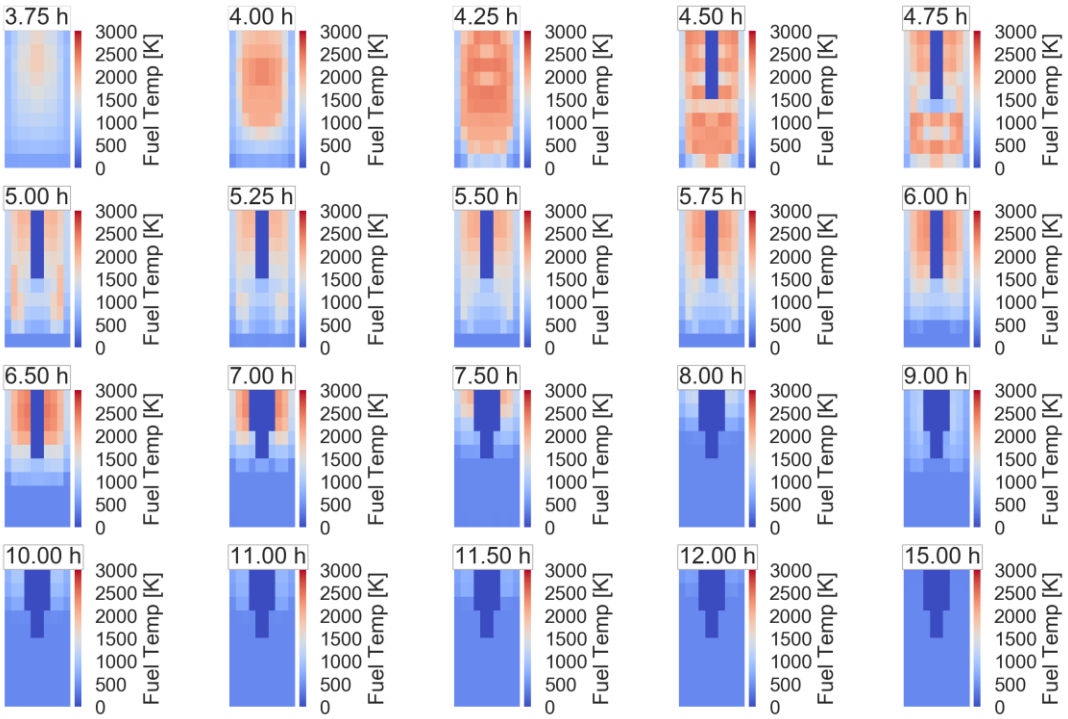

Figure B-7. Nodalized Core Temperature for Case 7, MELCOR

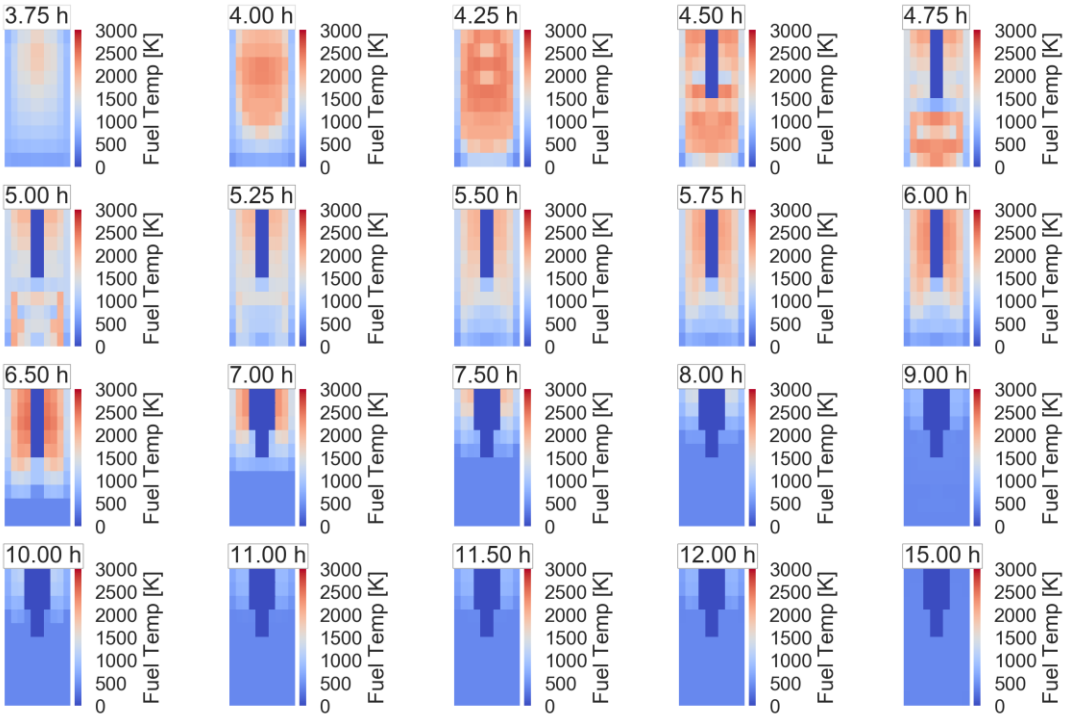

Figure B-8. Nodalized Core Temperature for Case 8, MELCOR

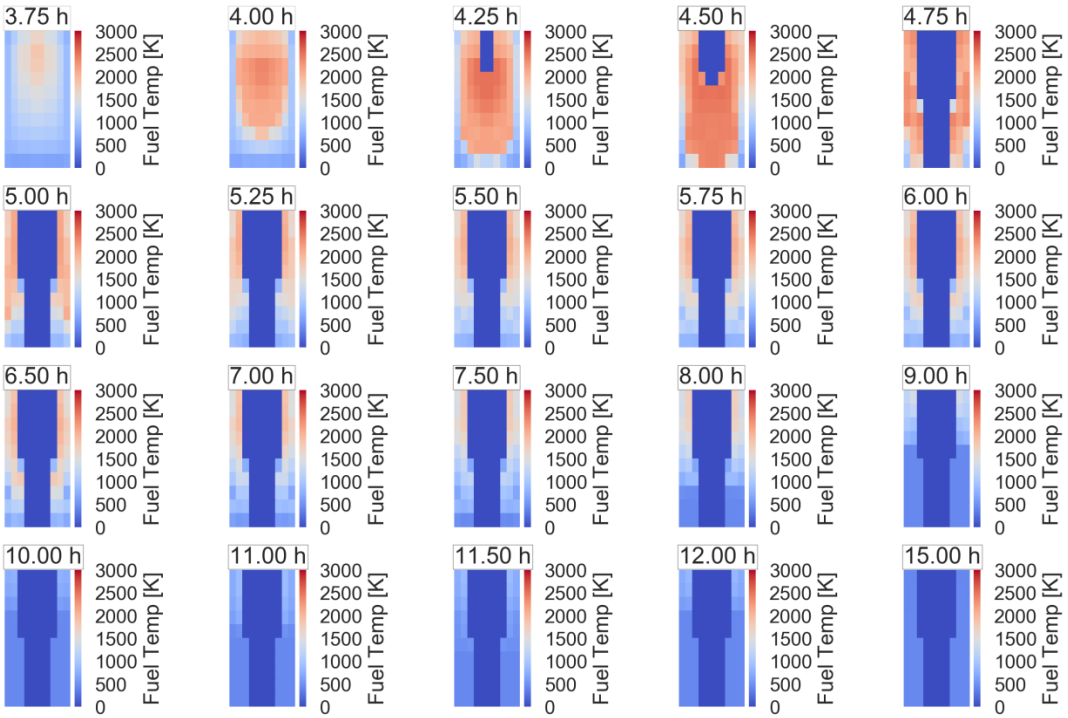

Figure B-9. Nodalized Core Temperature for Case 9, MELCOR

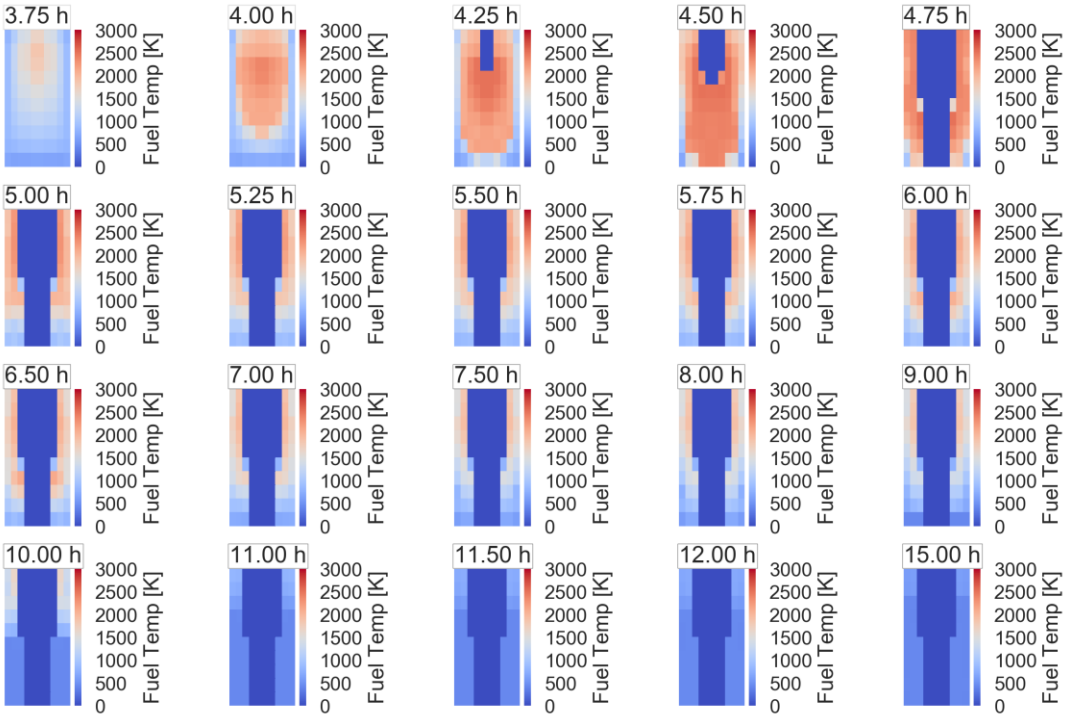

Figure B-10. Nodalized Core Temperature for Case 10, MELCOR

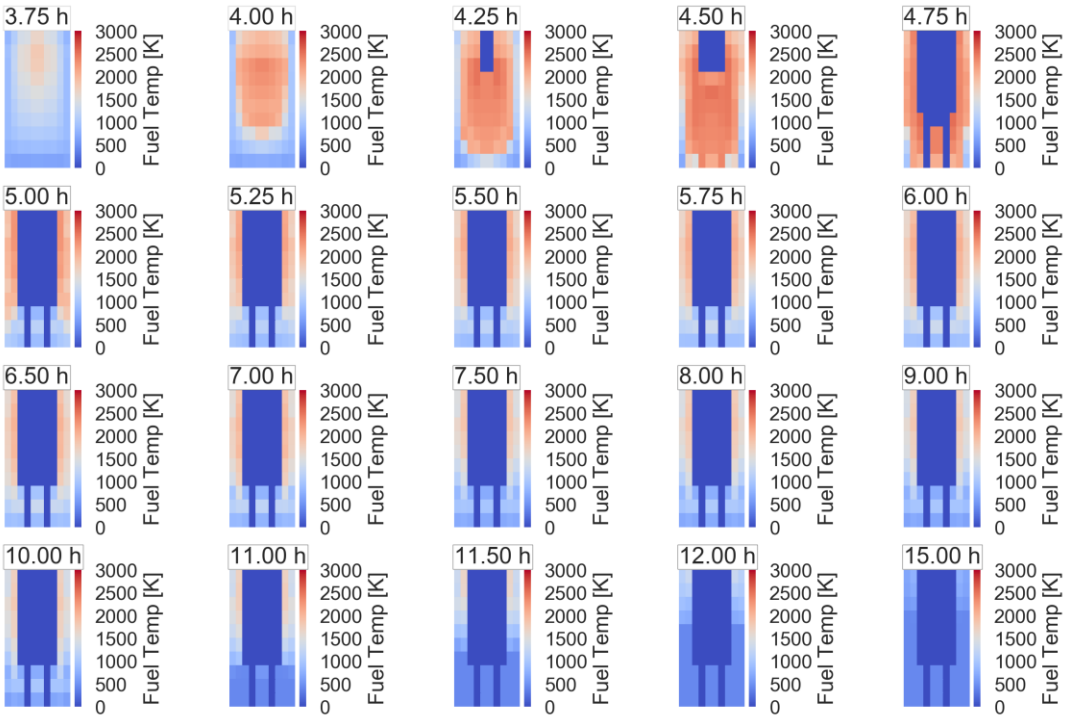

Figure B-11. Nodalized Core Temperature for Case 11, MELCOR

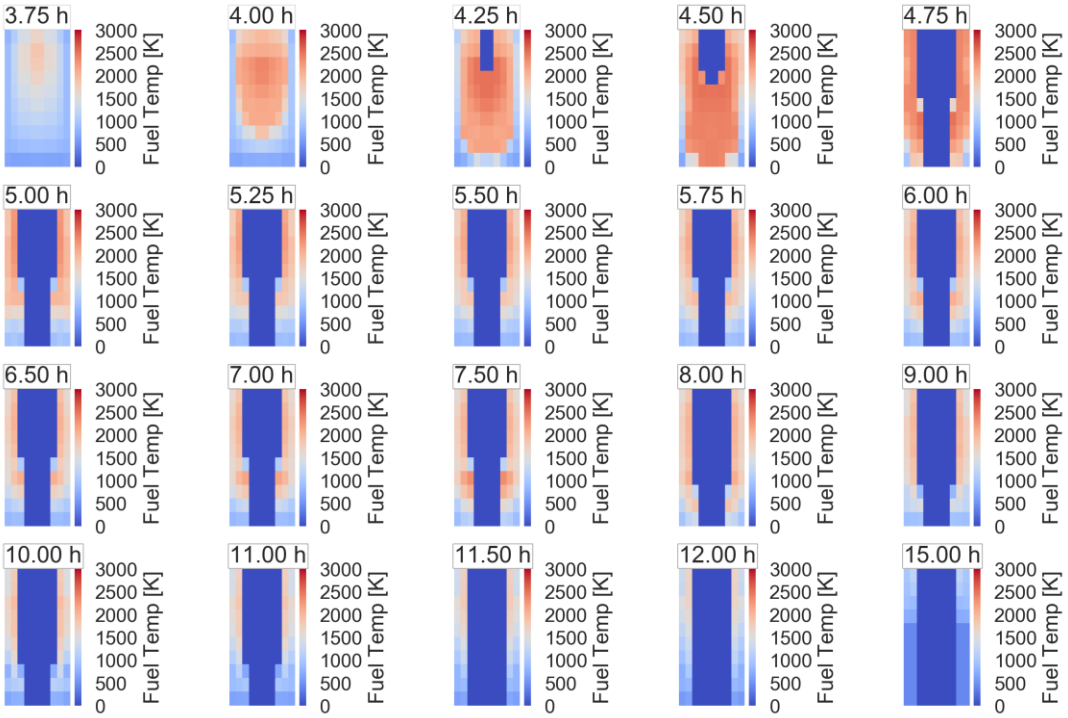

Figure B-12. Nodalized Core Temperature for Case 12, MELCOR

APPENDIX C. NODALIZED CORE BLOCKAGE FRACTIONS, MAAP

This appendix contains nodalized core blockage fractions diagrams for MAAP.

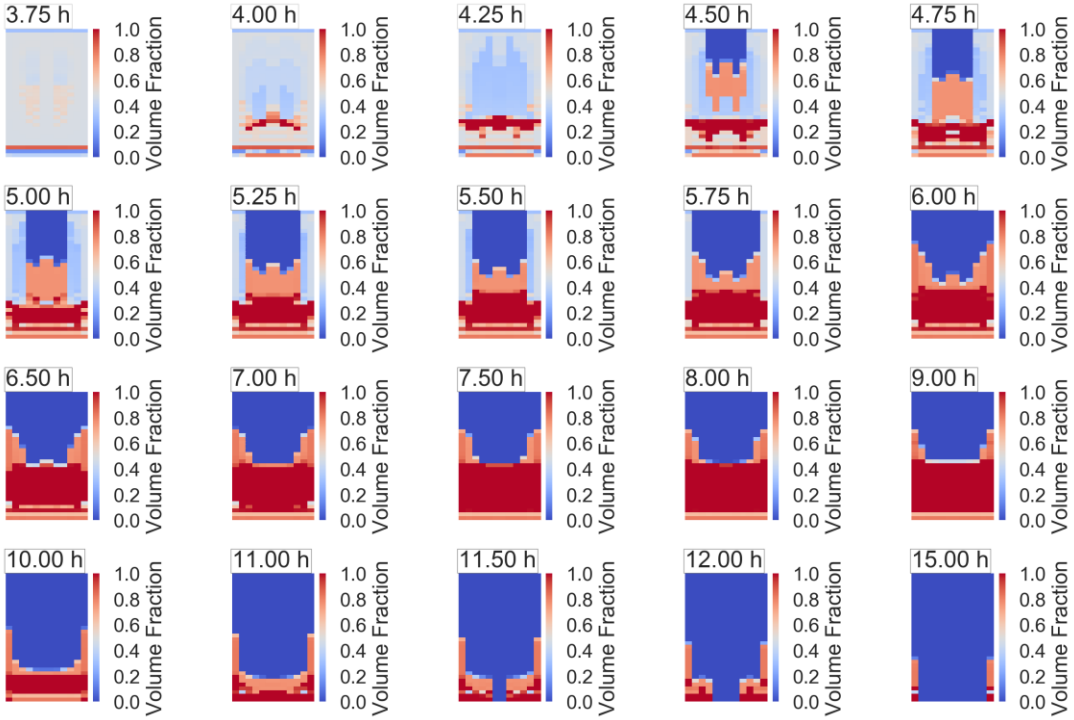

Figure C-1. Nodalized core blockage fractions for Case 1, MAAP

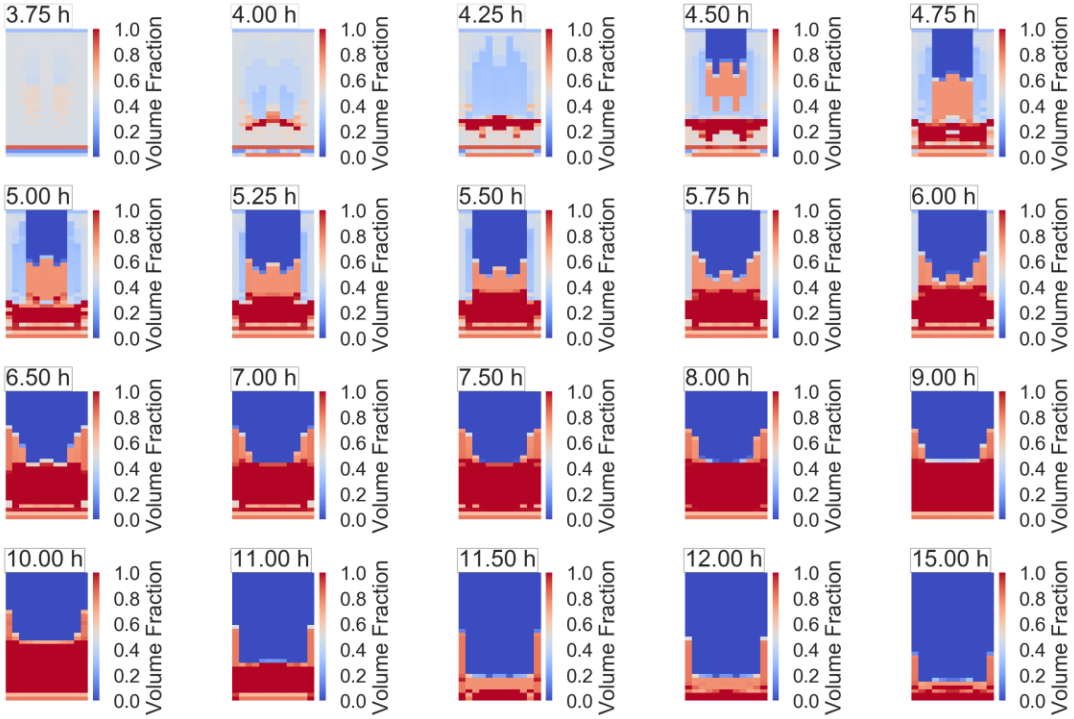

Figure C-2 Nodalized core blockage fractions for Case 2, MAAP

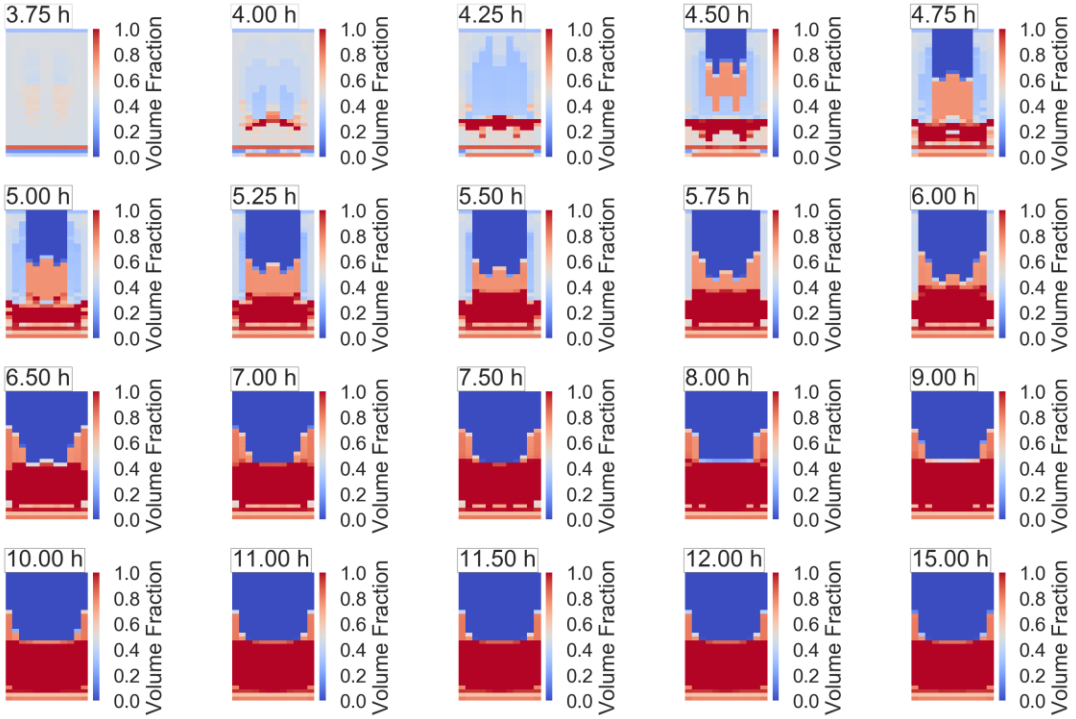

Figure C-3. Nodalized core blockage fractions for Case 3, MAAP

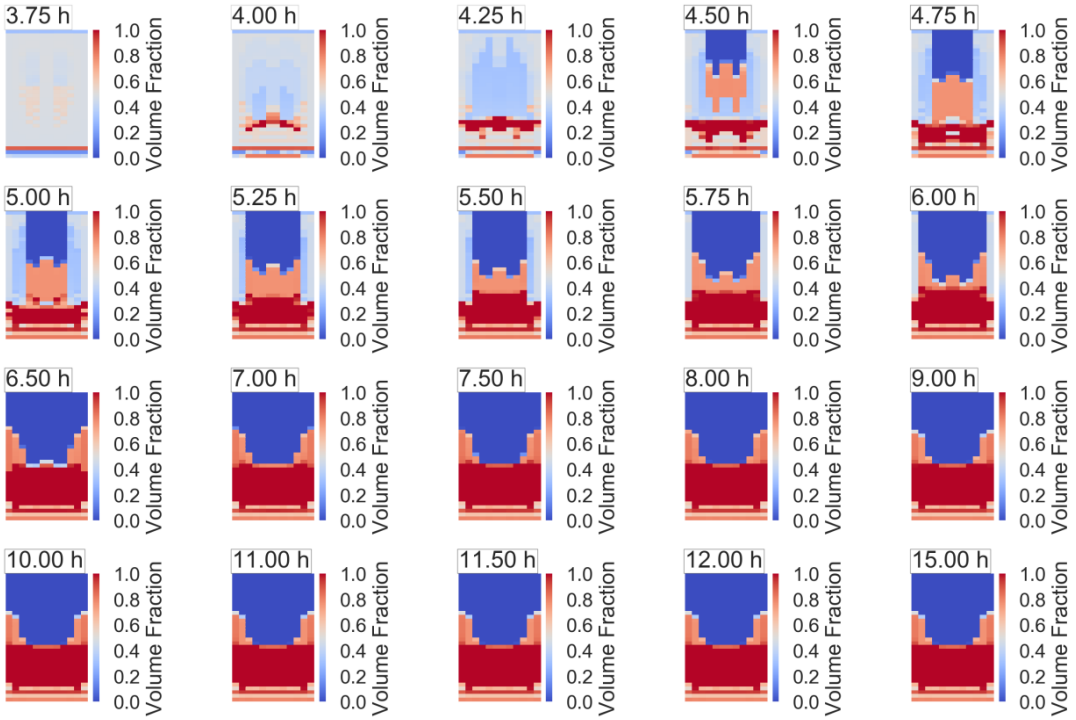

Figure C-4. Nodalized core blockage fractions for Case 4, MAAP

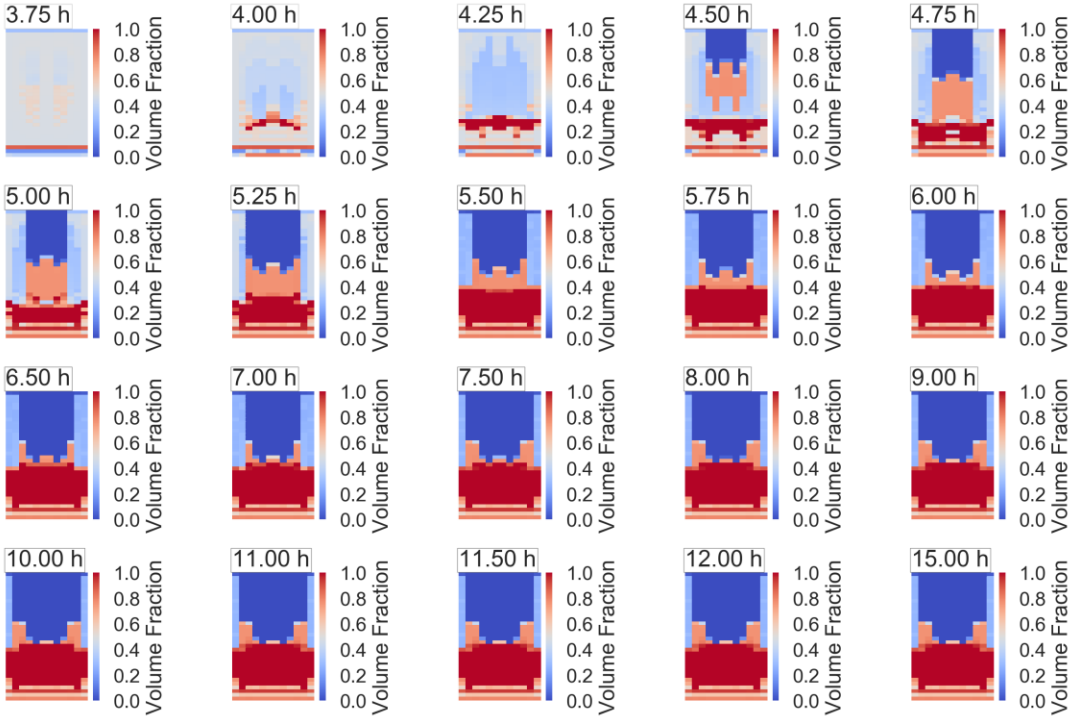

Figure C-5. Nodalized core blockage fractions for Case 5, MAAP

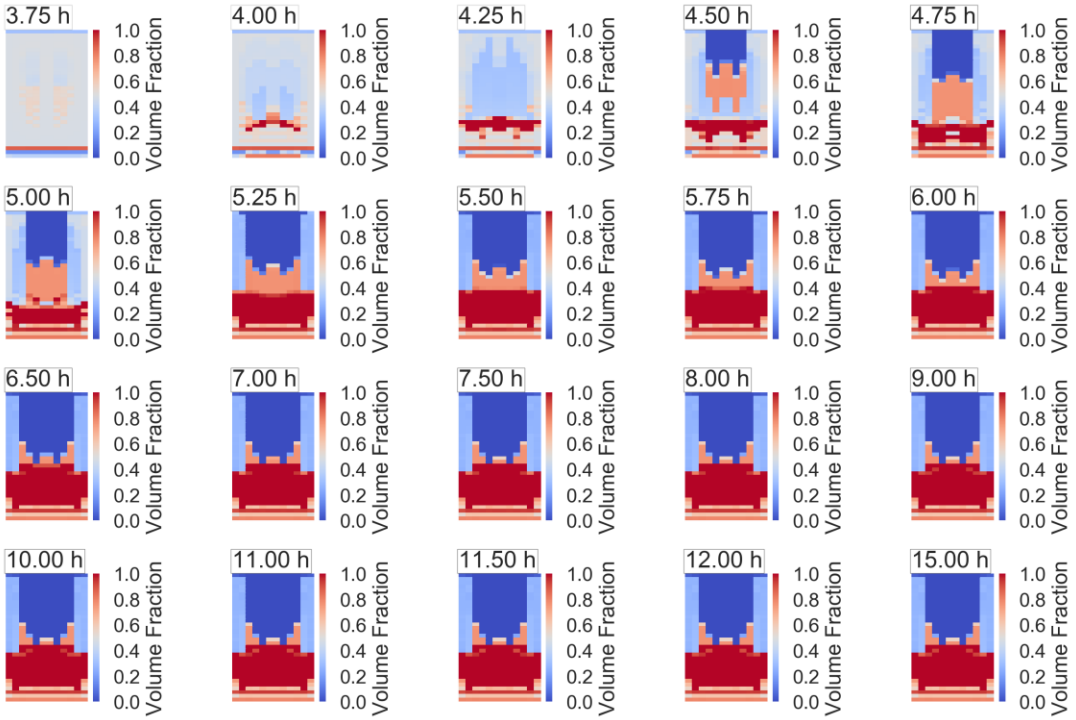

Figure C-6. Nodalized core blockage fractions for Case 6, MAAP

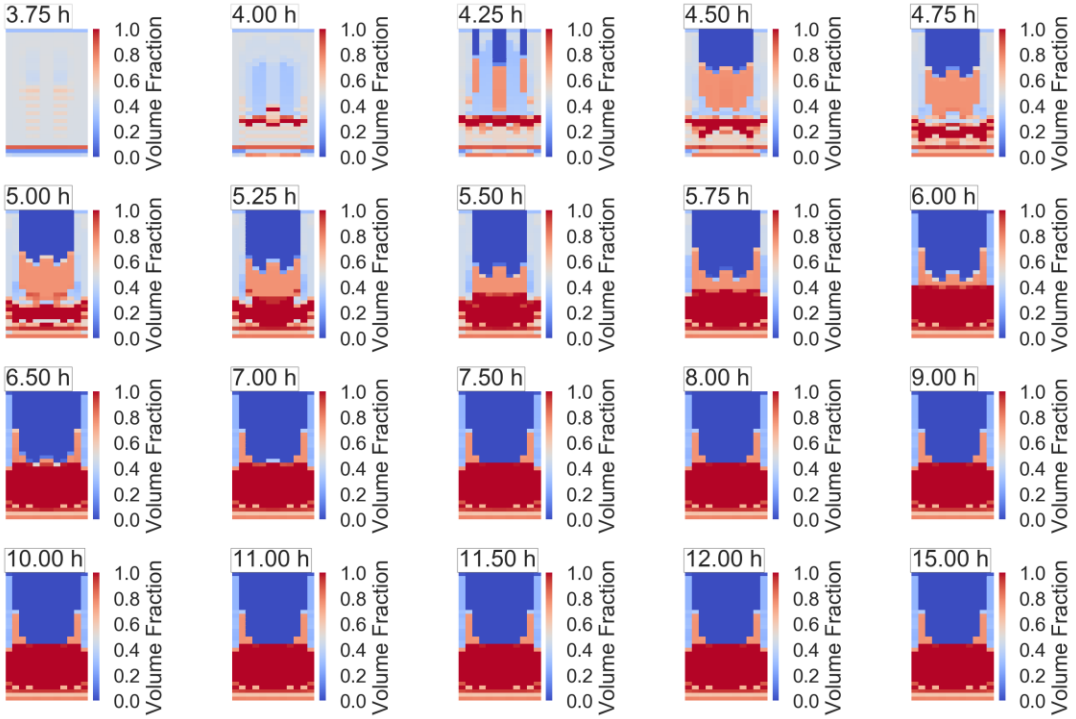

Figure C-7. Nodalized core blockage fractions for Case 7, MAAP

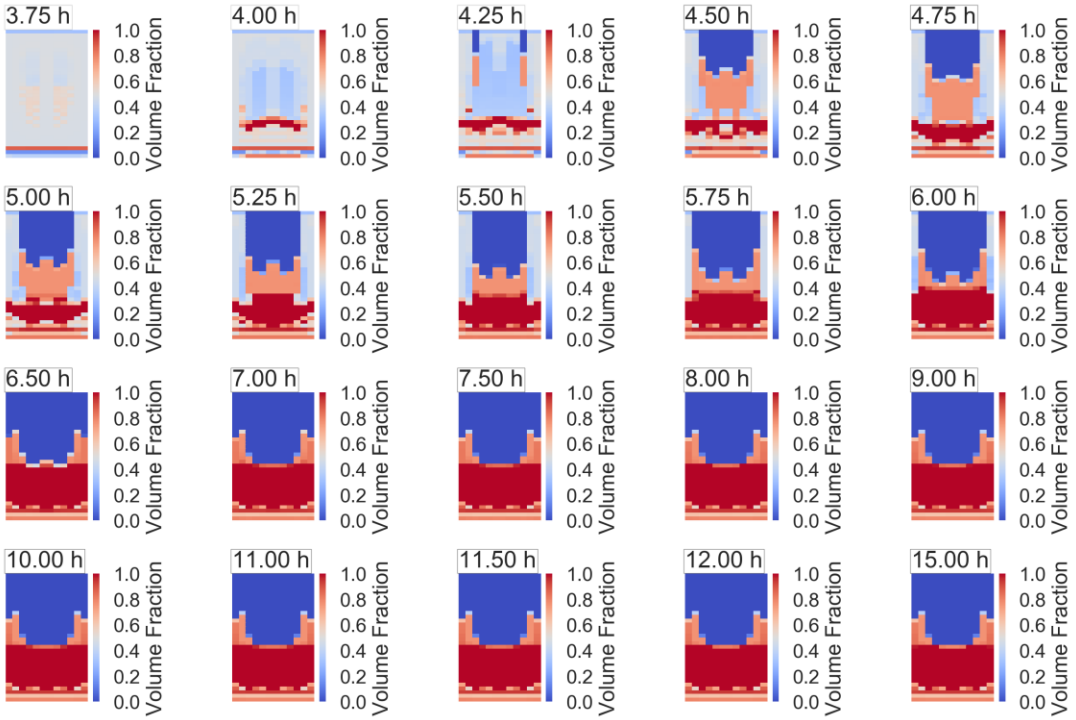

Figure C-8. Nodalized core blockage fractions for Case 8, MAAP

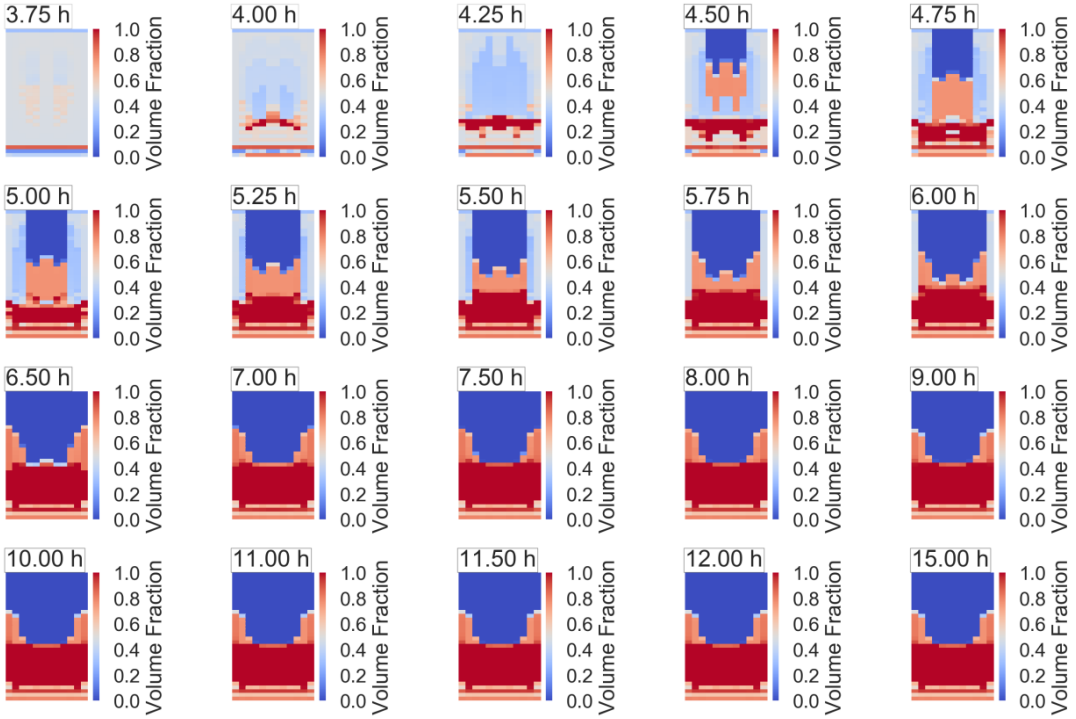

Figure C-9 Nodalized core blockage fractions for Case 9, MAAP

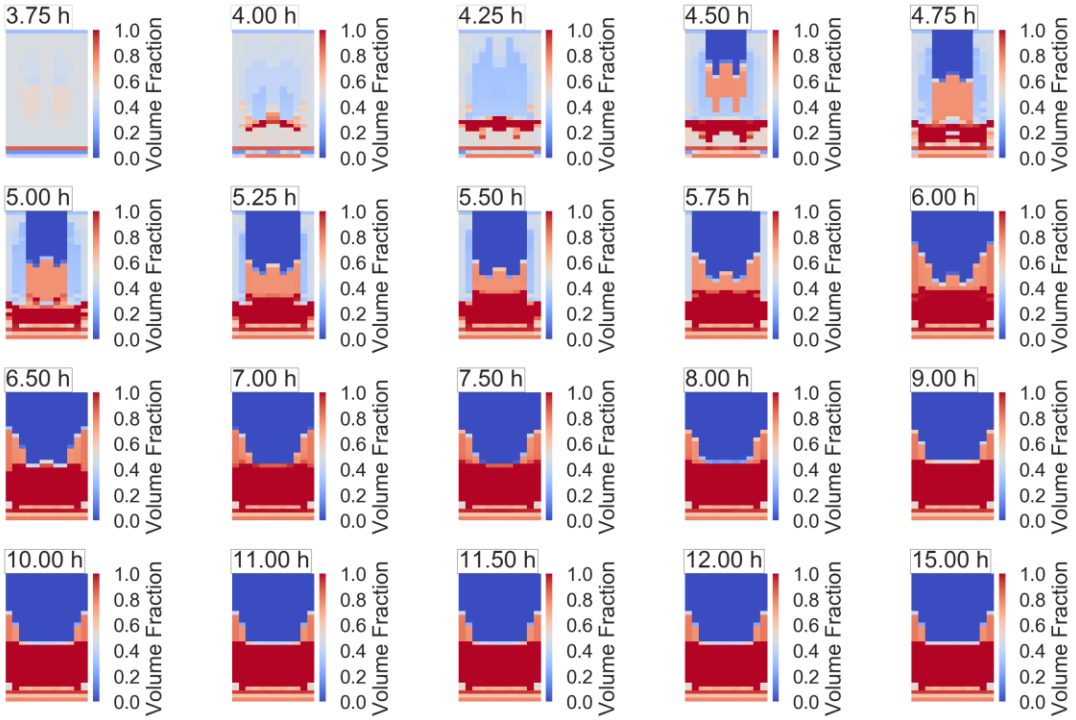

Figure C-10. Nodalized core blockage fractions for Case 10, MAAP

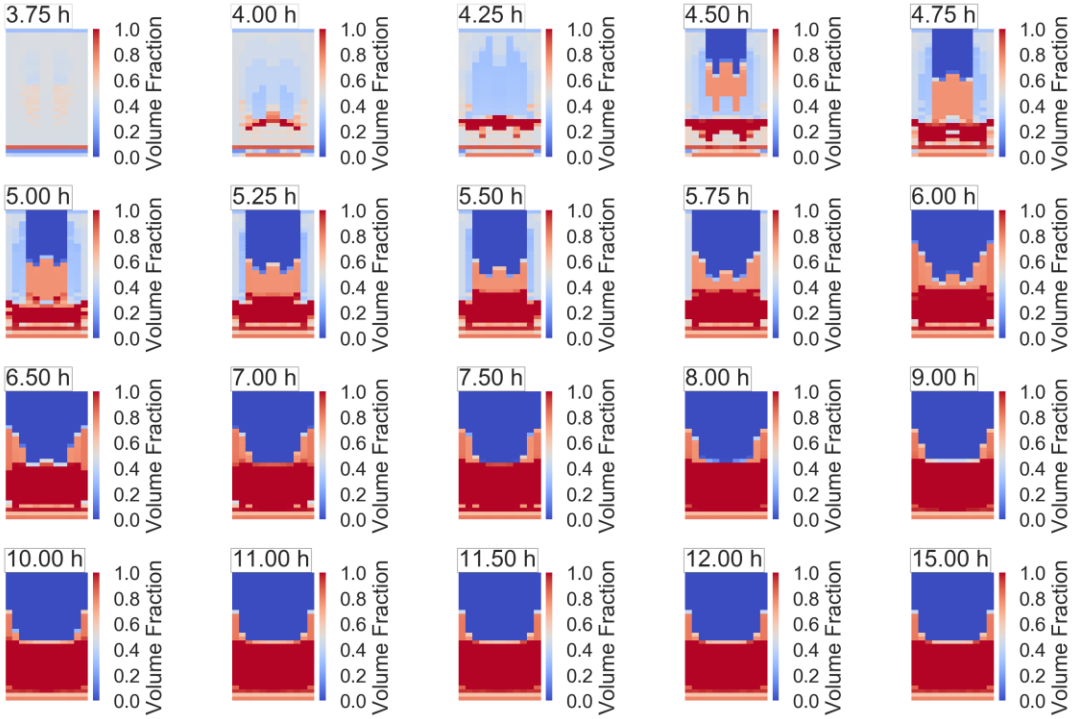

Figure C-11. Nodalized core blockage fractions for Case 11, MAAP

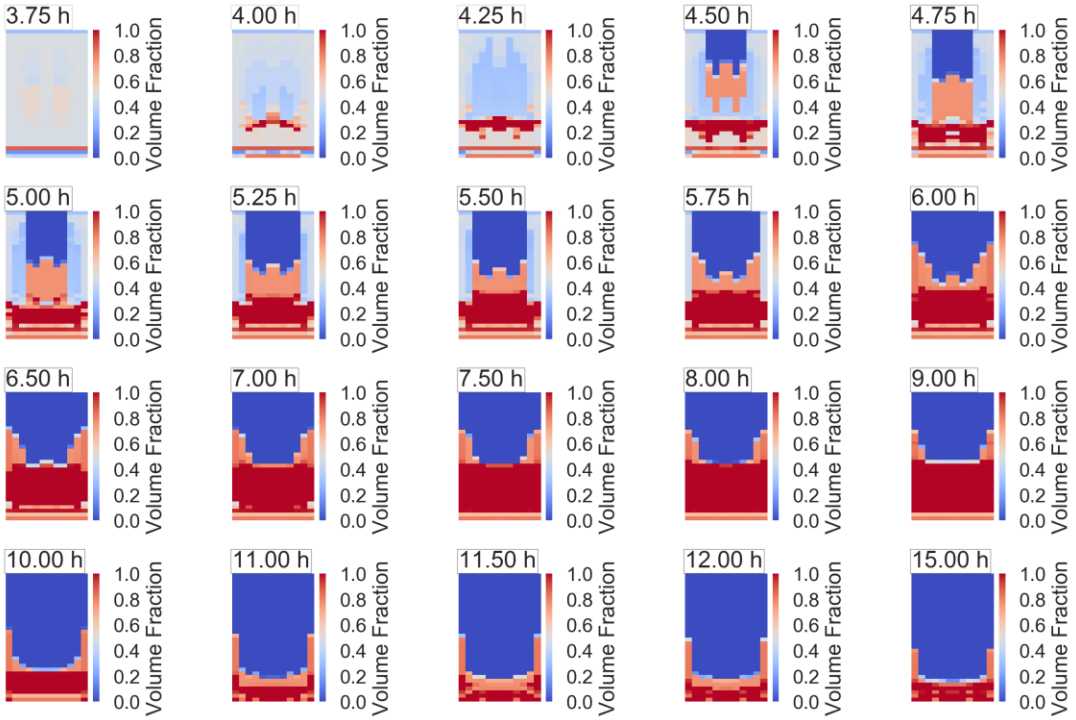

Figure C-12. Nodalized core blockage fractions for Case 12, MAAP

APPENDIX D. NODALIZED CORE BLOCKAGE FRACTIONS, MELCOR

This appendix contains nodalized core blockage fractions diagrams for MELCOR.

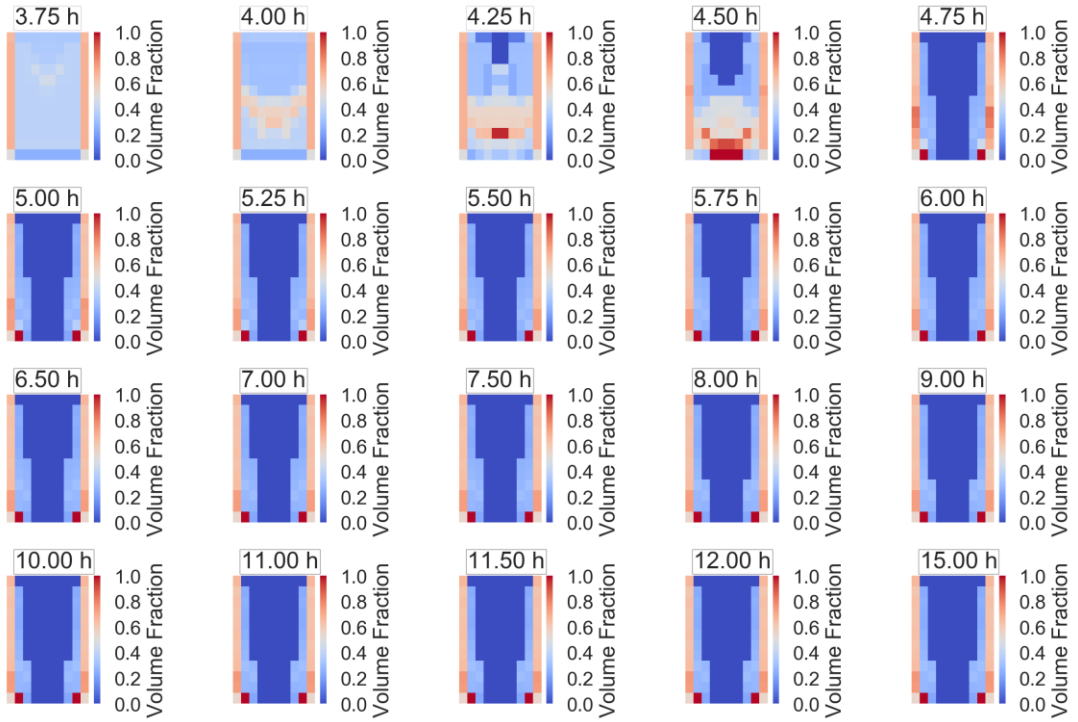

Figure D-1. Nodalized core blockage fractions for Case 1, MELCOR

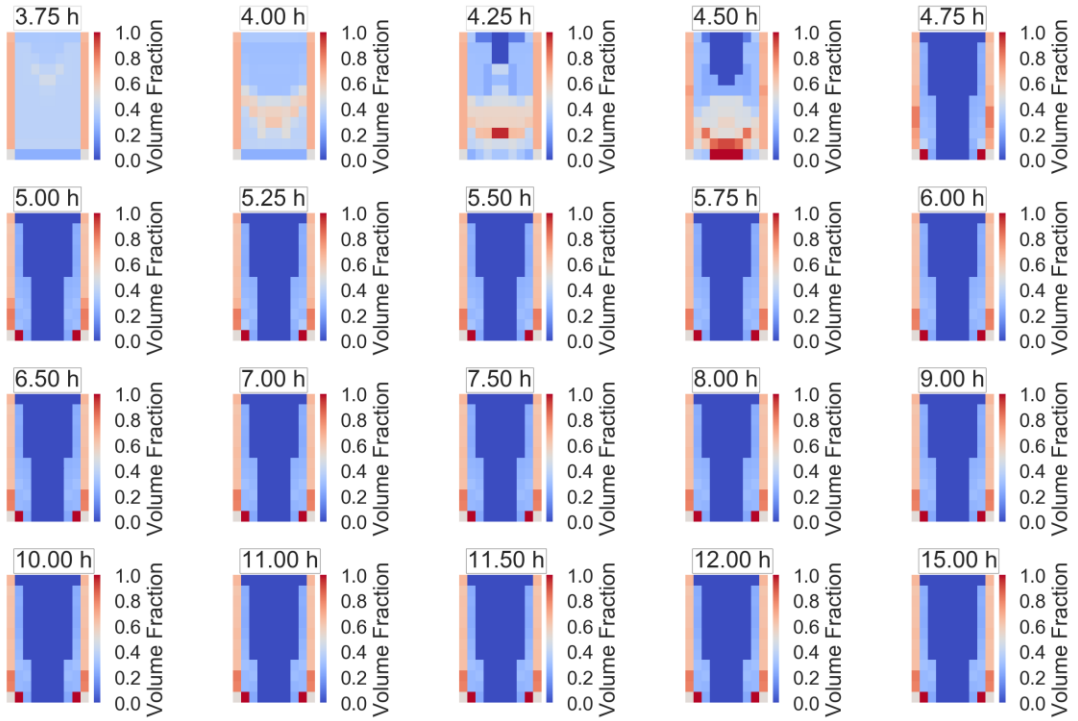

Figure D-2 Nodalized core blockage fractions for Case 2, MELCOR

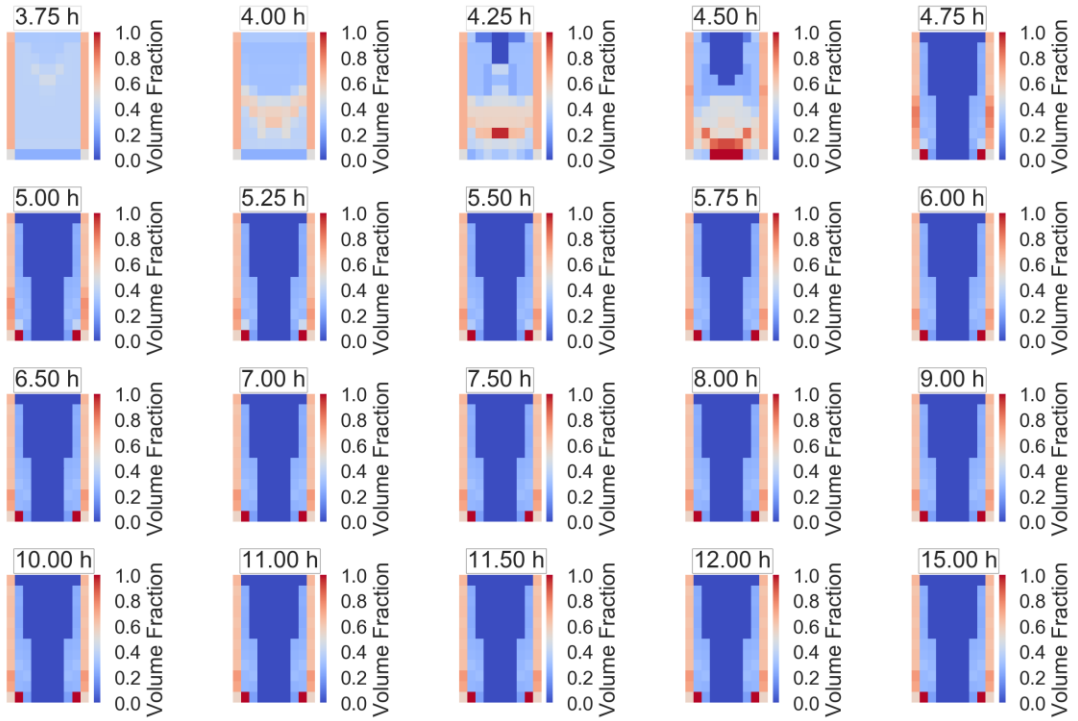

Figure D-3. Nodalized core blockage fractions for Case 3, MAAP

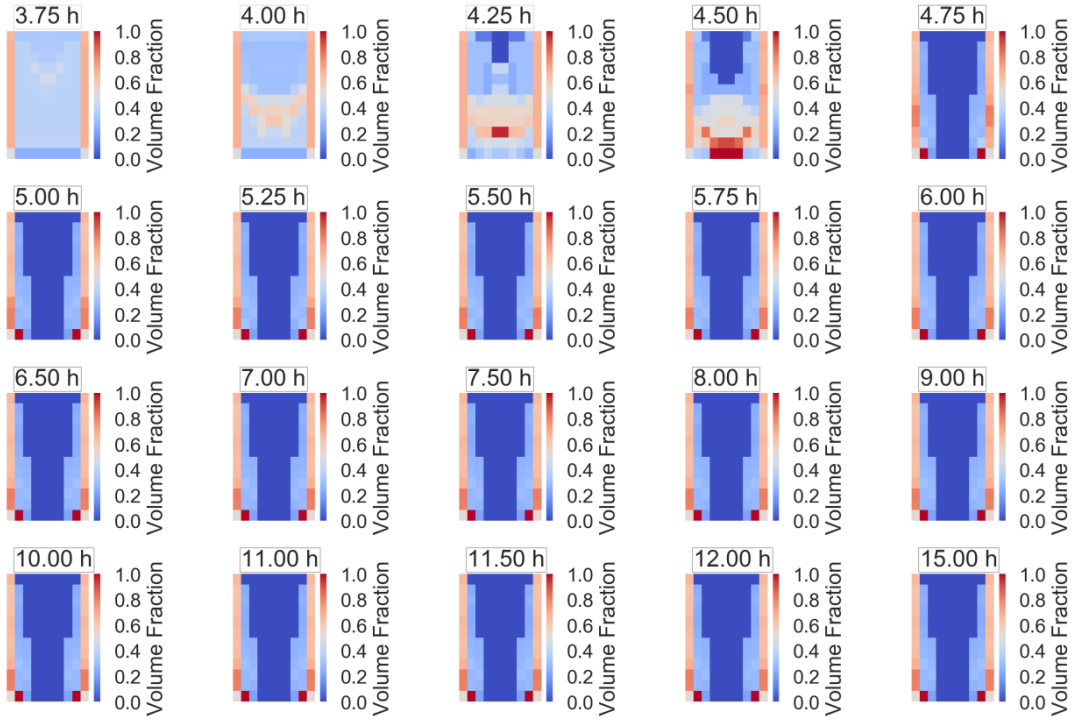

Figure D-4. Nodalized core blockage fractions for Case 4, MELCOR

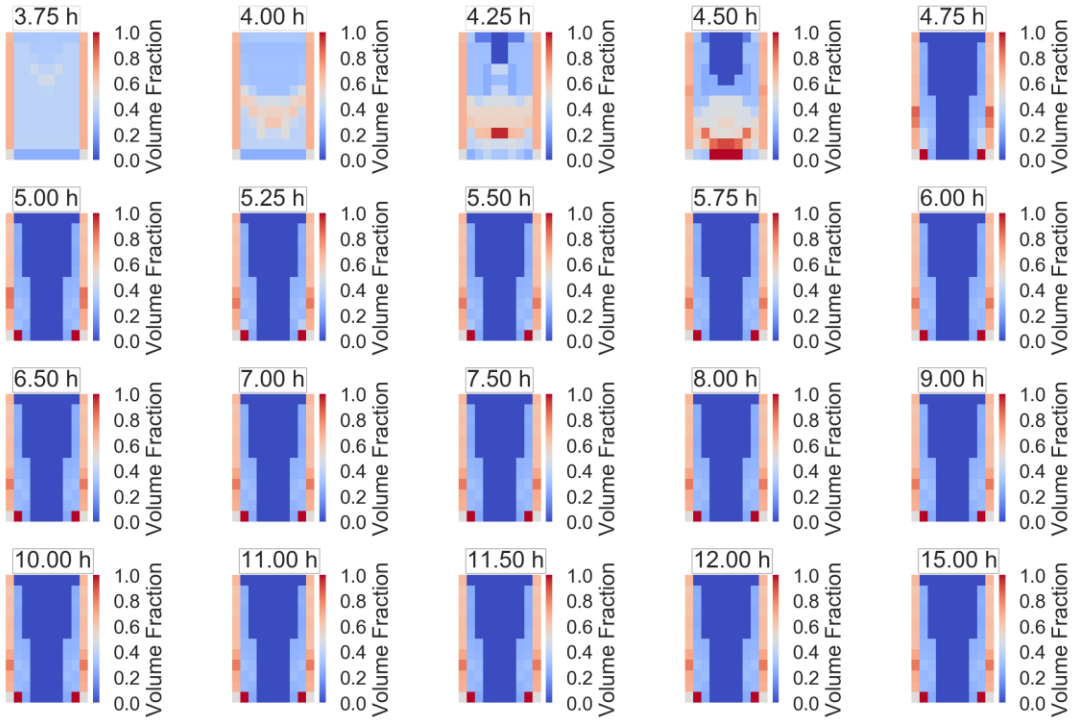

Figure D-5. Nodalized core blockage fractions for Case 5, MELCOR

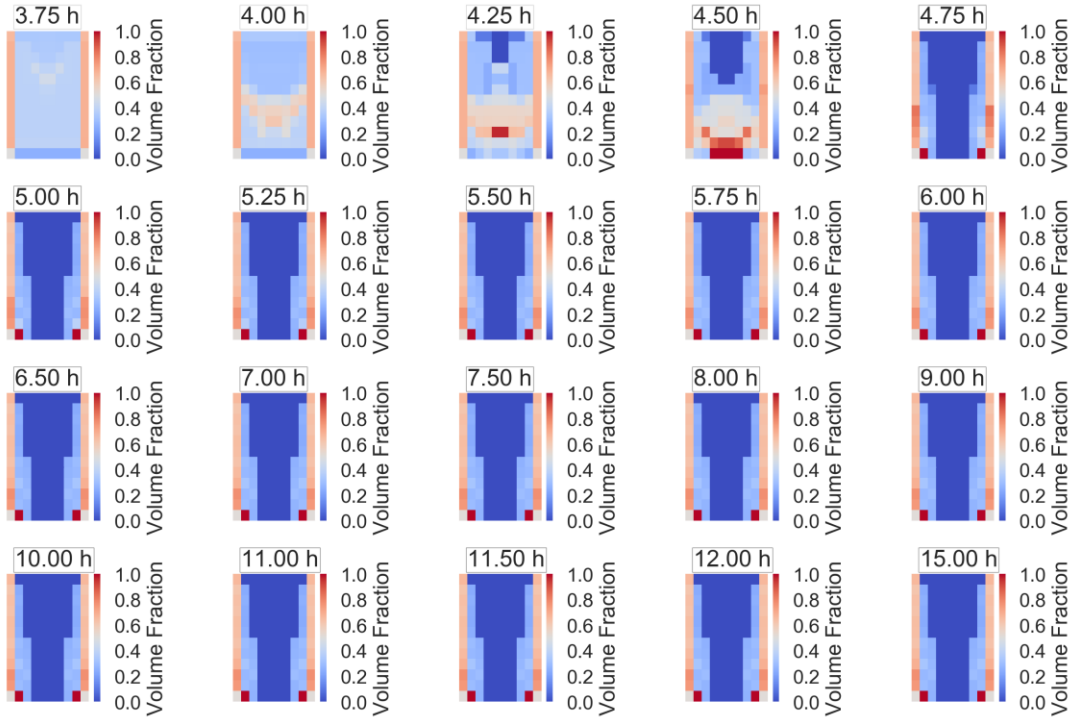

Figure D-6. Nodalized core blockage fractions for Case 6, MELCOR

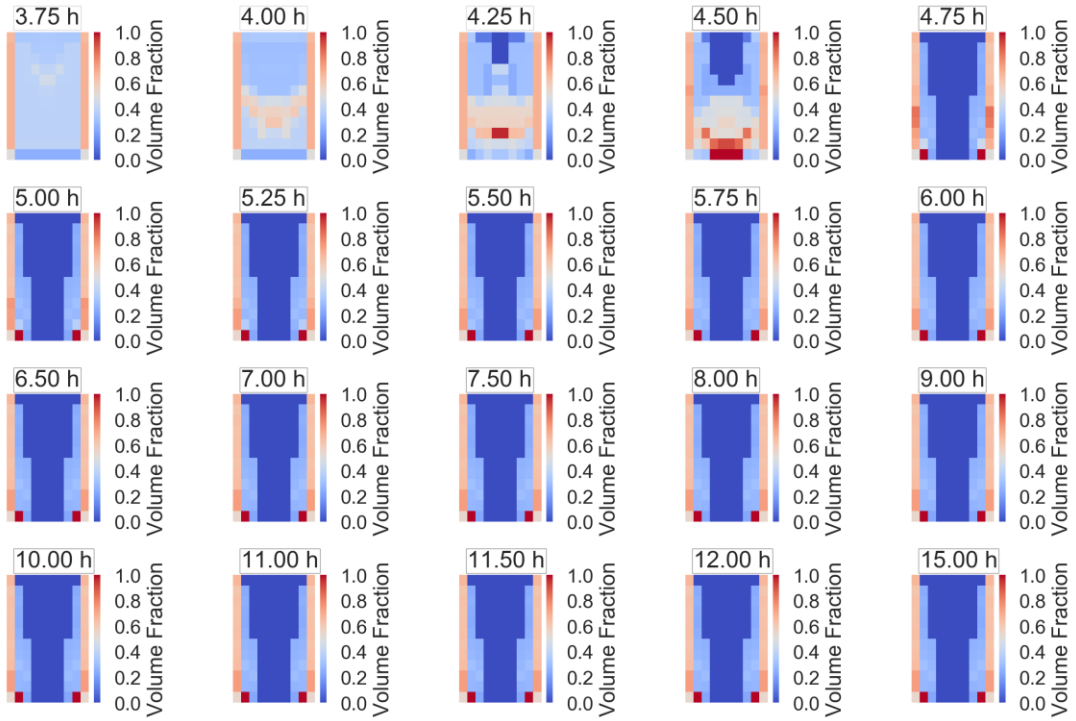

Figure D-7. Nodalized core blockage fractions for Case 7, MELCOR

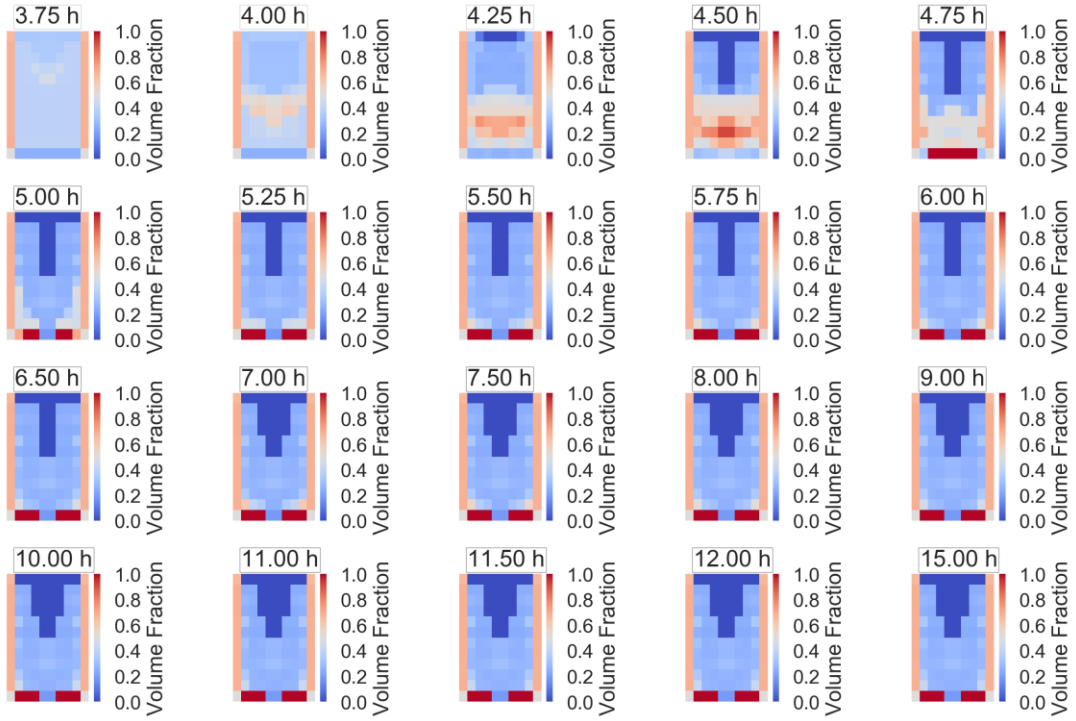

Figure D-8. Nodalized core blockage fractions for Case 8, MELCOR

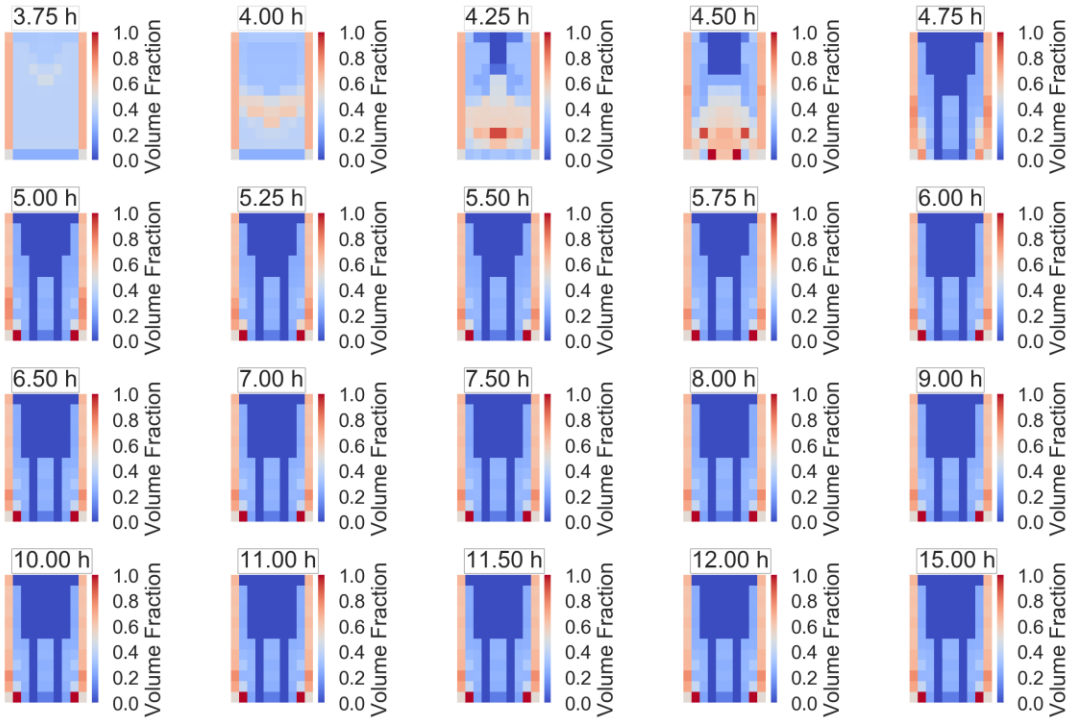

Figure D-9 Nodalized core blockage fractions for Case 9, MELCOR

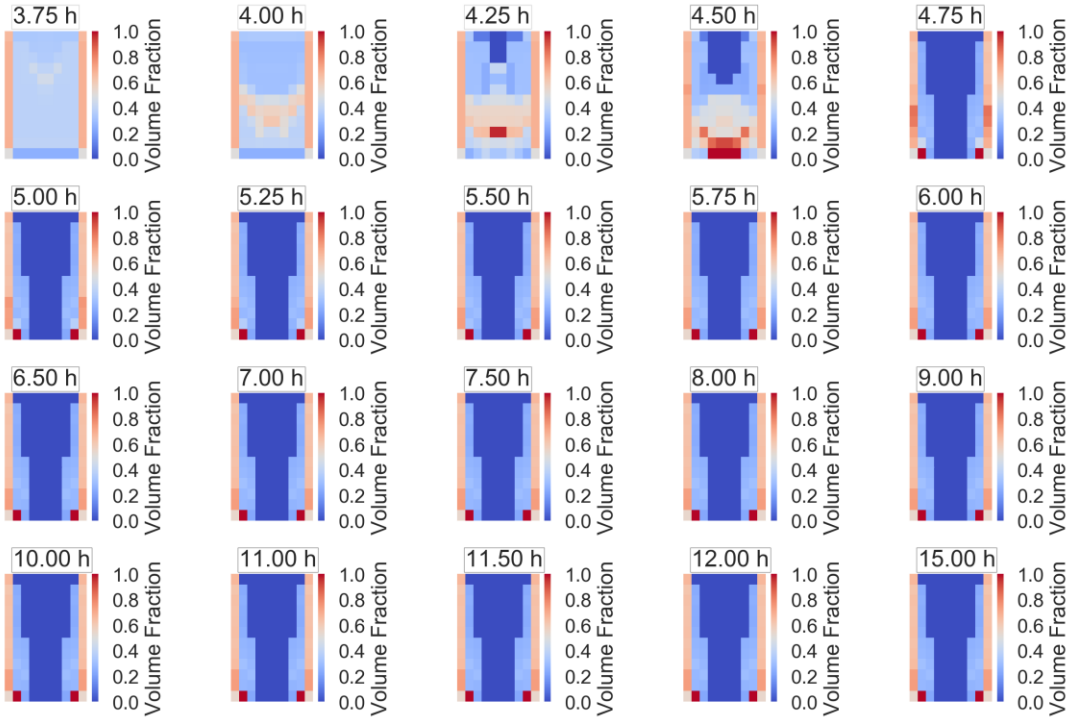

Figure D-10. Nodalized core blockage fractions for Case 10, MELCOR

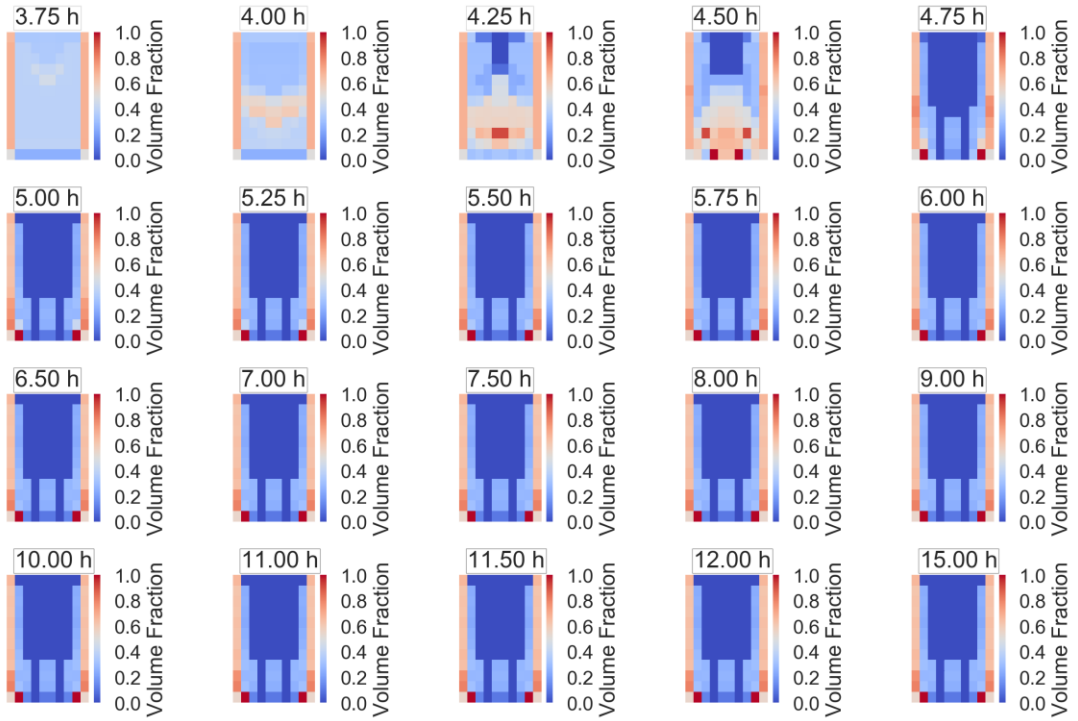

Figure D-11. Nodalized core blockage fractions for Case 11, MELCOR

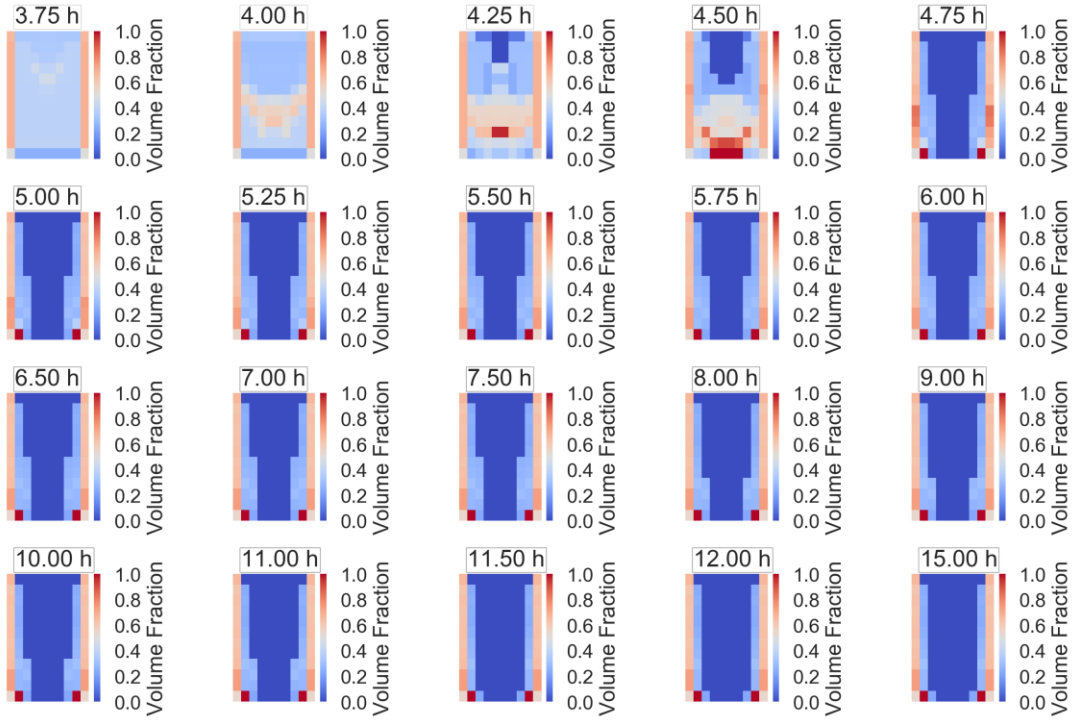

Figure D-12. Nodalized core blockage fractions for Case 12, MELCOR

APPENDIX E. WETWELL PRESSURES

This appendix contains wetwell pressure for all analysis cases.

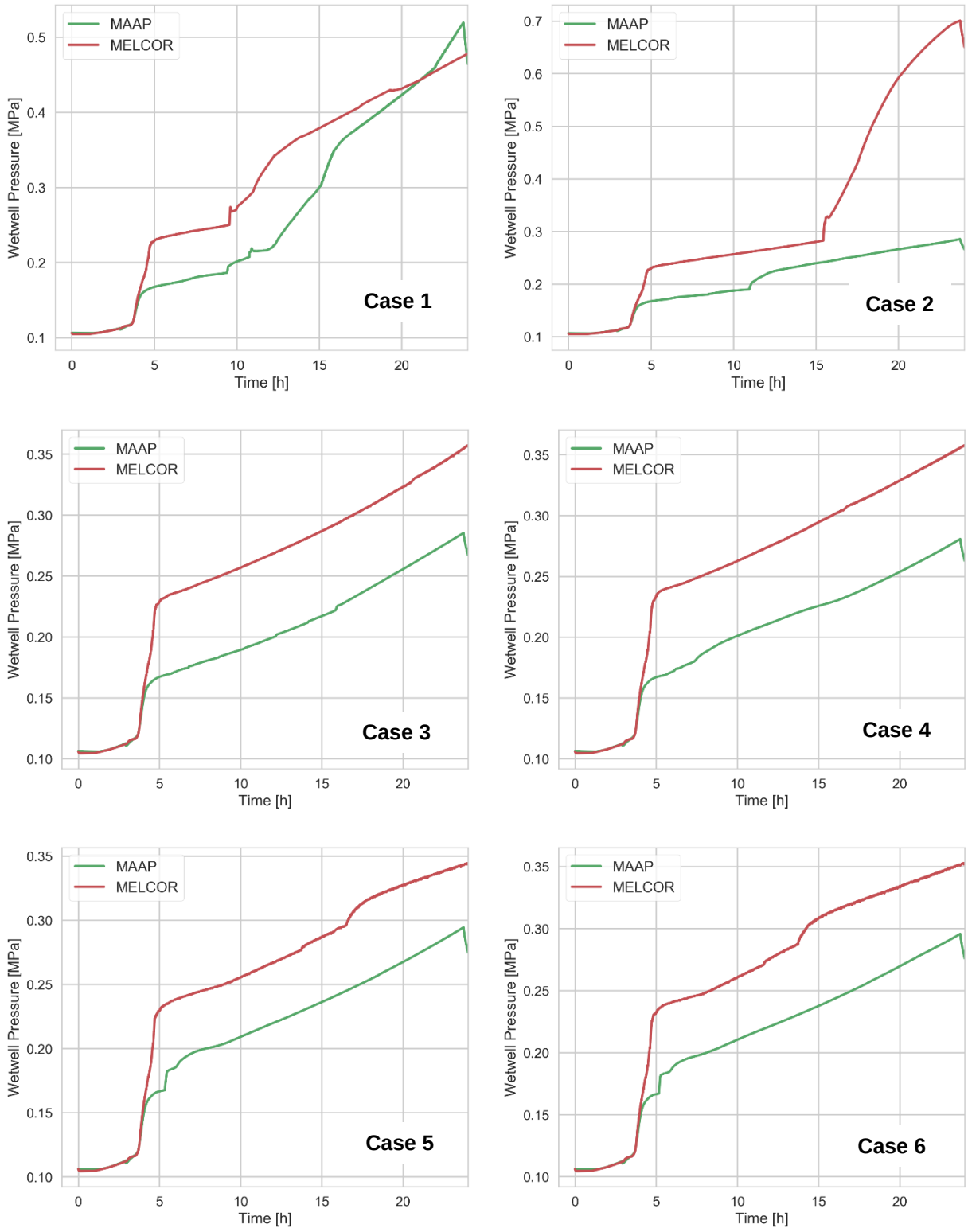

Figure E-1. Wetwell pressure for constant injection delay cases

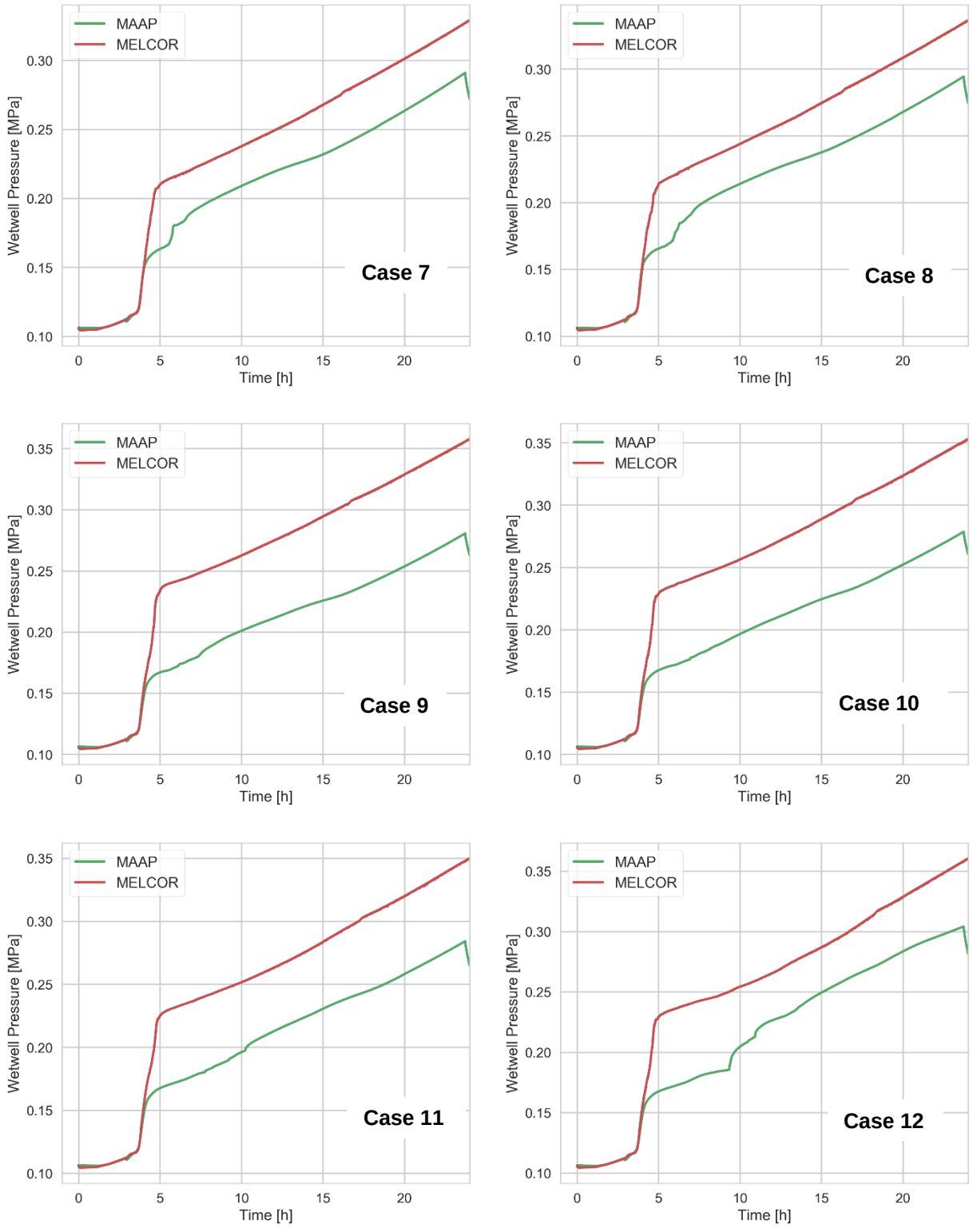

Figure E-2. Wetwell pressure for constant injection rate cases

DISTRIBUTION

1	MS0748	Nathan Andrews	8852
1	MS0748	Randall Gauntt	8852
1	MS0748	Christopher Faucett	8852
1	MS0748	Troy Haskin	8852
1	MS0748	Larry Humphries	8852
1	MS0748	Douglas Osborn	8852
1	MS0899	Technical Library	9536 (electronic copy)


Sandia National Laboratories